RAWASHDEH, RABEAH YOUSEF, Ph.D. Mechanistic Studies of Water Soluble Fullerenes as Free Radical Scavengers, Biological Antioxidants and NF-kappaB Inhibitors. (2014)
Directed by Dr. Ethan Will Taylor. 168 pp.

Since their discovery, fullerenes and fullerene derivatives have been the subject of intense research because of their unique properties and potential applications. The combination of a network of conjugated double bonds with high electron affinity makes them good electron acceptors, so that, despite being described commonly as antioxidants in the biological literature, they may act mechanistically as oxidants. Because of their ability to accept electrons, fullerenes can quench reactive oxygen species (ROS), particularly free radicals, by accepting their unpaired electron. Overproduction of ROS interferes with cell signaling and apoptosis, as well as causing generalized damage to biomolecules, through their interaction with lipids, DNA and proteins, thereby contributing to chronic diseases. The pro-inflammatory transcription factor NF-κB is known to be activated by ROS; modulation of NF-κB signaling is well established as a way to control inflammatory immune responses.

Although there are numerous studies on the biological roles of fullerenes, their mechanism of action is poorly understood. The main focus of this research is to clarify redox properties and bioactivity of fullerene derivatives, including their fundamental redox properties, their interaction with NF-κB and their biocompatibility involving the possibility of ROS generation vs. elimination by free radical scavenging. Different C_{60} and C_{70} fullerene derivatives used in these studies include hydroxylated fullerenes ($C_{60}OH_x$ and $C_{70}OH_x$), carboxyfullerene (C_3), amphiphilic liposomal malonylfullerene

(ALM), fullerene-tetraglycolate TGA and TTA, which were studied in comparison to common antioxidants such as ascorbic acid and N-acetyl cysteine.

The results from the ferric reducing antioxidant power (FRAP) assay demonstrate that fullerenes are very poor reducing agents, whereas the results of electro-paramagnetic resonance spectroscopy (EPR) confirmed their radical scavenging properties vs. superoxide ion. Taken together, the results of both studies (FRAP and EPR) emphasize the need to distinguish between antioxidant and antiradical properties of fullerenes, as the latter can occur via oxidation of free radical species.

Regarding their potential future use in clinical applications, an important finding is that hydroxy and carboxy fullerene derivatives exposed to ambient conditions in living cells neither produce ROS nor cause any cytotoxicity at nanomolar to micromolar concentrations, as shown using proliferation assays and redox sensitive fluorescent dyes. On the other hand, TTA and $C_{60}OH_x$ fullerenes were found to have a distinct effect on mitochondrial function of cells, implying their interference with proton transfer process of mitochondrial membrane. However, this effect is apparently not sufficient to decrease cell viability.

The activity of fullerenes as potential anti-inflammatory drugs was investigated using several cell-based assays involving an NF-κB reporter gene assay, coupled with visualization of nuclear translocation of exogenous (transfected) NF-κB, achieved via a construct with the NF-κB p65 gene fused to green fluorescent protein. The fullerene derivatives C_3 and $C_{60}OH_x$ were found to be effective inhibitors of NF-κB driven gene expression at micromolar concentrations. However, unlike some antioxidants such as α-

lipoic acid, they did not inhibit PMA-induced nuclear translocation of exogenous NF-κB even at high concentration (40 μM). Along with western blot analysis, this result strongly suggests that fullerene derivatives block NF-κB signaling downstream of the cytosolic activation pathway (the site of action of many antioxidants), possibly inhibiting NF-κB activation at a step penultimate to DNA binding in the nucleus (e.g., by interfering with the mandatory reduction of NF-κB by thioredoxin).

These studies suggest that the molecular basis of action of water soluble fullerenes has both similarities and differences to typical antioxidants. Like many antioxidants, they are active as NF-κB inhibitors, suggesting a potential role as novel anti-inflammatory agents, as they have low overall toxicity. However, they have a distinct mechanism of action, such as scavenging free radicals by oxidation, and lack activity as direct reducing agents.

MECHANISTIC STUDIES OF WATER SOLUBLE FULLERENES AS FREE RADICAL SCAVENGERS, BIOLOGICAL ANTIOXIDANTS AND NF-KAPPAB INHIBITORS

by

Rabeah Yousef Rawashdeh

A Dissertation Submitted to
the Faculty of the Graduate School at
the University of North Carolina at Greensboro
in Partial Fulfillment
of the Requirements for the Degree
Doctor of Philosophy

Greensboro
2014

Approved by

_____
Committee Chair

APPROVAL PAGE

This dissertation has been approved by the following committee of the Faculty of The Graduate School at The University of North Carolina at Greensboro.

Committee Chair _____
Ethan Will Taylor

Committee Members _____
Alice E. Haddy

_____
Christopher L. Kepley

_____
Marinella G. Sandros

_____
Dennis R. LaJeunesse

_____03/19/2014_____
Date of Acceptance by Committee

_____03/19/2014_____
Date of Final Oral Examination

ACKNOWLEDGMENTS

I would like to express my gratitude and sincere thanks to my advisor Dr. Will Taylor for his constant support and encouragement from the earliest stages of my study until the completion of this work. Thanks to him for giving me this research and for being generous in sharing his experience and knowledge with me. Without his guidance and patience this work would not have been possible. Thank you for giving me the choice to try new ideas and for your trust and confidence in my ability to accomplish the goals of this work, I deeply appreciate the time and effort you spent in advising me throughout this research.

Special thanks go for Dr. Alice Haddy for being part of my committee, for her generous time in running EPR reaction and for providing me with the reagents necessary to optimize the reactions. Thanks for the other members of my committee: Dr. Christopher Kepley for providing me with fullerene samples, Dr. Marinella Sandros for her various valuable suggestions and Dr. Dennis LaJeunesse for the help in using the confocal microscope.

Thanks to Dr. Taylor research group and especially Dr. Jan Ruzicka for his continuous help in my research by answering all my questions and helping in the technical aspects of my dissertation research. Many thanks for Dr. Autumn Carlsen for helping me in my study and for her friendship. Thanks for other great scientists that had meaningful contribution to my dissertations: Renuka Shivaji and Jenna Calender for helping me in running western blot experiment and for providing the supplies and

reagents necessary to accomplish the experiment. Dr. Brandie Ehrmann for the MS training and for the use of MALDI/TOF in her laboratory. Dr. Sarala Pamujula for sharing her expertise in technical work. Thanks to my fellow graduate students for answering some questions related to experimental work and for helping me finding some reagents: Jesse Plotkin, Anthony Dellinger, Lee Williams, Ashley Turner and Karshak Kosaraju. I am truly grateful for the University of North Carolina Greensboro, UNCG, and for the Joint School of Nanoscience and Nanoengineering, JSNN, for their financial support and learning experience.

Thanks also go to my friends and everyone who helped me to settle down in America: Karishma Fernandes, Ashley Ganoe, Najoua Elbourkadi, Krystal Bailey, Colleen Brown and Hiyas Junio. Thanks to Nafisa Sirelkhatim for her friendship and for all the good times we spent together. To Sana Daraghmeh, thanks for inviting me for dinner over your house for many times. Thanks to Dr. Hanan Malkwai and Dr. Reyad Sawafta for introducing me to both the Nanoscience and to the beautiful city Greensboro, the city that I now consider as my second home.

Very special thanks to my source of inspiration my lovely parents; my mother Jamelah and my father Yousef, your prayers and unconditional love have brought me to where I am. Thank you for encouraging me to follow my ambitions and for providing me with the support needed to overcome all the challenges and difficulties through my PhD study. To my brothers: Mohammad, Ahmad, Omar and Amer, thanks for your love and care.

TABLE OF CONTENTS

Page

LIST OF TABLES

Page

LIST OF FIGURES

Page

LIST OF ABBREVIATIONS

β-gal	β-galactosidase
DETAPAC	Diethylenetriaminepentaacetic acid
DLS	Dynamic light scattering
DMEM	Dulbecco's modified Eagle's medium
DMPO	5,5-dimethyl-1-pyrolline-N-oxide
DMSO	Dimethyl sulfoxide
EPR	Electron paramagnetic resonance
FCCP	Carbonyl cyanide 4-(trifluoromethoxy)phenylhydrazone
FRAP	Ferric reducing antioxidant power
FRTA	Free radical theory of aging
GFP	Green fluorescent protein
GPX or GPx	Glutathione peroxidase
HIV	Human immunodeficiency virus
H_2O_2	Hydrogen peroxide
HOMO	Highest occupied molecular orbital
LA	Lipoic acid
LUMO	Lowest unoccupied molecular orbital
LTR sequence	long terminal repeat sequence

MALDI/TOF	matrix assisted laser desorption/ionization time of flight mass spectroscopy
NAC	N-acetyl cysteine
NF-κB	Nuclear factor kappaB
$O_2^{\bullet-}$	Superoxide
PMA	Phorbol 12-myristate 13-acetate
PBS	Phosphate buffer saline
PBS-T	Phosphate buffer saline with Tween
ROS	Reactive oxygen species
SDS-PAGE	Sodium dodecyl sulfate/Polyacrylamide gel electrophoresis
SOD	Superoxide dismutase
TBHP	T-Butyl hydrogen peroxide
TGA	C_{70}- tetraglycol acid
TMRE	Tetramethylrhodamine ethyl ester perchlorate
TNF	Tumor necrosis factor
TPTZ	Tripyridyltriazine
Trx	Thioredoxin
TTA	C_{70}-TEG acid (tetraethylene glycol)

CHAPTER I

INTRODUCTION

This dissertation is focused on the investigation of redox properties of water soluble fullerene derivatives, and the assessment of their effect on NF-κB as an important transcription factor. This chapter will provide some background for the history of fullerenes, their recorded properties and biological activities, typical activities and interaction with macromolecules.

An Overview of Fullerene Discovery, Properties and Applications

Fullerenes have emerged as one of the most prominent and widely investigated classes of nanomaterials. Before their discovery, two main carbon allotropes were known to exist: diamond and graphite, but because of the effort of researchers from US and Europe [4], fullerenes were discovered in 1985 to present a new molecular form of carbon.

Fullerenes were later discovered in soot generated from laser ablation of graphite by a method developed for their mass production at Rice University [5]. Among the various fullerenes that can be formed with varying number of carbon atoms, such as C_{28}, C_{36}, C_{70}, C_{76}, C_{78} and C_{82} [6, 7], C_{60} was observed to be by far the most abundant of these. To explain the stability of this molecule, the research team of Harold W. Kroto, Robert F. Curl and Richard E. Smalley proposed a highly symmetrical structure of a close sphere

cage of sixty carbon atoms, which is considered to be three-dimensional analogue of benzene, however it is made entirely of carbon atoms arranged in a truncated icosahedron geometry [8] (Figure 1 .A) resembling that of a soccer ball, and lacking in aromaticity. This landmark discovery was awarded the Nobel Prize in Chemistry in 1996. C_{60} was given the name buckminsterfullerene, because its structure resembles the geodesic dome design of R. Buckminster Fuller. In addition to C_{60}, C_{70} has been the focus of extensive research. The C_{70} structure (Figure 1. B) is characterized by two reactive poles which allow for attachment of lipophilic, hydrophilic, or other functional groups, whereas the C_{70} equatorial region is relatively inert. The polar region has comparatively high reactivity due to the significant orbital overlap of its lowest unoccupied molecular orbital (LUMO) and highest occupied molecular orbital (HOMO) that is expected for sites of maximum radical reactivity. Because of these structural features, C_{70} molecules provide a novel platform for the preparation of various novel compounds, such as amphiphilic fullerenes [9].

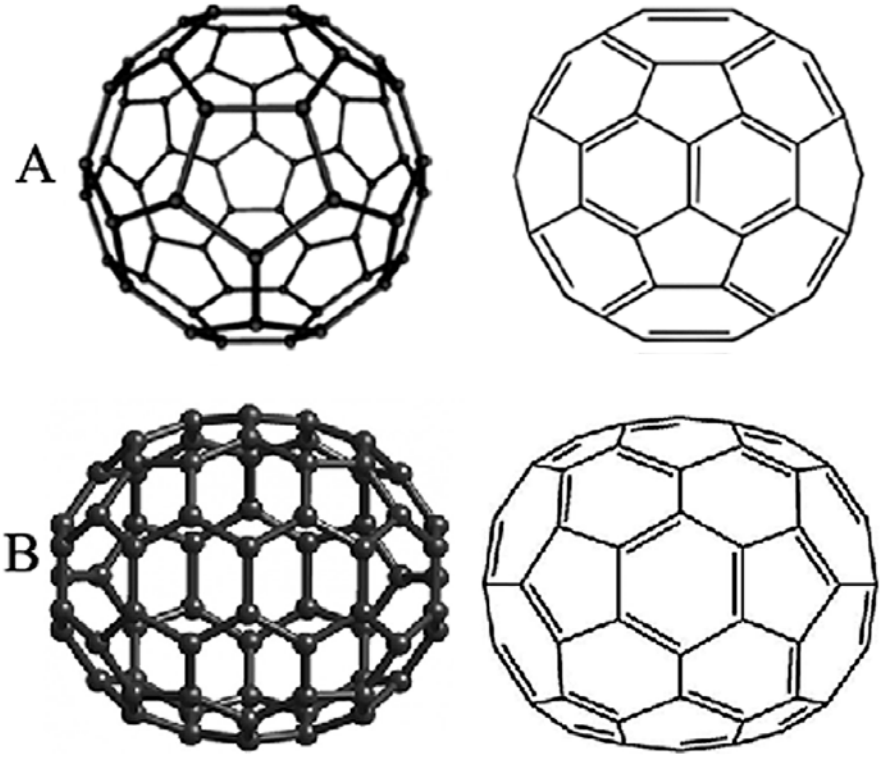

Figure 1. The unique structure of C_{60} and C_{70} molecules. A. A highly symmetrical 3D structure of icosahedral shape, C_{60} is made entirely of carbon atoms arranged in 12 pentagons and 20 hexagons; every carbon is bound to three other atoms, all in a state of sp2 hybridization. The conjugated double bonds are located at C5–C6 bonds (at the edge of hexagons). B. A less symmetrical structure, C_{70} is composed of 12 pentagons and 25 hexagons.

Fullerene chemistry, involving functional derivatization of various kinds, has been most extensively developed in the case of C_{60}, together with a less extensive body of work on C_{70}. At present most of the published papers described the chemical and physical properties of fullerenes C_{60} and C_{70}, with much less available on the chemistry on the higher fullerenes. The intensive investigation that has been done on the chemistry of C_{60} fullerenes over the last several decades shows the rich variety of reactivity of this compound and its derivatives. Despite the wealth of such information, given that it takes about 250 hours of work to produce just 1 mg of many of these molecules [10], much remains to be learned about their activities in biological systems.

Although fullerenes were first synthesized in the laboratory, they are produced naturally as a result of high energy events such as lightning strikes and have been found in meteorites and geological samples [11, 12], as well as occurring naturally in soot. While nanoparticles, in general are being produced and integrated into different products, for example in cosmetics and drugs (Figure 2), there is still a lack of data generated regarding their safety and application (Figures 3 & 4). Production of extensive data is the first step in the process of issuing guidelines and setting regulations regarding use and safety of nanomaterials in general by regulatory agencies. Moreover, the availability of more information about those molecules will definitely enhance the marketing and commercialization of nano products in general.

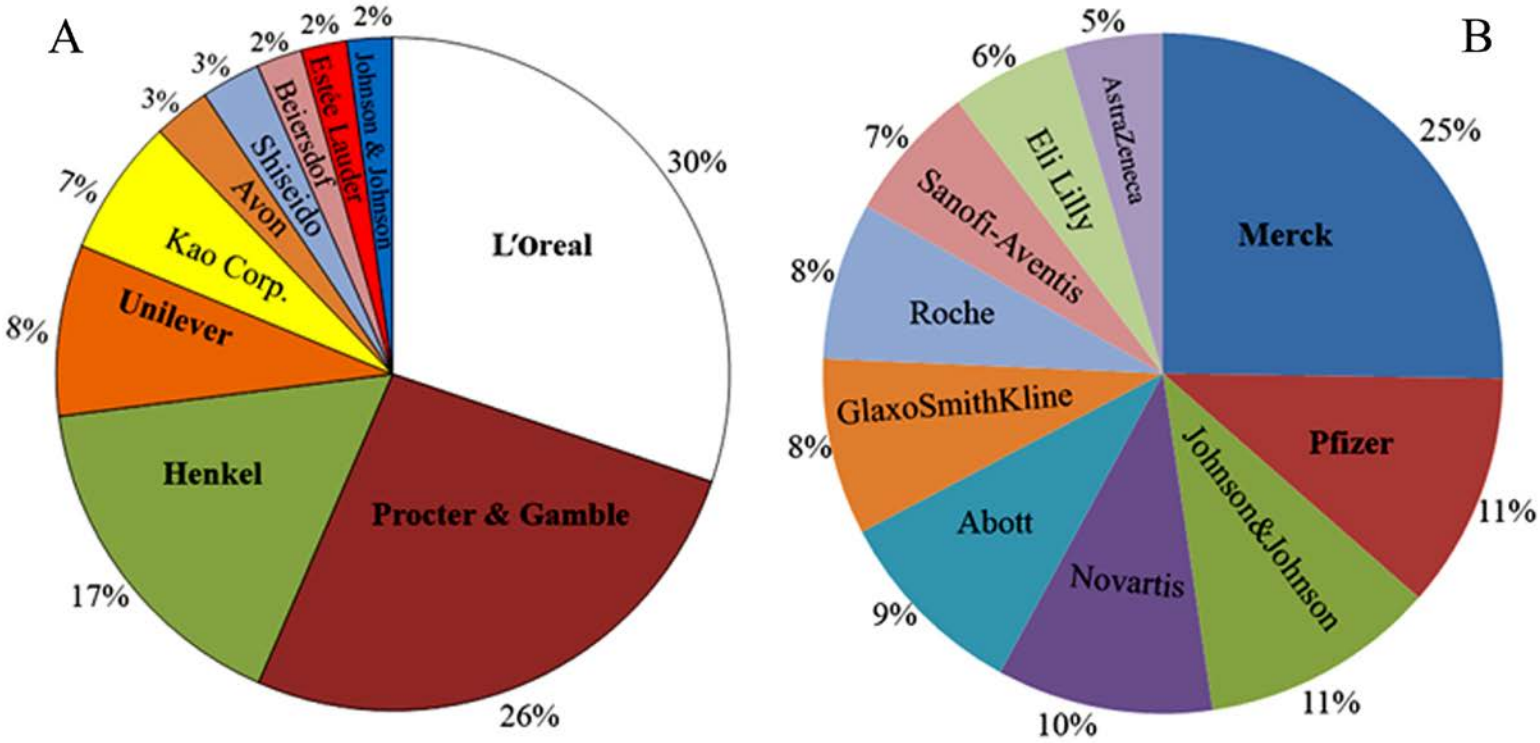

Figure 2. The two graphs are based on Espacenet database, show the estimated percentages of NANO-related patents of the top 10 COSMETIC (A) and PHARMACEUTICAL (B) companies of the world in 2009 [1, 2].

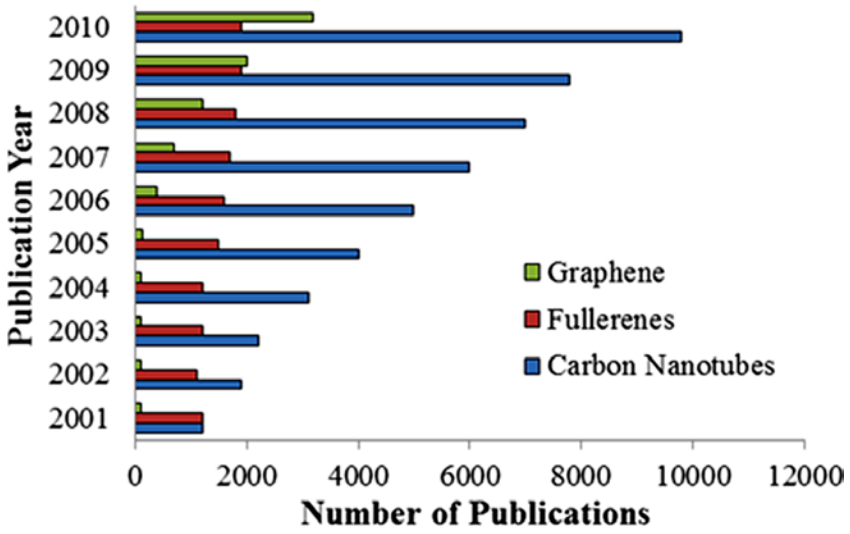

Figure 3. The estimated number of publications of carbon nanomaterials from 2001 to 2010. Science Citation Index Expanded/Web of Science [13].

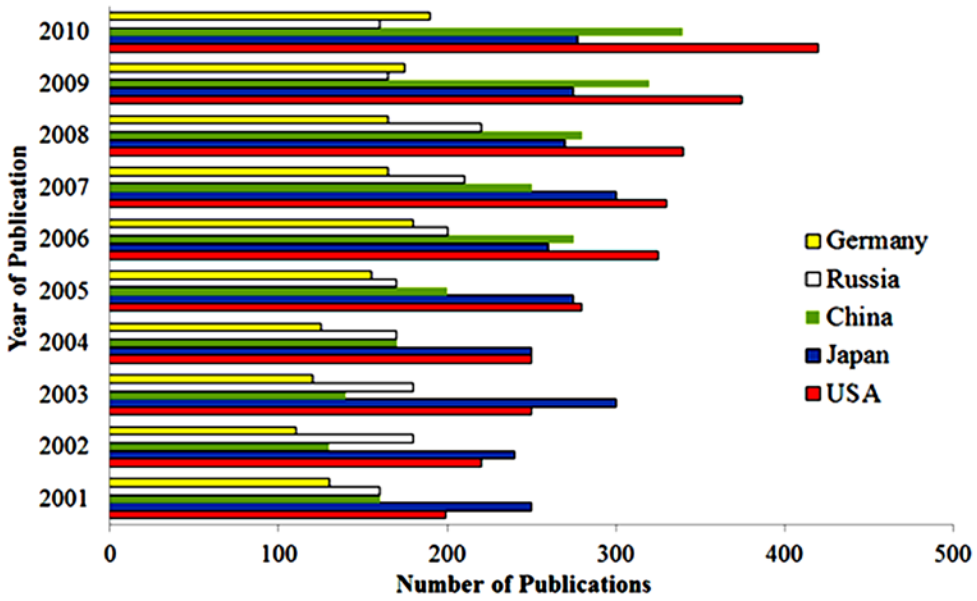

Figure 4. The estimated number of publications in FULLERENES in leading countries from 2001 to 2010. Source: Science citation index [13].

In spite of the production of workable quantities of fullerenes, their application is restricted, particularly in nanomedicine, due to their poor solubility in water. Underivatized C_{60}, also known as pristine C_{60}, is a hydrophobic molecule that is most easily dissolved in organic solvents. Some procedures can be used to enhance their dispersion in aqueous suspension, such as long term stirring in water [14, 15] and incorporation into water soluble supramolecular structures such as cyclodextrin [16]. In addition to that, the covalent attachment of various polar groups (e.g., –OH, NH_2, –COOH) to fullerene cage results in the formation of functionalized fullerene molecules; this procedure, known as exohedral functionalization, allows water to establish bonds with hydrophilic addends of fullerene [17-19], enhancing the solubility.

Research in the field of water soluble C_{60} fullerene derivatives has increased dramatically and many distinguishable biological properties of water soluble fullerenes have been exhibited so far including; neuroprotection [20, 21], antiviral activity [22-24], antimicrobial activity [25], antiapoptotic activity [26], DNA photocleavage [27] , drug delivery [17, 28], magnetic resonance imaging MRI [29] and contrast agents [30, 31].

Fullerenol, a polyhydroxylated C_{60} derivative, was the first water soluble fullerenes to be successfully synthesized, in 1992 [32, 33] (Figure 5). Fullerenol (C_{60}-OH_x) can function as a free-radical scavenger [34], a neuroprotective agent [20] and an antiproliferative agent for vascular smooth muscle cells [26]. A fullerene-carboxylic acid derivative, C_3 (Figure 5), was found to play a role as a neuroprotective agent [21]. The biological functions of the soluble fullerenes have commonly been attributed to their

antioxidant properties [34]. However, the reality is more complex, as will be shown later in this Dissertation.

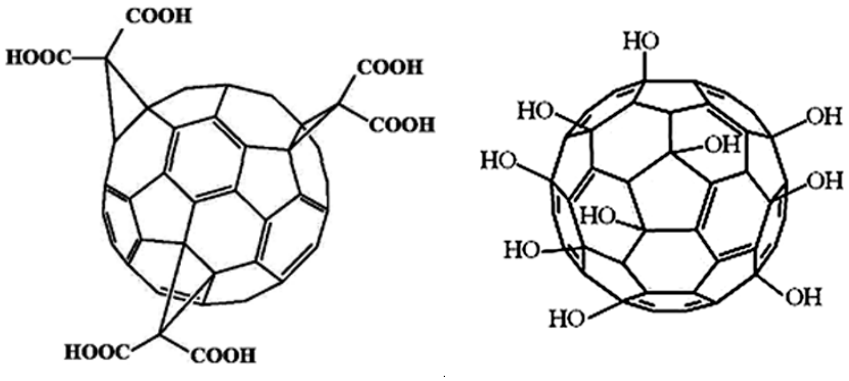

Figure 5. The tris malonyl C_{60} compound known as C_3 (left); the three malonyl groups are attached to fullerene compound through [6,6] bonds, and the hydroxylated fullerene $C_{60}[OH]_{22}$ (right).

The unique electrochemical features of water soluble fullerenes allow them to quench reactive oxygen species (ROS) [21], which have been implicated in aging and various degenerative diseases, such as diabetes, neurological and cardiovascular diseases and cancer [35-38].

Role of Free Radicals and Antioxidants

A free radical can be defined as any molecule or atom with unpaired electrons, e.g. as a result of losing one electron from the outer shell, causing it to become relatively unstable and highly react with other molecules, from which it can extract an electron in order to stabilize its own electron configuration. Free radicals form as metabolic intermediates through many different biochemical reactions. However, the

overproduction or uncontrolled generation of free radicals resulting from metabolic dysfunction can cause damage to many biological macromolecules [39]. Free radicals are distinguished as highly reactive molecules that explain their toxicological activities, examples; superoxides ($O_2^{\bullet -}$) and hydroxyl radicals ($^{\bullet}OH$) (Figure 6).

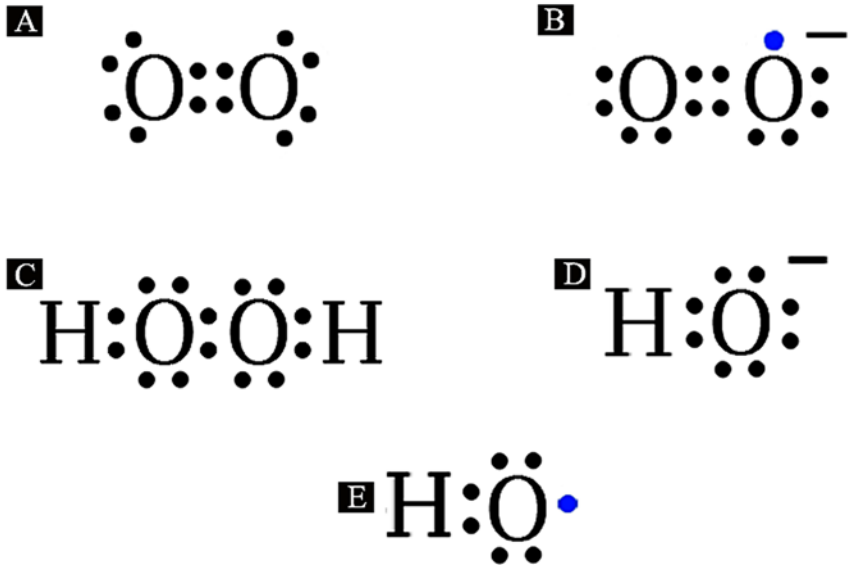

Figure 6. Lewis electron configuration of Oxygen (A), Superoxide anion (B), Hydrogen peroxide (C), Hydroxide ion (D) and Hydroxyl radical (E). The difference between radicals and the non-radical oxygen species is in the unpaired electron; therefore of the molecules shown, superoxide and hydroxyl radicals are the only radical species. The unpaired electron is shown in blue.

The mechanisms underlying aging have yet to be fully elucidated, and the emergence of every new aging theory makes it even harder for researchers to recognize the entire mechanisms of aging due to the multidisciplinary perspectives involved. One of the earliest and most well-known theories of aging, called the free radical theory of aging (FRTA), postulates that accumulation of damage to macromolecules caused by free radicals causes aging and ultimately death as a consequence [40]. However other data

support the evolution of the hyperfunction theory placed by Blagosklonny M. [41]; this theory emphasis that aging is not the only factor contributing to death through molecular damage and the real cause of aging is hyperfunction, especially excess biosynthesis. This hypertrophy is driven by cellular signaling networks that control growth (and thereby, reproduction) including insulin, insulin-like growth factor 1 (IGF-1), and in particular, the target of rapamycin (TOR) kinase pathways [41]. Furthermore, several biological clocks were found to be associated with aging such as telomere length and DNA methylation level.

Since the advent of genetic technologies such as gene knockout organisms, various studies have been done to attempt to extend or modify lifespans involving genomic mutation or RNA interference for the inhibition of mitochondrial proteins expression [42-44]. Surprisingly, it was found that normal to increased oxidative damage as a result of superoxide dismutase gene knockouts failed to decrease the lifespan of the mutants, as would be predicted by the FRTA. Moreover, it was found that elevated levels of superoxides contributed to remarkable longevity of both C. elegans wild type and mitochondrial respiratory mutants [45, 46]. Therefore it was concluded that molecular damage accumulation due to ROS is not the primary cause of aging.

While life extension studies have been directed at slowing down the biological process to extend the average lifespan [47], it is not well understood if aging occurs in parts, for instance, Is it the aging of molecules? organelles? cells or tissues? or the entire organism? Scientific data collected so far do not resolve the mystery of aging. This bring up the question, Is aging curable? Is there really a treatment? And if yes, Does the

treatment stop the whole process of aging? Or does it only deal with one aspect of it? Despite the claims of some drug companies, a real anti–aging drug has not yet been realized.

The FRTA posits that the main players in the process of aging are the free radicals or oxidation inducing molecules, i.e. reactive oxygen species (ROS). Any type of interference with mitochondrial function affects the mitochondrial production of ROS, considering mitochondria as the main site of ROS. ROS in turn interfere with various cellular processes, causing oxidative damage that impacts aging (Figure 7).

ROS have clearly detected roles in interference with cell signaling and apoptosis through their interaction with lipids, DNA and proteins [48] resulting in a cellular death, Moreover, reaction of macromolecules (lipids, sugars, proteins, and DNA) with ROS generates by products that are sometimes more dangerous than the initial ROS [49]. Therefore an increase in ROS and the simultaneous decrease in antioxidant mechanisms can shift the reduction-oxidant balance toward the oxidation state.

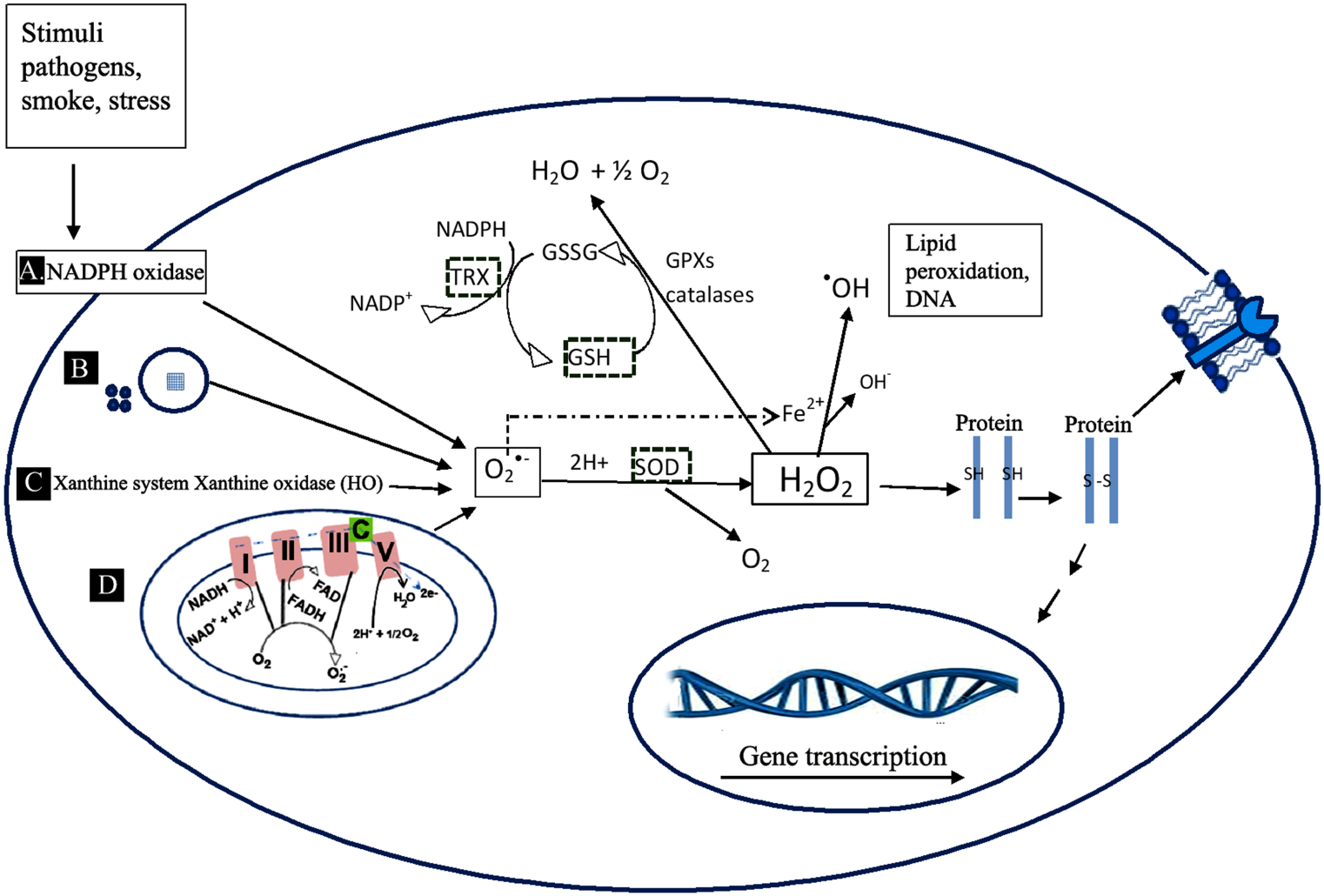

Figure 7. A representative diagram of cellular sources and pathways of ROS.

Superoxide anion results from normal cellular metabolism and physiological process or from exposure to environmental stimulus such as light and smoke. Cellular sources of superoxides, A. NADPH oxidase enzymes, B. Microsomes and Peroxisomes, the later produce H_2O_2 by the function of enzymes such as amino acid oxidase enzymes. C. Xanthine system (xanthine oxidases XO catalyze the reaction of hypoxanthine to xanthine forming superoxide anion and xanthine to uric acid to form hydrogen peroxide). D. Mitochondria as the main source of reactive oxygen species through the electron transport chain (ETC) as well as Cytochrome P450, electron (e-) transfer from NADH and $FADH_2$ through complexes I and II, respectively, and then to complex III. Cytochrome c transfers electrons from complex III to complex IV, which reduces O_2 to form H_2O. Leaking of electrons from complexes I and III generates superoxide. Moreover, electrons are substracted from cytochrome c to produce O_2. Via the ROS redox pathway, superoxide is removed by the dismutation reaction of superoxide dismutases, cytoplasmic Cu/Zn superoxide dismutase (SOD-1) and mitochondrial Mn superoxide dismutase (SOD-2) SOD2 in the matrix to generate hydrogen peroxide. Under stress conditions, superoxides release iron from iron containing enzymes, where ferric ion is reduced to ferrous (Haber-Weiss reaction) as a first step, the second step is the generation of hydroxyl radical ($^{\bullet}OH$) by the Fenton reaction. H_2O_2 is reduced to H_2O by glutathione peroxidase (GPX) using glutathione GSH resulting in an oxidized glutathione (GSSG) which is reduced back to GSH by glutathione reductase. H_2O_2 is a toxic molecule that has been associated with tissue damage in cancer and inflammatory disorderes [50].

Under normal conditions, ROS levels are counteracted by antioxidant system, which is classified into enzymatic antioxidant defense such as superoxide dismutase (SOD), glutathione peroxidase (GPx), catalase, thioredoxin reductase (Trx-Trx) [51-54] (Figure 7) and the non-enzymatic small molecule dietary antioxidants such as thioredoxin (Trx), glutathione, carotenoids, vitamins E (α-tocopherol) and vitamin C (ascorbic acid) [55-57]. Figure 8 shows structures of some antioxidants like N-acetyl cysteine (NAC) and Lipoic acid (LA).

Antioxidants preferably interact with compounds containing functional groups with electron-rich double bonds such as sulfides and phenols that are easily oxidized. The mechanism behind the activity of common antioxidants against free radicals is well known, one mechanism involves the reduction of radicals (**R**·) by the thiol group of sulfur containing antioxidants like N-acetyl cysteine (NAC) and Lipoic acid (LA) [58],

$$\mathbf{R}^{\cdot} + \text{NACSH} \longrightarrow \text{RH} + \text{NACS} \quad (\text{RH= reduced radical})$$

The second mechanism is the donation of the hydrogen atom from phenolic group of non thiol antioxidants, such as ascorbic acid ($AscH_2$) to reduce radical anions, via electron transfer process [59].

$$\mathbf{R}^{\cdot} + \text{AscH} \longrightarrow \text{RH} + \text{Asc}^{\cdot -}$$

Along with the capability to remove radicals, thiol or enzymatic antioxidants have protective role against protein oxidation, the presence of cysteine residues in their active reduce the oxidized protein thiols contributing to an intracellular redox hemostasis.

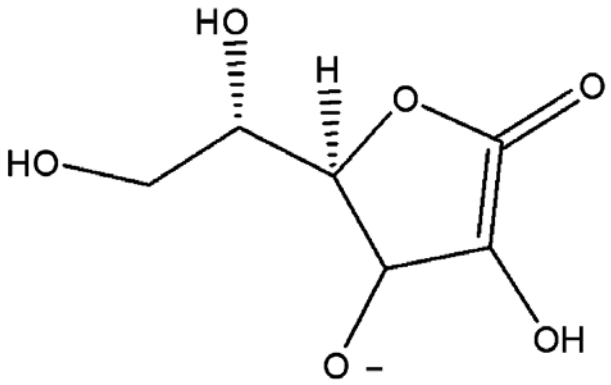

Ascorbic Acid, $C_6H_8O_6$, turns into ascorbate anion $AscH^-$ at pH 7.4

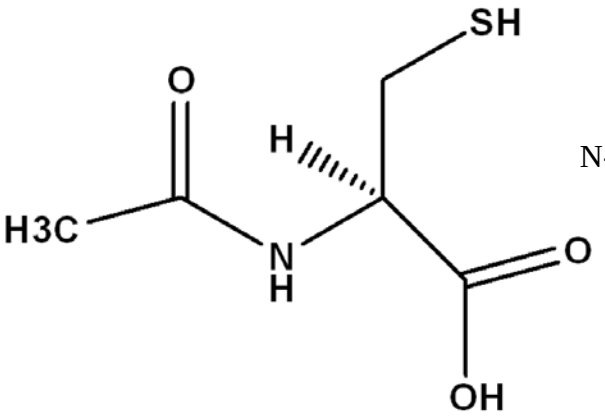

N-acetyl cysteine, NAC, $C_5H_9NO_3S$

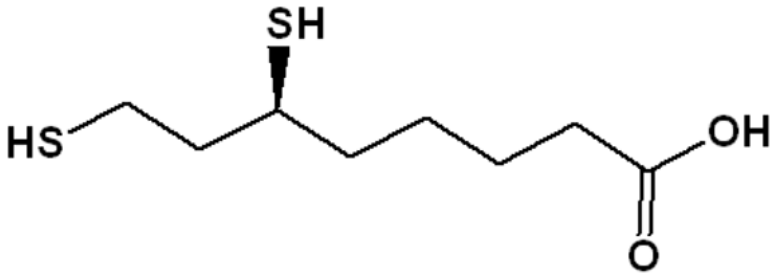

Lipoic Acid, reduced form (Dihydrolipoic acid), $C_8H_{14}O_2S_2$

Figure 8. Structure of common non enzymatic antioxidants. Ascorbic Acid, N- acetyl cysteine, NAC and Lipoic Acid.

Oxidized proteins are more susceptible to proteolysis and an increase in oxidized proteins attacked by ROS might affect certain biochemical functions [60] and decrease cell viability (Figure 9). The cysteine thiol groups involved in protein structures are part of redox signaling in cells [61] (Figure 9). The disulfide bridge RS-SR (oxidized status) formed as a result of redox reaction of cells leads to stabilization of protein structure. Cysteine thiol group can act as a nucleophilic site in many critical sites of the proteins such as active sites; typically, thiol groups of cysteine side chains are the most potent nucleophile of all amino acids. Under the influence of pathophysiological stimuli, thiol RSH is oxidized by hydrogen peroxide to sulfenic acid RS-OH. Cysteine groups on glutathione and thioredoxin are critical for their action as peptide/protein reducing agents and redox modulators.

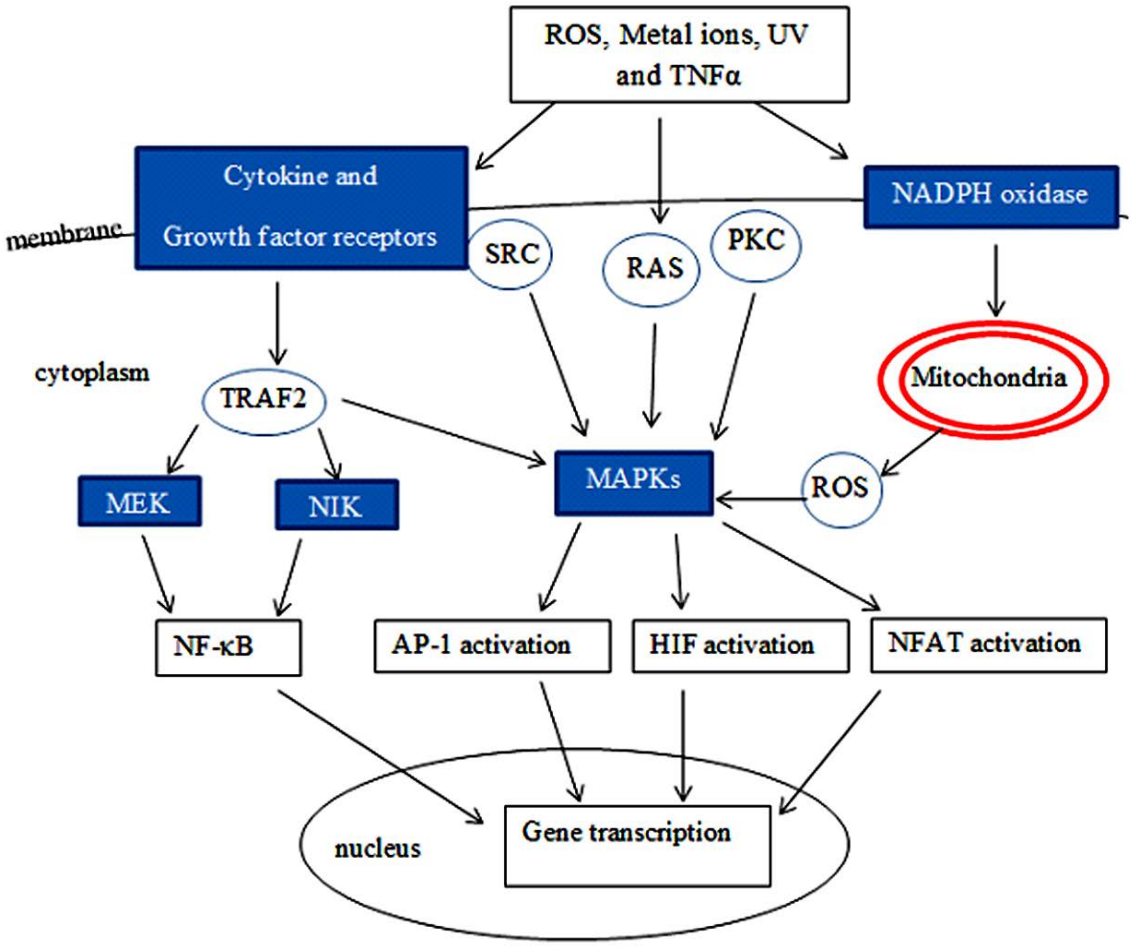

Figure 9. A representative diagram of cellular stimulation by certain factors (ROS, UV and cytokines such as TNFα). The stimulation of cells results in the activation of NIK (NF-κB inducing kinases) and (MAP) mitogen-activated protein (MAP) kinases mediated by c-Jun amino-terminal kinases (JNK) and p38 which are activated by TRAF2 leading to the subsequent activation of transcription factors. This diagram also shows the interference of ROS with protein signaling pathways by oxidization of sulfhydryl groups on protein cysteine residues. Changes in protein structure (Oxidation of thiol groups) leads to the dysregulation of several signaling cascades such as growth factor kinase-, src/Abl kinase-, mitogen-activated protein kinase (MAPK) which activates several redox-regulated transcription factors such as activator protein 1 (AP-1), NF-κB, p53, hypoxia-inducible factor 1 (HIF-1) and nuclear factor AT (NFAT)]. These factors control gene expression involved in DNA repair, cell growth and differentiation and the immune system.

Mechanism of Action of Fullerenes as Free Radical Scavengers

It was not until early 1990s that C_{60} and C_{70} were found to react with free radicals [62, 63] and the fullerene core characterized as being a free radical sponge. The details of the mechanism underlying the protective function of fullerene derivatives remain elusive. The delocalized π double bonds increase the reactivity of C_{60} and allow them to react in different ways. Free radicals can react with C_{60} molecules by direct binding through the delocalized π electrons, via addition to the carbon-carbon double bond [62]. Andrievsky [64] theoretically estimated that a total of 60 radicals can bind to a single pristine C_{60}, based on the fact that one carbon double bond can scavenge two radicals (Figure 10). However, the number of radicals able to react with modified fullerene derivatives having fewer double bonds than pristine C_{60} could be much less,depending on the number and position of the attached chemical groups, and how the latter modify the electronic structure of the molecule.

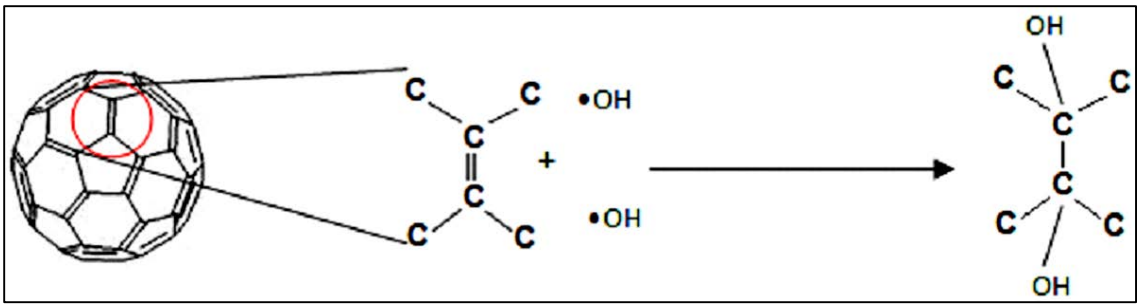

Figure 10. Simplified representation of the net reaction of OH radical with C_{60}. C_{60} core acts as sponge and scavenge free radical by direct binding.

Instead of direct binding of free radicals to C_{60} double bonds, an alternative mechanism of superoxide dismutation was suggested for the SOD-mimetic C_3 carboxylic fullerene [65, 66], although the ability of C_3 to scavenge superooxides was found to be lower than SOD1 and SOD2 (superoxide dismutastion enzymes). C_3 acts as nucleophilic with super delocalizability and was found to fom a complex with $O_2^{\bullet-}$. In fact Liu [67] claimed to be the first to detect the catalytic dismutation activity through $O_2^{\bullet-}$ oxidation within an electron transfer process.

We hypothesized as a result of using FRAP assay (ferric reducing/antioxidant power) and an electron paramagnetic resonance (EPR) spin trapping technique (Rawashdeh et al. 2014) that the existence of conjugated double bonds makes fullerene derivatives a good electron acceptor not donors therefore they act as oxidants rather than reductants. Fullerenes are involved in redox reaction in the cells. Fullerenes go through a reduction-oxidation chain, where the electron transfers from superoxide to fullerene in the first place to result in oxidizing the superoxide into oxygen and reducing fullerene into fullerene anion. The generated fullerene anion donates the extra electron to another superoxide resulting in its being reduced to peroxide ion. This net dismutation of

superoxide by C_3, and related results for other fullerene derivatives, has led researchers to label fullerene derivatives as biological antioxidants. However, they appear to work, at least in part, by an oxidative mechanism:

$$F + O_2^{\bullet -} \rightarrow F^{\bullet -} + O_2 \quad \text{(oxidation)}$$

$$F^{\bullet -} + O_2^{\bullet -} \rightarrow F + O_2^{-2} \quad \text{(reduction)}$$

Based on these results (detailed in chapter 2), water soluble fullerenes can be considered to have redox cycles, analogous to those seen in the redox cycles of other biological antioxidants like glutathione, thioredoxin (Trx) and vitamin C.

The biological activity of fullerene derivatives is due to their unique properties such as; their large surface area: mass ratio, which makes them important as catalysts in chemical reactions; therefore, fullerene derivatives could scavenge intracellular ROS and regulate NF-kappaB activation.

NF-KappaB Signal Transduction Pathway as a Target of Free Radicals

Nuclear factor kappaB (NF-κB) is one critical protein that might be targeted by ROS where the reactive oxygen intermediates have been proposed to be involved in activation of NF-κB [68-71]. It has been proposed that the initial response to inducers is the production of superoxide anion followed by the generation of H_2O_2 [70]. The activation of NF-κB signal transduction pathway (a set of protein reactions that activate

NF-κB, see Figure 11) by ROS mediates pathological disorders such as inflammatory diseases; rheumatoid arthritis and lung diseases [72].

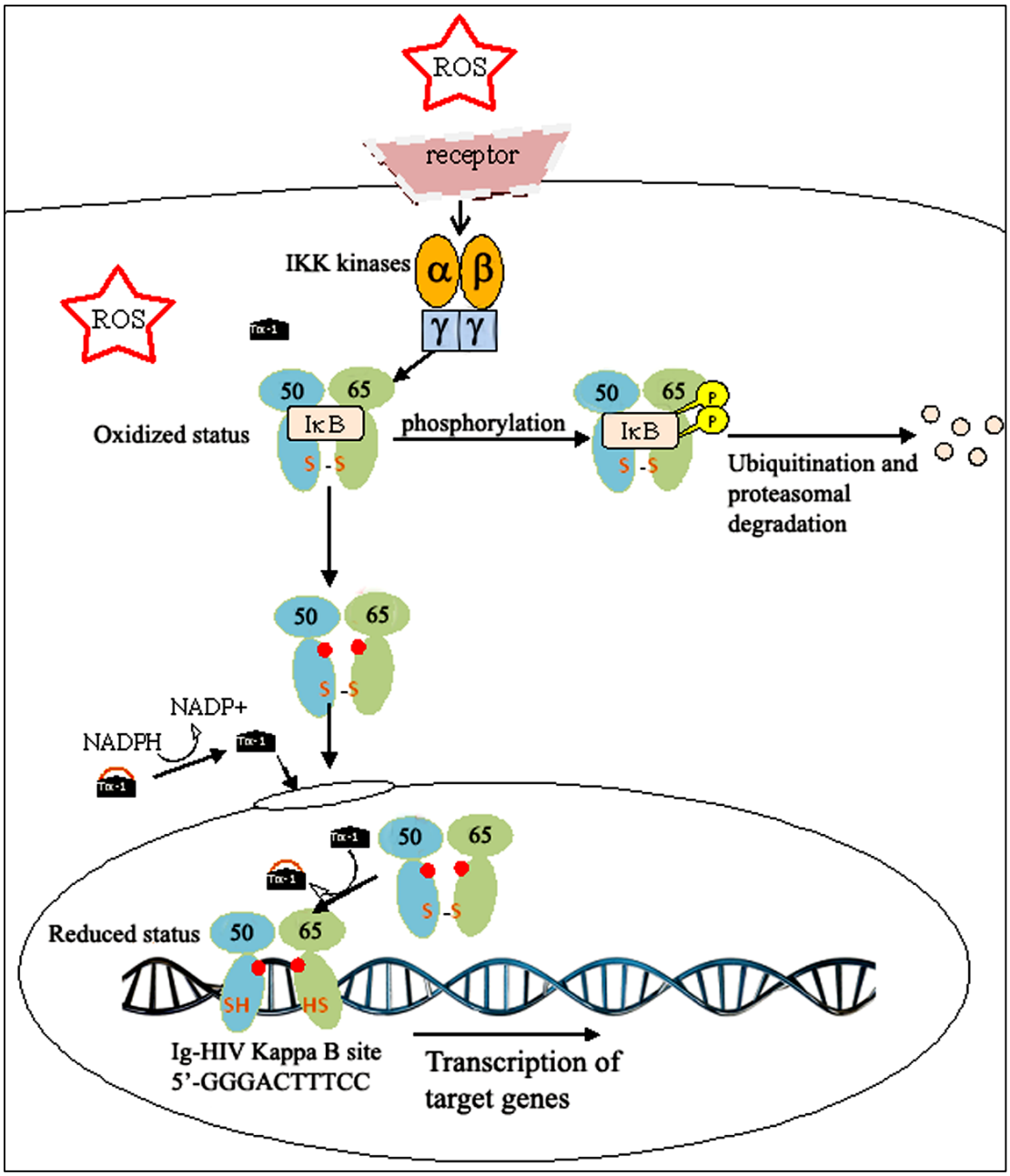

Figure 11. Canonical NF-κB regulation pathway of the heterodimer RelA/P65. Stimuli (such as TNFα, PMA, ROS and smoke) induce the phosphorylation of IKB at Ser32/Ser36 through TRAF2/6–NIK kinase pathway. Phosphorylated IKB undergoes proteosomal degradation releasing NF-κB and allowing it to translocate into the nucleus. Trx-1 reduces NF-κB in nucleus and NADPH reduces the oxidized Trx. NIK is NF-κB inducing kinase. (●) is the nuclear localization signal (NLS) that guides NF-κB translocation into the nucleus. Trx-1 represents an oxidized Trx-1.

This study was inspired by the extensive research that is widely done showing the bio-protective and anti-inflammatory roles of water soluble C_{60} fullerenes. The aim of this research is to study electrochemical and redox properties of water soluble fullerene derivatives; $C_{60}OH_x$, C_3, TGA, TTA and amphiphilic liposomal malonylfullerene ALM and correlate their structure with possible mechanism of interaction with NF-κB and ROS. Evaluation of antioxidant and free radical scavengers properties were done by FRAP and EPR respectively (Chapter 2). Electron paramagnetic resonance (EPR) spectroscopy is a magnetic resonance technique used to detect free radicals.

The activity of NF-κB pathway in the presence of fullerenes was tested by using two plasmids separately, one that has multiple kB sites driving expression of the B-galactosidase reporter gene and the other having p65 tagged to GFP for fluorescence intracellular localization studies (Chapter 3). Fullerene derivatives were kindly provided by Luna nanoWorks (Luna Innovations Inc. VA) as suspensions in ionic solution (phosphate buffer saline, PBS). To our knowledge this study is one of the first to directly study the effects of water soluble fullerenes on NF-κB driven gene expression, and the underlying mechanisms.

CHAPTER II

THE FULLERENE PARADOX: BIOLOGICAL ANTIOXIDANTS WITH LOW INHERENT REDUCING ABILITY

Abstract

Fullerene derivatives have been studied for a wide variety of applications in the physical and life sciences. Their unique combination of spheroidal structure with an extensive conjugated bond network enables electron delocalization and mobility, making them highly suitable for electron transfer applications. This property underlies many applications and activities of fullerene derivatives, e.g., as acceptors moieties for photovoltaics. This is consistent with their high electron affinity, which should make them potential oxidizing agents. Paradoxically, in biological applications, fullerenes have an established reputation as antioxidants, which appears to be based largely upon their ability to scavenge free radicals. We tested 6 different fullerene analogs for their ability to reduce ferric to ferrous iron, a standard test for reducing power (FRAP assay); at concentrations up to 10μM, none had significant activity, as compared to N-acetylcysteine and vitamin C as positive controls. In line with previous reports, we found that the tris-malonate fullerene derivative C_3 was able to scavenge superoxide, as assessed by EPR spectroscopy. Because our results confirm that fullerenes lack direct reducing ability, we conclude that native fullerenes scavenge superoxide radicals initially

by oxidizing them, accepting an electron from superoxide to generate molecular oxygen, along with a reduced fullerene molecule having an extra electron ($F^{\cdot -}$). The latter, a fullerene anion, could function as a direct reducing agent by donating its electron, contributing to the reported antioxidant activities of fullerene derivatives. Finally, we propose a fullerene redox cycle analogous to those of other biological antioxidants like glutathione, thioredoxin and vitamin C.

Introduction

Fullerenes are now routinely produced in useful quantities and studied for engineering applications such as photovoltaics and, increasingly, for biomedical uses. However the later application is restricted by the poor solubility of native fullerenes in water. Pristine C_{60} is a hydrophobic molecule that is best dissolved in organic solvents. Some procedures can be used to enhance their dispersion in aqueous suspension, such as the addition of surfactant [15] long term stirring in water [14] and incorporation into water soluble supramolecular structures such as cyclodextrins [16]. In addition, exohedral chemical functionalization, which involves the covalent attachment of various functional groups (e.g., –OH, NH_2, –COOH) to the fullerene cage, results in the formation of ‘‘functionalized’’ fullerene molecules that are able to establish bonds with water molecules via hydrophilic extensions [22-24, 73].

Research in the field of water soluble fullerene derivatives (e.g. trismalonic acid C_{60}, known as C_3, Table 1) [15] has increased dramatically and many distinguishable biological properties of fullerenes have been exhibited so far, including: neuroprotection [21], protection against excitotoxic stimuli [20], antiapoptotic activity [20, 26], antiviral

activity [22-24], anti-aging effects [74], anti-inflammatory activity [9, 75, 76] and protection against oxidative stress induced by UV radiation [77] iron [78] or peroxides [77, 79]. Indeed, most of these biological activities of fullerene derivatives have been thought to be due to their antioxidant or free radical scavenging activity. Many of these studies hypothesize that antioxidant activity mediates functional biological responses, based upon either the demonstration of free radical scavenging ability, or an endpoint such as a decrease in lipid peroxidation products, or increased cell viability.

Biological antioxidants are important for living systems because they function as a defense mechanism against reactive oxygen species (ROS), the most reactive of which are free radicals such as hydroxyl radical (·OH) and superoxide (O_2·⁻). ROS can be produced during normal cellular processes such as oxidative metabolism, or from exposure to environmental stimuli such as light and smoke. Under normal condition ROS levels are kept in check via natural antioxidants, which can be peptides (e.g. glutathione), proteins (e.g. thioredoxins, glutathione peroxidases and superoxide dismutases) [53, 80-82], or small molecules (dietary antioxidants) including α-lipoic acid, vitamins E, C and carotenoids [55, 57, 83]. ROS have well established roles in interference with processes such as cell signaling and apoptosis through their interaction with lipids, DNA and proteins, which if unchecked by antioxidant defenses can result in cell death and organ failure [84]. An increase in ROS with a concomitant decrease in antioxidant mechanisms can shift the oxidation-reduction balance toward the oxidation state. Oxidized proteins are more susceptible to proteolysis and an increase in oxidized proteins attacked by ROS can affect various biochemical functions. Thus, the possibility that fullerene derivatives

can serve as biological antioxidants or free radical scavengers is of considerable importance for the development of novel therapeutic entities.

A case can be made that most of the applications of fullerenes, both physical and biological, are based primarily upon their electronic properties, and to a lesser extent upon their shape and other aspects. Their unique combination of a spheroidal structure with an extensive conjugated bond network enables electron mobility and partial delocalization, making them highly suitable for electron transfer applications. Physical and computational data suggest that fullerenes are much better electron acceptors than electron donors. The electron affinity of C60 is quite high (2.65 eV) [85], approaching that of the halogens (3-3.6 eV), with energy being released on binding an electron; in contrast, an even greater amount of energy must be expended to remove an electron from C60 (first ionization energy ≈ 7.7 eV) [86]. Hence, fullerenes react primarily as electrophiles, so that much of the chemical functionalization of fullerenes is achieved via nucleophilic additions to the carbon cage, using various reagents. Furthermore, native C_{60} has 60 pi electrons, so that 12 additional electrons would be needed to form a closed shell configuration of 72 electrons, as required for spherical aromaticity by the $2(N+1)^2$ rule [87]; this state is attainable in alkali fullerides such as $K^+_{12}C_{60}{}^{12-}$ [88].

This propensity to accept electrons underlies many applications and activities of fullerene derivatives, e.g., their use as acceptors moieties for photovoltaics [89]. Paradoxically, the biological literature is full of references to fullerenes as antioxidants, although the evidence cited is typically of roles as free radical scavengers. Yet it is rarely if ever noted in such contexts that their avidity for electrons would make it more likely

for a fullerene derivative to be an oxidizing agent than an antioxidant, in the strict chemical sense of an antioxidant as a molecule with reducing ability, i.e., an electron donor. We will explore the hypothesis that the apparent antioxidant and radical scavenging abilities of some fullerenes may arise not from any inherent activity as reducing agents (electron donors), but from their ability to oxidize free radicals (i.e., accept their unpaired electrons), so that they are not direct acting reducing agents. However, oxidation of a free radical or other species by a fullerene can generate an anionic fullerene species ($F^{\bullet -}$), which does have the capacity to act as a reducing agent by giving up its electron(s).

The majority of the reports like those cited above of the "beneficial" effects of fullerenes, involving free radical scavenging and protection against oxidative challenge, have used fullerenes functionalized with hydroxyl or carboxylate-bearing groups, like those shown in Table 1. In contrast, reports that fullerenes can cause oxidative stress and free radical damage [90-93] have generally involved studies of native (unfunctionalized) C_{60} or C_{70}, which are also much less soluble than the functionalized oxygenated fullerenes. This hydrophobicity may target them to cell membranes, which are highly susceptible to oxidant damage. However, it has also been reported that C_{60} incorporated in a water-soluble liposomal preparation showed both free radical scavenging and cytoprotective abilities. These results are hard to reconcile, unless it is simply the solubilization of fullerenes (either by functionalization, and/or by physical means such as liposomes) [94] that promotes their anti-radical anti-oxidative stress profile, and

somehow limits their ability to induce oxidative stress via their inherent potential as oxidizing agents (due to the avidity of the fullerene core for electrons).

To shed light on the question of whether soluble fullerene derivatives are functioning as biological antioxidants due to an inherent ability to act as reducing agents, or indirectly via an anti-radical activity that could involve oxidation of free radicals, we tested the ability of a panel of soluble fullerenes (shown in Table 1) to act as direct reducing agents.

For this purpose, we used the FRAP assay (originally the ferric reducing ability of plasma assay [95] also known as ferric reducing antioxidant power), which is an electron transfer-based assay that is commonly used to test the antioxidant capacity of foods, fruit extracts and dietary supplements. FRAP has been reported to be the most efficient assay in terms of reproducibility, simplicity and rapid performance among different antioxidant assays including ORAC (the oxygen radical absorption capacity), ABTS (2,2-azinobis (3-ethyl-benzothiazoline-6-sulfonic acid) and DPPH (2,2-diphenyl-1-picrylhydrazyl) [96]. Thus it should be an appropriate technique for the assessment of fullerene antioxidant activity. In the FRAP assay, as shown in the equation below, antioxidant (reducing) activity is assessed via the reduction of Fe^{+3} (ferric) ion to Fe^{+2} (ferrous), which at low pH results in the formation of a ferrous-tripyridyltriazine (TPTZ) complex with an intense blue color, having a peak absorption at λ= 593nm [95].

$$Fe^{+3}(TPTZ)_2 \text{ (colorless)} + e^- \rightarrow Fe^{+2}(TPTZ)_2 \text{ (blue)}$$

Note that in the general formulation shown above, the electron is donated by the reducing agent (antioxidant) being tested. The ability to reduce Fe^{+3} to Fe^{+2} would be expected for a typical water-soluble antioxidant [96].

For assessing the free radical scavenging activity of water soluble fullerenes, electropara-magnetic resonance (EPR) spectroscopy has been used in various studies, due to its ability to detect free radical species (see appendix A. for principles of EPR spectroscopy). Because the soluble carboxyfullerene C_3 has been reported to be a functional mimic of superoxide dismutase [65, 67, 74] we focused our EPR studies on that compound, to confirm its ability to scavenge superoxide.

In the current study, we will show that, as expected from the fundamental electronic properties of fullerenes reviewed above, a set of typical water soluble fullerenes (Table 1) including C_3 and $C_{60}OH_x$ show negligible reducing ability in the FRAP assay. Thus, the mechanism underlying their documented free radical scavenging properties (which we confirm for C_3) requires a more nuanced explanation than their labeling as “antioxidants” would suggest.

Table 1. Structures of various water soluble fullerene derivatives

Name	Chemical structure	Molecular weight g/mol
C_{70}-TTA C112 H68 O28	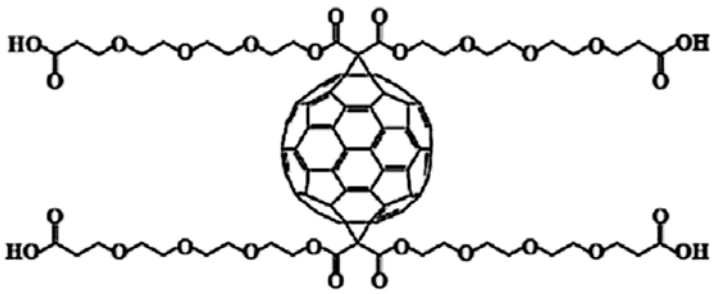	1860
C_{70}-TGA C84 H12 O16	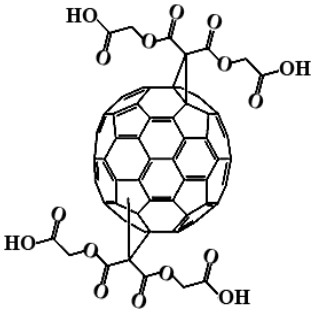	1276
$C_{60}OH_x$ X=~22-29 Hydroxylated fullerene (Fullerenol)	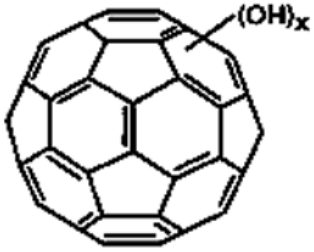	~1146[a]

C_3 Trismalonic acid C_{60}	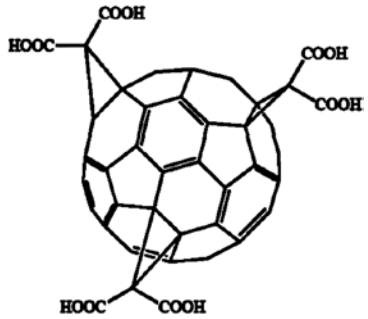	1027
$C_{70}OH_x$ X=~20	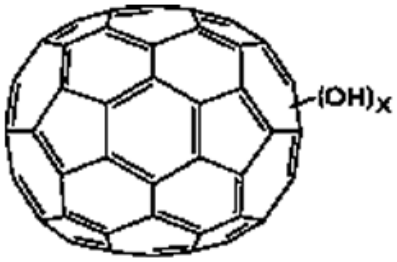	~1181[a]
ALM Amphiphilic liposomal malonylfullerene	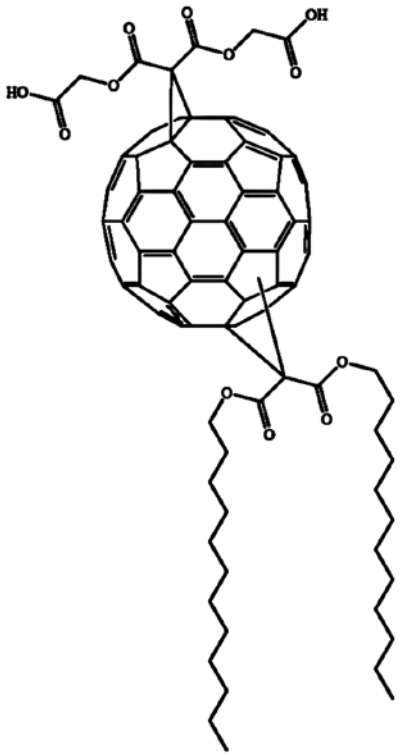	1498

[a]The molecular weight is approximate as the exact number of OH groups is variable (see appendix A, p.134)

Materials and Methods

Fullerene samples. Fullerene derivatives were kindly provided by Luna nanoWorks (Luna Innovations Inc., Danville, VA) as 1 mg/ml solutions or suspensions in ionic solution (Phosphate buffer saline, PBS).

FRAP Assay. The FRAP assay was performed according to Benzie and Strain [95] with some modifications. This involves 3 stock solutions, including a 300 mM acetate buffer, pH 3.6 (3.1 g sodium acetate.$3H_2O$ and 16 ml glacial acetic acid in 1 liter distilled water), which was stored for later use. Fresh solutions of a) 20 mM Ferric chloride and b) 10 mM 2,4,6-tripyridyl-s-triazine (TPTZ, 0.031 g in 10 ml of 40 mM HCL dissolved at 50 °C on a water bath) were prepared at each use. For a single microplate, an adequate volume of the fresh working solution (FRAP reagent) is prepared by mixing 10 ml acetate buffer with 1ml TPTZ solution and 1ml $FeCl_3$ solution. Assays were conducted in 96 well microplates; in individual wells, 11 µl of sample was tested in a total reaction volume of 111 µl (100 µl FRAP reagent + 11 µl sample or PBS for blanks). Absorbance measurements were taken on a BioTek Synergy MX plate reader using Gen5 software version 1.09.8 (BioTek Instruments, Inc., Highland Park, Winooski, VT).

Vitamin C and N-acetyl cysteine (NAC) were used as positive controls in the FRAP assay. Ferrous sulphate was used as the assay standard. FRAP reagent alone was read as background (blank); the average blank absorbance was subtracted from sample absorbance values obtained at 593 nm. Because the fullerene solutions have significant opacity, particularly at high concentrations, they have baseline absorption across the visible spectrum. To correct for this, the blank value was customized for each fullerene

dilution by addition of a value corresponding to the absorbance due to the fullerene alone at that dilution. The latter contribution was determined by mixing 11 μl of each fullerene dilution with 100 μl of distilled water, measuring the absorbance of that solution at 593 nm and subtracting from it the absorbance of 111 μl of distilled water. The resulting number was then added to the blank value for FRAP reagent alone, giving a custom blank value for each fullerene at each concentration tested.

Electron paramagnetic resonance (EPR) spectroscopy. EPR spectroscopy was used to monitor changes in superoxide levels in the presence of fullerene derivatives. As most radical species are difficult to detect because of their short life span, the spin trapping reagent DMPO (5,5-dimethyl-1-pyrolline-N-oxide) is generally used for the detection of radicals; this forms a persistent aminoxyl spin-trapped adduct with a longer life-span. In the presence of DMPO, the adduct DMPO-·OOH is formed from superoxide; detection of this adduct correlates to superoxide levels (Figure 12).

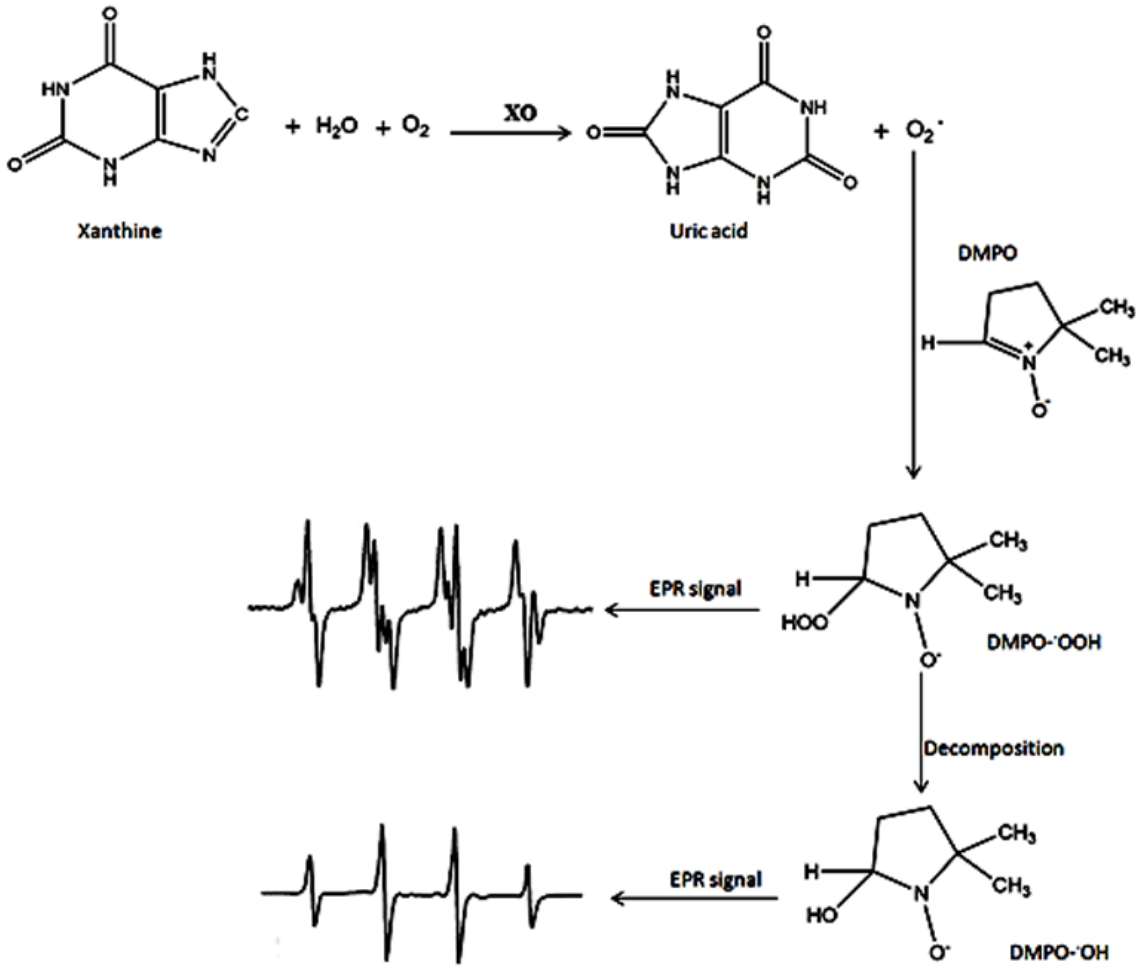

Figure 12. Generation and detection of superoxide radical by electron paramagnetic resonance (EPR) spectroscopy (after Fig. 1, Togashi et al. [3]). Xanthine oxidase (XO) oxidizes xanthine to uric acid and the released electrons react with oxygen molecules forming superoxide ions. The spin trapping reagent DMPO (5,5-dimethyl-1-pyrolline-N-oxide) is used to trap superoxide radicals by forming a DMPO-·OOH adduct. DMPO-·OOH is unstable and decomposes to DMPO-·OH; both have characteristic EPR signals.

Superoxide ($O_2^{\cdot -}$) was generated from the reaction of xanthine/xanthine oxidase at a concentration of 0.5 mM and 50 mU/ml respectively and in the presence of 1mM diethylenetriaminepentaacetic acid (DETAPAC) and 100 mM DMPO in PBS as the control and also in the presence of either 40 or 100 μM of fullerene C_3, or 40 μM ascorbate (vitamin C), as $O_2^{\cdot -}$ scavenging agents (see appendix A, pages;129,130, 131, 132 & 133). EPR spectroscopy was carried out using a Bruker Instruments EMX 10/12 EPR spectrometer equipped with a standard cavity (ER4102ST). Collection of EPR spectra was initiated approximately 3 minutes after the introduction of xanthine oxidase to the sample on ice and transfer to a glass capillary tube with inner diameter of 0.8-0.9 mm. EPR spectra were collected using the following conditions: temperature 296ºK, microwave frequency 9.8GHz, microwave power 20mW, modulation amplitude 1 G and modulation frequency 100 kHz. The total scan time for each spectrum was around 6 minutes.

Results

FRAP Assay. All of the fullerene derivatives shown in Table 1 were tested for ability to reduce Fe^{+3} to Fe^{+2} in the FRAP assay. Of these, TTA, TGA, C_3, C_{70}-OH_x and C_{60}-OH_x were tested at final concentrations up to 20 μM (Figure 13); due to limited quantity, ALM was tested only up to 5μM, at which its FRAP activity was not significant. It is of interest that the absorbance values for ascorbate were approximately double those of the equivalent concentrations of ferrous ion, which is consistent with its ability to provide 2 electrons in becoming fully oxidized to dehydroascorbate, i.e., one molecule of ascorbate can reduce 2 Fe^{+3} ions to Fe^{+2}. In contrast, absorbance readings for NAC are close to

those for the equivalent Fe^{+2} concentrations. FRAP values of all of the fullerenes tested were not significantly different from the corresponding blank values, except at the highest concentration tested, where the values for TTA, C_3 and $C_{60}OH_x$, although quite small, were significant at $p < 0.05$; however, these values are less than 10% of the FRAP value for ascorbate at the same concentration (see appendix A. p. 135; for the color change as a result of reduction). If real, that would suggest that it would take at least 5 fullerene molecules to reduce a single Fe^{+3} ion to Fe^{+2}. It is more likely that the absorbance here is an artifact of the opacity of the fullerene solutions at high concentrations, which our blank correction protocol cannot perfectly correct for. In any case, the results show that, under these assay conditions, the water soluble fullerenes tested are at best extremely weak reducing agents.

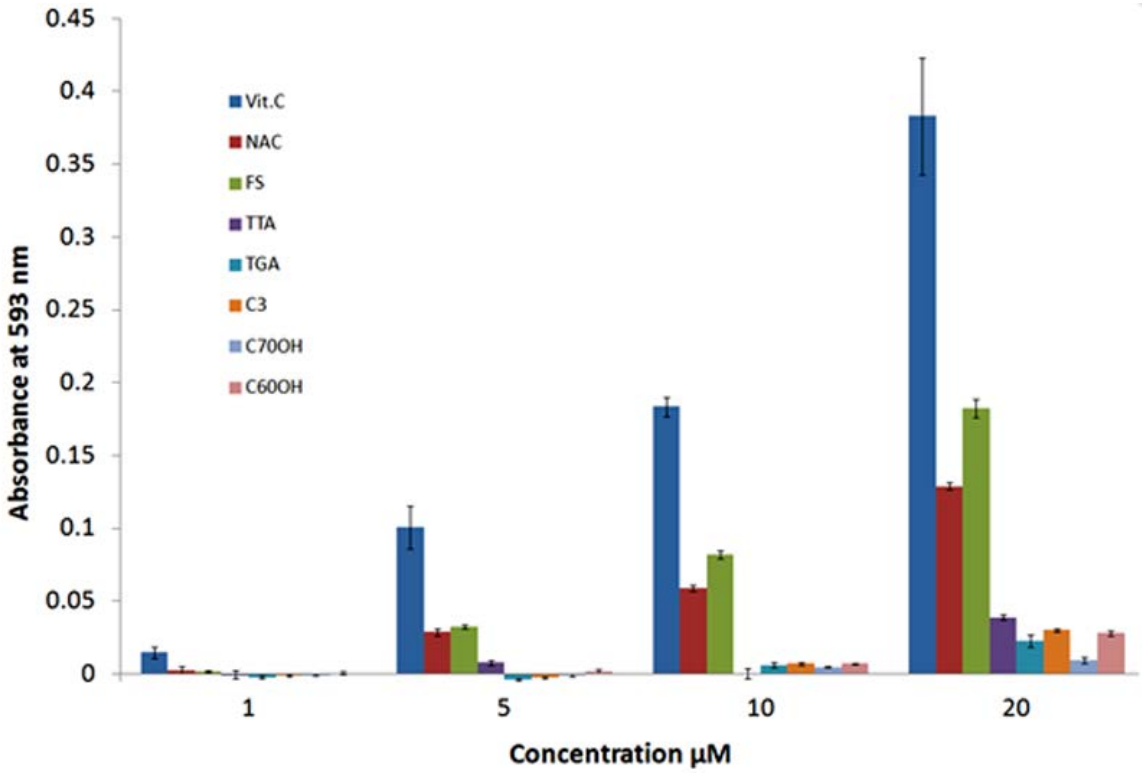

Figure 13. FRAP assay results for soluble FULLERENES as compared to typical thiol (N-acetyl-cysteine, NAC) and non-thiol (ascorbate) ANTIOXIDANTS used as standards. Data are plotted as raw absorbance values after subtracting the blanks (see methods section); these values correlate to the amount of ferrous ion generated by reduction of Fe^{+3}, which relates to the antioxidant power of the tested compounds. Results shown as FS are from the corresponding concentrations of ferrous sulfate, used for calibration. Various fullerenes (TTA, TGA, C_3, C_{70}-OH_x, and C_{60}-OH_x) were tested at final concentrations up to 20 µM; due to limited quantity, ALM was tested only up to 5µM, at which its FRAP activity was not significant. In contrast to the positive controls ascorbate and NAC, the near-zero FRAP values of the fullerene derivatives show that they do not possess sufficient antioxidant power to reduce ferric ion in this assay. The values are the average of three independent experiments, ± S.E.M.

Electron paramagnetic resonance (EPR) spectroscopy. EPR spectroscopy was used in this study to detect the scavenging of superoxide anion radicals by C_3 fullerene. Previous studies have used various concentrations to demonstrate the scavenging capability of water soluble fullerenes. The carboxyfullerene C_3, as one of the most extensively studied fullerene ROS scavengers, was reported to quench ROS signals at 40μM concentration [97]. Based on that result and in an attempt to detect similar activity, 40μM concentration was chosen to evaluate the scavenging activity (for EPR spectra at 40μM concentration of different fullerene derivatives; see appendix A. pages;129, 130, 131, 132 & 133). Some researchers have used higher concentrations of fullerenol and C_3 to detect their ROS quenching capability; for example, a concentration of 100μM was used in study of Dugan et al. to demonstrate ROS quenching of fullerenol [20] and by Yin et al. using carboxyfullerene and fullerenol [98]. We used the xanthine/xanthine oxidase system to generate superoxide, with DMPO as the spin trapping agent. As shown in Figure 14, the superoxide signal was reduced in the presence of C_3 fullerene at 40μM, and nearly eliminated by C_3 at 100μM. However, the ability of fullerenes to quench the superoxide signal is less than that of an equivalent concentration of vitamin C, which eliminated the superoxide signal at 40μM.

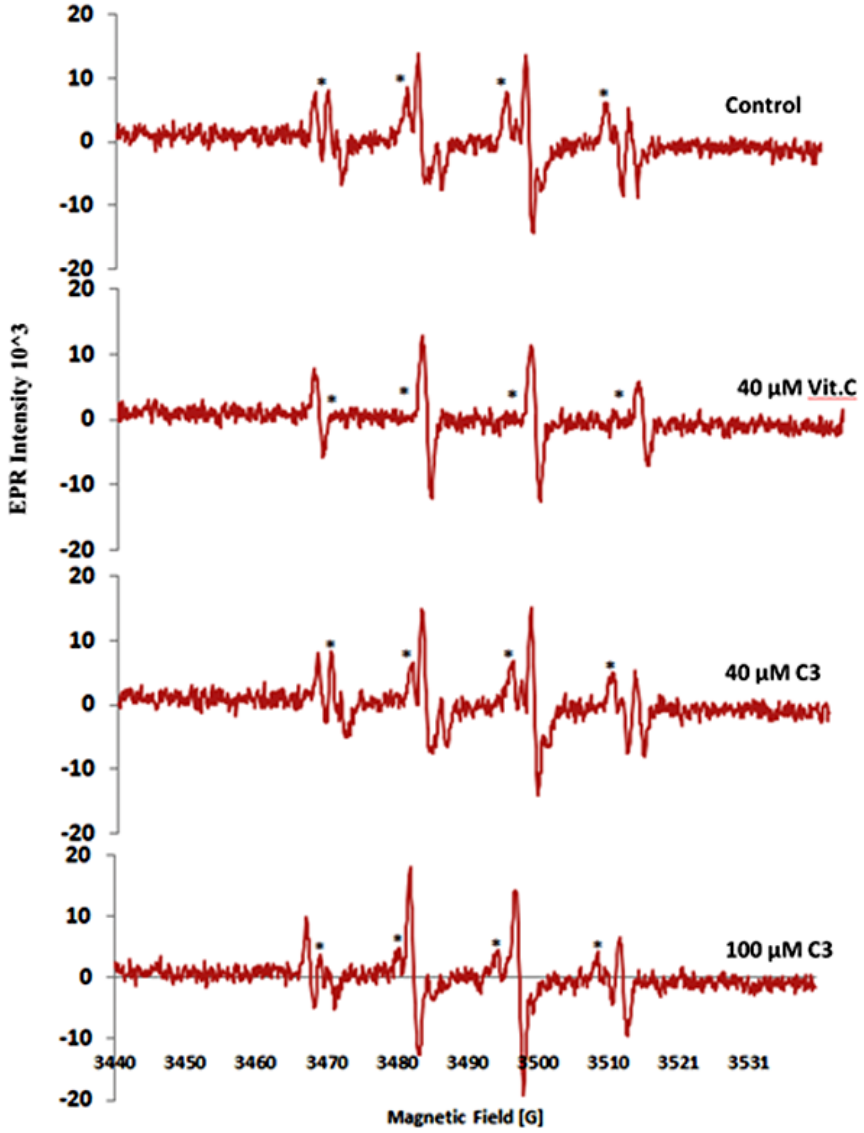

Figure 14. EPR spectra of DMPO-·OOH (superoxide adduct) generated from xanthine/xanthine oxidase in the absence and presence of vitamin C or C_3. Asterisks point to peaks characteristic of superoxide. Collection of the EPR spectra was initiated approximately 3 minutes after the introduction of xanthine oxidase to the samples. The top spectrum represents the control (superoxide generated in the absence of any scavenging agent). The superoxide EPR signal was decreased in a dose-dependent fashion by C_3 fullerene at 40 and 100 µM concentrations. The signal was not detectable in the presence of 40 µM of vitamin C.

Discussion

The 6 water-soluble fullerenes listed in Table 1 ($C_{60}OH_x$, C_3, C_{70}-ALM, $C_{70}OH_x$, TTA and TGA) showed very weak ability, if any, to reduce ferric to ferrous iron in the FRAP assay (Figure 13). This finding is consistent with the known electrochemical properties of the fullerene core reviewed in the Introduction, which suggest it is much more likely to function as an electron acceptor, as opposed to an electron donor, making it less favorable for fullerene derivatives in general to act as reducing agents.

Given the extensive body of evidence that many fullerene derivatives, e.g. hydroxylated and carboxylated analogs, can act as free radical scavengers in both cell-based and cell-free systems, which we have confirmed in the present study in the case of the tris-malonate derivative C_3 (Figure 13), our results strongly support the conclusions of Liu et al.[67] in regard to the mechanism by which carboxy fullerenes act as mimics of superoxide dismutase SOD. As stated by those authors, based on cyclic voltammetry, spectrophotometric, and submillisecond mixing UV/Vis stopped flow measurements, for the carboxy fullerenes studied, "the higher the reduction potential (ability to be reduced by $O_2^{\bullet -}$) the higher the SOD activity.. the electron transfer from $O_2^{\bullet -}$ to the fullerene plays a key role in the overall catalytic dismutation of superoxide"[67] .

Thus, Liu et al. make a compelling case that carboxy fullerenes that act as SOD mimics (including C_3 and closely related compounds such as their structure **V**) do so by oxidizing superoxide radicals in the first case, accepting an electron from superoxide to generate molecular oxygen, along with a reduced fullerene molecule having an extra electron ($F^{\bullet -}$), i.e., a fullerene anion:

$$F + O_2^{\bullet -} \rightarrow F^{\bullet -} + O_2$$

Their results also support the hypothesis that, by donating its extra electron, the fullerene anion generated in the first reaction is able to scavenge a second molecule of $O_2^{\bullet -}$ by reducing it to peroxide ion, regenerating the original native fullerene in the process:

$$F^{\bullet -} + O_2^{\bullet -} \rightarrow F + O_2^{-2}$$

Along with the initial oxidation of $O_2^{\bullet -}$ to O_2, this forms a complete dismutation cycle in which two molecules of $O_2^{\bullet -}$ are converted to O_2 and O_2^{-2} (peroxide) in successive steps [67]. Significantly, this scavenging of the second $O_2^{\bullet -}$ by a fullerene anion is a genuine reduction, so that, to the extent such fullerene anions are available *in situ* as a result of native fullerene molecules oxidizing radicals like superoxide, they would be expected to further contribute to the widely reported free radical scavenging and antioxidant activities of fullerene derivatives.

It is of interest to view these reactions of the native fullerene and fullerene anion with superoxide as part of a redox cycle, analogous to those of other biological antioxidants like glutathione, thioredoxin (Trx) and vitamin C. In such schemes, the redox molecule of interest (e.g. Trx) exists in both oxidized and reduced forms. Figure 15.A shows such a scheme, in which the native or pristine fullerene is shown with an asterisk (F^*), with the reduced form being the fullerene anion ($F^{\bullet -}$). It is notable that, in analogous schemes, e.g. for the redox cycling of Trx shown for comparison in Figure 15.

B, the position occupied by F^* corresponds to the oxidized form of the redox molecule. This suggests that, as we have indicated via (Ox) next to the F^* species, it is appropriate to think of the native fullerene as a (relatively) oxidized form, able to accept electrons as it oxidizes $O_2^{\cdot -}$ [67] and possibly other ROS that are susceptible to scavenging via oxidation.

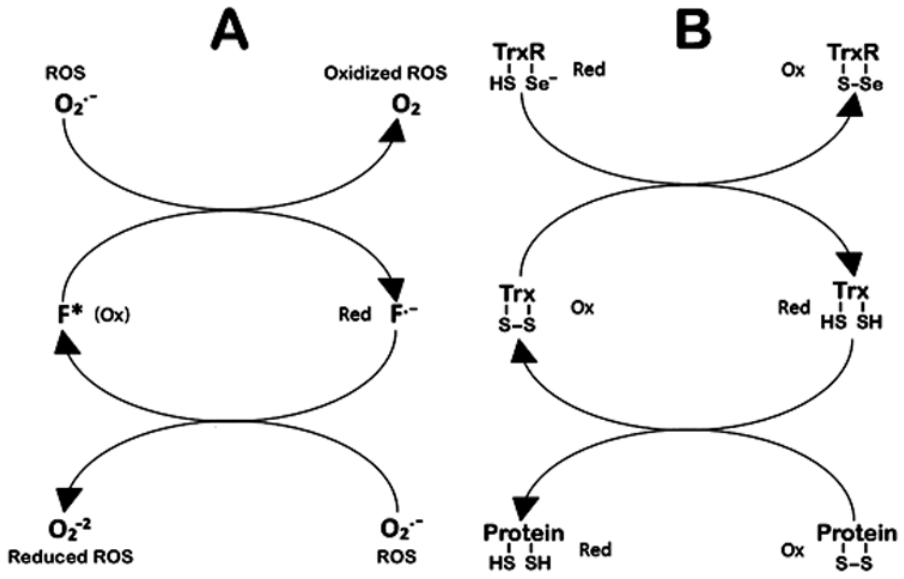

Figure 15. REDOX cycle for A) the reactions of a generic NATIVE fullerene F^* and fullerene ANION $F^{\cdot -}$ with superoxide, compared to B) an analogous scheme for thioredoxin (Trx), a typical thiol reducing agent. In such schemes, the redox molecule of interest exists in both oxidized and reduced forms. In A, the native fullerene is indicated with an asterisk (F^*), with the reduced form, after accepting an electron, being the fullerene anion $F^{\cdot -}$. Note that the position occupied by F^* corresponds to the oxidized form of the redox molecule (i.e. TrxS2 in the middle left of scheme B). As indicated via (Ox) next to the F^* species, this suggests that the native fullerene is acting as a (relatively) oxidized form, able to accept electrons as it oxidizes other species such as $O_2^{\cdot -}$. In contrast, the resulting fullerene anion $F^{\cdot -}$ is able to act as a direct reducing agent by donating its electron, reducing superoxide to peroxide [67] and possibly reducing other ROS as well (lower reaction of scheme A). In scheme B (after Holmgren et al.[80]), TrxR represents Trx reductase.

Of course, the scheme shown in Figure 15.A could also be extended to the left, by showing the loss of an electron by F^* to give an F^+ species, via an interaction with a sufficiently powerful oxidizing agent; in that case, F^* would be the (relatively) reduced form in relation to a more oxidized F^+ state. However, the point is that given the proclivity of the fullerene core to accept electrons rather than donate them, the redox scheme shown in Figure 15.A is likely to be the most relevant for an understanding of the redox behavior of water-soluble oxy- and carboxy-fullerenes and related derivatives

under physiological conditions. So, we conclude that, mechanistically, in living cells a native fullerene F^* is more likely to be acting in the role of an oxidized form (and as an oxidizing agent), in a redox scheme such as 15.A. In this scheme, it is the cognate fullerene anion $F^{\cdot -}$ that, as the reduced form, could act as a direct reducing agent. At the bottom of Figure 15.A, this is shown reducing $O_2^{\cdot -}$ to peroxide ion, but it could also act to directly reduce other ROS, as suggested in the figure.

One other fascinating physical property of solubilized fullerenes relevant to this discussion is that of their color in solution. Martínez et al. [99] have suggested an association between the natural pigmentation of certain compounds and the mechanism of their antiradical activity, which can be achieved by either donating or accepting electrons from the radical species. Their results suggest that the antioxidant vitamins and natural products that neutralize free radicals by reduction (by donating electrons to them) tend to be colorless or yellow, while the carotenoids that are better electron acceptors, and neutralize free radicals by oxidizing them, tend to be red in color. In essence, they propose that "red pigments are better electron acceptors than yellow or colorless substances" [99].

This is of interest in regard to the water soluble fullerenes, some of which (including C_3) tend to be red or reddish brown in solution (Figure 16). C_{60} itself is known for forming purplish or pink solutions in many solvents, and C_{70} solutions are a deep red. Given the data presented here confirming that they are poor reducing agents, and evidence that they scavenge superoxide by oxidizing it [67], the water soluble fullerenes also appear to align with the trend suggested by Martinez et al. We also find considerable

merit in their proposal that the more descriptive term “antiradical” be used instead of “antioxidant” to describe radical scavengers that act as electron acceptors, and therefore scavenge radicals by oxidizing them.

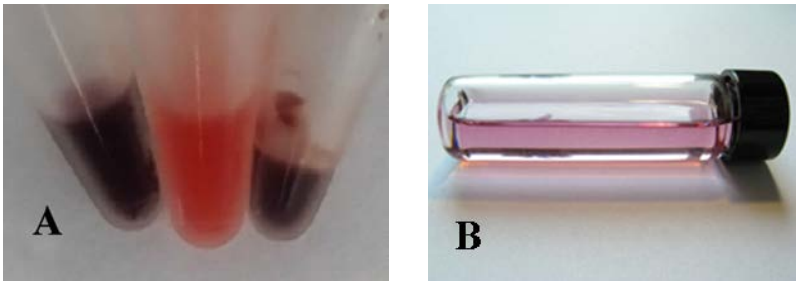

Figure 16. Colors of fullerenes in solution. A. Stock solutions of TTA, C_3 and TGA (left to right), each at 1 mg/ml concentration; all are red or reddish-brown. B. C_{60} in solution in an organic solvent [100].

Conclusions

To our knowledge this study is the first to test the antioxidant properties of fullerenes using the FRAP assay, which is a simple way to assess their ability to donate electrons. Taken together, our FRAP and EPR spectroscopy results show that these compounds are poor reducing agents, yet can be active free radical scavengers. These results emphasize the need to distinguish between antioxidant and antiradical activity, at least, if one hopes to understand the mechanism of action of the molecular species involved, which is critical for rational drug design. The possible need for this distinction may well hinge on the definition of antioxidant, which could be stated so as to leave open the possibility of an indirect antioxidant action such as free radical scavenging, rather than direct reduction of an oxidizable substrate.

Consider one of the more formal attempts to define an antioxidant, by Halliwell and Gutteridge, as “any substance that, when present at low concentrations compared to those of an oxidisable substrate, significantly delays or prevents oxidation of that substrate” [101]. Even this definition fails to distinguish between direct and indirect effects. Does it apply only when the two species are isolated in solution in a cell free system, where a direct reduction is more likely to be required? Or if a molecule blocks lipid peroxidation indirectly by scavenging certain ROS by oxidizing them, thereby limiting free radical chain reactions that underlie the process, does that fall under the definition? Even those eminent authors go on to say that “there may be cases which the definition does not include”, giving an example of the sequestering of metal ions by plasma protein binding. But they express reluctance to broaden the definition to include “any substance that inhibits oxidative damage to a target under the assay conditions being used”, as this would open the door to almost everything being either an antioxidant or a prooxidant [101].

So it is unlikely that the current work will induce a change in the use of the term “antioxidant” to describe the cellular action of various fullerenes that are not really functioning as reducing agents. Fullerenes nonetheless do fall under a broad definition of antioxidant, which could include indirect actions and an overall antioxidant effect on the cellular redox status.

Perhaps more significantly, our analysis of the mechanism of action of fullerenes that show significant “antioxidant” activity raises several important questions that merit further investigation:

1) If these compounds tend to act initially as oxidizing agents, by accepting electrons, why is it that we do not see more evidence of oxidative damage to cells, rather than the opposite? Could there be something about their structure that makes it easy for them to accept electrons from highly reactive free radicals like $O_2^{\bullet -}$, but more difficult for them to oxidize typical biomolecules?

2) If the native fullerenes have sufficient affinity for electrons from various sources (including superoxide), is it possible that the resulting anionic fullerene species $F^{\bullet -}$ (or F^{-n} with n>1) may be present in significant concentrations, such that they could be providing genuine reducing power, further contributing to the predominantly antioxidant effects that have been widely documented in cells? If so, why did their presence not show up as activity in the FRAP assay?

It is of interest that, although the fullerene redox scheme shown in Figure 15.A has been clearly established for superoxide as substrate in both directions [67], not all free radicals could be easily oxidized by loss of an electron, as appears to be the case for the oxidation of $O_2^{\bullet -}$ to O_2 by C_3 and other fullerenes (shown in the upper part of the cycle in Figure 15.A. However, a high turnover of $O_2^{\bullet -}$ to O_2 could generate enough $F^{\bullet -}$ to enable scavenging of other radicals that may only be scavenged by donation of an electron, i.e., reduction (shown in the lower part of the cycle in Figure 15.A. Such an asymmetric redox cycle in regard to preferred substrates could help explain the “net” antioxidant effects of these compounds, i.e., $O_2^{\bullet -}$ may be selectively oxidized to generate reducing equivalents ($F^{\bullet -}$) for the reduction of other ROS species that are not amenable to elimination by oxidation.

Until some of these questions can be answered, the fullerene paradox remains exactly that.

CHAPTER III

SOLUBLE FULLERENES INHIBIT NF-κB DRIVEN GENE EXPRESSION, VIA A MECHANISM OTHER THAN BLOCKADE OF NUCLEAR TRANSLOCATION

Abstract

The transcription factor Nuclear Factor κB (NF-κB) is the terminal effector of the predominant pro-inflammatory signal transduction pathways in animals. The effects of various fullerene derivatives on NF-κB signaling were investigated using cell-based assays, including an NF-κB-driven reporter gene assay, coupled with visualization of nuclear translocation of exogenous (transfected) NF-κB, via an NF-κB-GFP fusion protein expression construct. We report here for the first time direct evidence that some fullerene derivatives (specifically C_3 and $C_{60}OH_x$) are effective inhibitors of NF-κB driven gene expression at micromolar concentrations. However, unlike some antioxidants such as α-lipoic acid, they do not inhibit PMA-induced nuclear translocation of NF-κB, even at high concentration (40 μM). These and other results strongly suggest that fullerene derivatives block NF-κB signaling downstream of the cytosolic activation pathway (the site of action of many antioxidants), possibly inhibiting NF-κB activation at a step penultimate to DNA binding (e.g., the reductive nuclear activation of NF-κB by thioredoxin). For fullerene derivatives to be clinical useful as anti-inflammatory agents, they must have acceptably low toxicity. Using cell proliferation/viability assays and

redox sensitive fluorescent dyes, we found that in living cells, several hydroxy and carboxy fullerene derivatives neither produce ROS nor cause any cytotoxicity, even at high micromolar concentrations. On the other hand, TTA and $C_{60}OH_x$ fullerenes were found to decrease the intensity of tetramethylrhodamine methyl ester live cell staining, implying perturbation of the mitochondrial transmembrane potential. However, this effect is apparently not sufficient to decrease cell viability. Despite this caveat, taken as a whole, our results suggest that fullerenes are a promising class for the development of NF-κB inhibitors.

Introduction

Because of their unique molecular structure that is exclusively made of carbon atoms bonded in fused conjugated rings, fullerenes (C_{60} and C_{70} in particular) and their derivatives are the focus of many studies for elucidation of their properties and potential applications. Many interesting chemical and physical properties have been demonstrated, and significant biological properties are still being discovered.

Fullerene research is advancing by developing their biological applications; several approaches are used to enhance their dispersion in aqueous suspension including exohedral functionalization [17, 19, 67, 102, 103] which is the addition of chemical groups on the surface of the fullerene cage. Those structurally modified fullerenes hold great promises in medical applications including; drug delivery [17] and magnetic resonance imaging MRI [29]. However a particular focus of recent studies has been to determine what researchers tend to describe as potential antioxidant properties of

fullerene derivatives, referring to their in vivo and in vitro biological roles [34, 66, 98, 103-110].

Because of their ability to act as a free radical sponge, fullerenes are able to protect against oxidation- induced molecules, or what are known as reactive oxygen species. Reactive oxygen species (ROS) such as hydroxyl radicals, peroxides and superoxide radicals are produced from several cellular organelles as a result of cellular metabolic reactions. An electron transport chain occurs in mitochondria where electrons move in a stepwise path to reduce an oxygen molecule to form a water molecule; however, cellular dysfunction or injury induced as a result of chemical or environmental stress leads in turn to premature electron leakage to oxygen and therefore oxygen is reduced by fewer electrons, forming superoxide ($O_2^{\bullet -}$) and, subsequently, hydrogen peroxide H_2O_2.

Reactive oxygen species ROS have clearly detected roles in interference with cell signaling and apoptosis as well as causing generalized damage to biomolecules, through their interaction with lipids, DNA and proteins, thereby contributing to chronic diseases [40, 84, 111]. Interestingly it is important to know that many diseases are developed as a result of interference or modulation of cell redox pathways (reduction-oxidation balance) along with modification of various macromolecules [84]. Accordingly, an excess production of ROS as a result of cellular dysfunction or exposure to environmental stimuli such as light and smoke, coupled with the simultaneous decrease in antioxidant mechanisms, can shift the redox balance toward the oxidation state responsible for the

eventual development of many disorders such as cancer, cardiovascular diseases, and aging.

Natural oxidative system like NADPH oxidase, mitochondria respiratory chain, xanthine-xanthine oxidase system generate reactive oxygen species in cells; superoxide ($O_2^{\bullet -}$), hydroxyl radical ($^{\bullet}OH$) and hydrogen peroxide (H_2O_2). However our bodies neutralize or detoxify ROS by antioxidant systems such as superoxide dismutase (SOD), glutathione (GSH) and glutathione peroxidase (GPx) [53, 112-115]. The protective role of these protein or peptide antioxidants against protein oxidation is due to the presence of cysteine thiol residues in their active sites that reduce the oxidized protein disulfides by thiol exchange, contributing to an intracellular redox hemostasis [53, 54, 116-118].

Oxidized proteins are more susceptible to proteolysis and an increase in oxidized proteins produced by ROS might affect certain biochemical functions. Nuclear factor κB (NF-κB) is the terminal effector of the predominant pro-inflammatory signal transduction pathways in animals. NF-κB is a redox-regulated transcription factor found essentially in all cell types. NF-κB signal transduction can be activated by various noxious stimuli, including ROS, as well as pro-inflammatory cytokines, TNF and interleukins (IL-1, IL-2), pathogen-associated molecules like lipopolysaccharide (LPS), H_2O_2 and T-cell receptor induction [68-71]. ROS may thereby mediate changes in gene expression leading to interference with the nucleolus redox signaling [51, 119]. By binding to DNA, specifically to a sequence called a κB site (immunoglobulin kappa light-chain enhancer) [120], NF-κB controls the expression of an exceptionally large number of genes responsible for immune activation and inflammation, including cytokines, growth factors,

extracellular matrix protein, immune receptors, TNF-receptors (TNFR) and T-cell receptors [68]. Furthermore NF-κB, specifically its p65 subunit, plays an important role in apoptosis and cellular proliferation [121]. NF-κB is localized in the cytosol in an inactive form, as a result of binding to an inhibitor, a protein complex known as IκB. Stimulators regulate its activity by two pathways [122]; the canonical pathway is the classical NF-κB activation pathway that is stimulated by signals emanating from several cytokine receptors: TNF-receptors, interleukin (IL-1, IL-2) receptors, antigen receptors and pattern-recognition receptors, including most of the Toll-like receptors. Stimulation of NF-κB involves the disruption of NF-κB/IκB complex by IκB degradation. IκB kinase (IKK) phosphorylates IκB, consequently initiating its ubiquitination and proteasomal degradation. The IKK complex consists of IKKα, IKKβ, and IKKγ as the regulatory subunit (NEMO). This well elucidated signal transduction pathway activates p50/65 and p60/Rel-c heterodimers [123]. In contrast to canonical activation that is mediated by IKKβ- and NEMO- dependent manner, the non-canonical pathway depends on IKKα phosphorylation of p100, leading to proteasomal degradation of its C-terminus to generate p52, which forms transcriptionally active p52/RelB heterodimers of NF-κB [124]. The noncanonical pathway is triggered by certain TNF family cytokines, such as CD40L and lymphotoxin-β (LT-β).

Notably, fullerene derivatives have attracted considerable interest as potential therapeutic drugs for treatment of diseases resulting from redox imbalance. Examples include: poly hydroxylated fullerenes known as fullerols or fullerenols (e.g. $C_{60}OH_x$) [34, 108, 110, 125] which were shown to inhibit the production of angiogenesis factors, and

metastasis. $C_{60}(OH)_{24}$ was reported to inhibit carcinogenesis, malignant growth and doxarubicin induced cytotoxicity. Moreover, $C_{60}(OH)_{24}$ showed anti-genotoxic effects against anticancer drug-induced DNA damage, as well as a tissue-protective effect in irradiated cells. Likewise, carboxylated C_{60} fullerenes showed anti-apoptotic and neuroprotection activity [65, 74].

The redox properties of fullerenes can be predicted from their electrochemical structure. Their extensive conjugated double bonds and the delocalized LUMO with high electron affinity (2.683 eV for C_{60} and 2.765 eV for C_{70}) make them function exceptionally well as electron acceptors. They tend to be electrophiles, accepting electrons from nucleophiles; consequently, fullerenes can be considered as potential oxidizing agents. A recent study made by our group involved the use of the FRAP assay (ferric reducing/antioxidant power) and an electron paramagnetic resonance (EPR) spin trapping technique for the elucidation of fullerene redox properties; results showed that fullerenes are poor reducing agents, suggesting the need for a reformulation of fullerene redox properties [126]. The ability to oxidize free radicals may be the basis of their activity as free radical scavengers, yielding a next antioxidant effect in cells. Therefore native fullerenes (prior to accepting additional electrons) are mostly likely not reductants or antioxidants, but are still able to function as free radical sponges via oxidation. However, the fullerene radical anion ($F^{\cdot -}$) formed by oxidizing a free radical (by accepting its unpaired electron) could then function as a direct reducing agent by donating its electron. Together these factors (oxidative radical scavenging, and the reducing ability of the fullerene anions so generated) are probably the basis of the

apparent antioxidant activity of fullerene derivatives reported by many previous investigators.

The current study was designed to investigate our hypothesis that fullerenes could act as anti-inflammatory agents by inhibition of the NF-κB signal transduction pathway. The aim of this research is to investigate NF-κB signaling and redox responses in MDCK cells after exposure to different fullerene derivatives (see Table 1 p. 32) and the possible mechanism of interaction of fullerene derivatives with NF-κB and cellular redox status.

Studies of the mechanisms by which fullerene analogs are able to inhibit NF-κB driven gene expression involved examination of steps along the NF-κB signaling pathway, particularly the nuclear translocation of NF-κB, which is known to be enhanced by oxidative stimuli and increased ROS levels. Thus, by using an engineered conjugate of NF-κB with a fluorescent protein (GFP), the ability of NF-κB to enter the nucleus was assessed with and without the presence of the fullerenes.

Materials and Methods

Fullerene preparation. Fullerene samples were obtained as suspension in phosphate buffer saline PBS, from Luna Innovations, Inc. Samples was kept at 4°C when not in use. A different batch of hydroxylated fullerene was obtained from a commercial source in a powder form: $C_{60}(OH)_{24}$ (41182-MB 65-01-01, Alfa Aesar, A Johnson Matthey Company, Ward Hill, MA). The sample was dissolved in 1X PBS with long stirring for 24-48 hours.

Cell Culture. MDCK (Madin-Darby canine kidney) cells (American Type Cell Culture ATCC, Catalog No. CCL-34, CCL-34) were grown under 5% CO_2 at 37 °C, in Dulbecco's Modification of Eagle's Medium, DMEM, 1X (4.5 g/L glucose & sodium pyruvate without L-glutamine & phenol red) (cat.# 17-205-CV, Cellgro, Mediatech, Inc, Manassas, VA). This media was supplemented with 2 mM of L-Glutamine 200mM (100x) solution (Hyclone), 0.1 mM non-essential amino acid solution 100x (Sigma M7145) and 10% Fetal Bovine Serum. Cells used in the assays were at a passage number less than 20 (see appendix B).

Cell Cytotoxicity. Cytotoxicity of water soluble fullerenes was tested at different concentrations against MDCK. The MTT and MTS proliferation assays were used (see appendix B, p. 141). MTT is reduced by certain enzymes and converted from yellow tetrazole (3-(4,5-dimethylthiazol-2-yl)-2,5-diphenyltetrazolium bromide) to insoluble purple formazan in living cells; dimethyl sulfoxide DMO is added to dissolve the insoluble purple formazan product into a colored solution. Using a spectrometer, the colored solution can be detected at an absorbance at 500-600 nm. MTS (CellTiter 96® AQ_{ueous} one solution reagent, Promega) cell proliferation assay is composed of solutions of a novel tetrazolium compound [3-(4,5-dimethylthiazol-2-yl)-5-(3-carboxymethoxyphenyl)-2-(4-sulfophenyl)-2H-tetrazolium] in the presence of the electron coupling reagent, phenazine methosulfate (PMS). The MTS assay is similar to the MTT, but it uses one solution instead of two. MTS creates a water soluble reaction product, thereby eliminating the DMSO solubilization step required with MTT. MTS is

reduced by intracellular metabolic enzymes into a soluble formazan product that can be detected at absorbance at 490-500 nm.

Cells were seeded at a density of 2.0 x 10^5 cells/ml per well in a 96 well plate and incubated for 24 hours at 37 °C in 5% CO_2. Cells were exposed to various concentrations of fullerene derivatives; for the MTT assay, a range of concentration of 0.003, 0.03, 0.39, 0.79, 4.69 and 8.6 µM of ALM, $C_{60}OH_x$ and C_3 were tested while for MTS a range of concentrations: 1, 10, 40 and 100 µM of $C_{60}OH_x$, TGA, TTA and C_3 were tested. T-Butyl hydrogen peroxide (TBHP) was used as a positive control.

Measurement of NF-κB inhibition in 5KBpHIVLacZ transfected cells by β-galactosidase reporter gene activity. Cells were transfected with a modified version of the plasmid pHIVlacZ which was obtained from NIH AIDS Research & Reference Reagent program (Cat# 151) and subsequently engineered by the insertion of additional copies of the κB site (5'-GGGGACTTTCC-3') into LTR sequence, for a total of 5 κB sites in the final construct pHIV-5κB-LacZ, to maximize cellular response to NF-κB [127] (see appendix C. p.144). Potential inhibitory activity of the three water soluble fullerenes; $C_{60}OH_x$, C_3 and ALM against the HIV 3'LTR promoter activity was studied by the transfection of MDCK cells with pHIV-κB-LacZ using 96 well plates. MDCK cells with 50-70% confluency were tryptinized at 37 °C and 5% CO_2 for 30 minutes, then resuspended in DMEM and seeded onto 96 well plates at a density of 2.0 x10^4 cells/well. After 24 hours further incubation at 37 °C and 5% CO_2, the cells were transfected using 0.22 µg DNA and 0.5 µl lipofectamine for each well, at a ratio of 1:2.3 plasmid DNA and lipofectamine 2000, diluted in OptiMEM medium. The DNA and Lipofectamine were

mixed together and allowed to stand for 20 minutes at room temperature before addition to the micro-plates. After one hour of transfection, a range of different concentrations of fullerenes (8.6×10^{-6}, 4.69×10^{-6}, 7.85×10^{-7}, 3.9×10^{-7}, 2.74×10^{-8} and 3.04×10^{-9} M) were added to cells. Phorbol myristic acid (PMA) was added at a concentration of 300 nM after 3 hours to stimulate transfection (2 hours after the addition of fullerenes) (see appendix C, p.146 for more details).

Enhanced β-Galactosidase Assay Kit (genlatis A10100K) uses the chromogenic substrate chlorophenol red-β-D-galactopyranoside (CPRG). The expression of β-galactosidase (β-gal) is measured by its cleavage of CPRG subsequently resulting in production of chlorophenol red, which is measured by colorimetric assay using a standard 96 well plate reader. The assay was done following the manufacture instructions and absorbance was read at 575 nm with a microtiter spectrophotometer (see appendix C, p.147).

A visual intracellular localization study for the determination of fullerene effects on PMA induced NF-κB nuclear translocation. MDCK cells were transfected with GFP-RelA obtained from Addgene. Cells were seeded in 96 well plates at a concentration of 2.0×10^5 cells/ml, after 24 hours of incubation, cells were transfected with GFP-RelA. Transfection was done using 0.22 µg DNA and 0.5 µl lipofectamine 2000 (Invitrogen 11668-019) for each well, at a ratio of 1: 2.3 of plasmid DNA and lipofectamine 2000, diluted in OptiMEM medium. The DNA and Lipofectamine were mixed together and allowed to stand for 20 minutes at room temperature before the addition to plates. After 24 hours of transfection, cells were treated with fullerenes at a final concentration of 40

μM. Nuclear transfection was induced after 24 hours of fullerene treatment by using Phorbol 12-myristate 13-acetate, PMA (Sigma, P1585-1MG, $C_{36}H_{50}O$ MW: 616.83).

Determination of mitochondrial membrane potential (ΔΨm) and ROS level. The fluorescent dye TMRE (Tetramethylrhodamine ethyl ester perchlorate, Sigma, 87917-25MG, LOT # BCBK3586V) was used for the detection of mitochondrial membrane potential. (ΔΨm). MDCK cells were seeded at a density of $2x10^5$cells/ml in four chambers cell dish, after 24 hours incubation, cells were labeled with 100 nM of TMRE for 5-10 minutes followed by incubation for 90 minutes with the absence (control) or presence of 40 μM of the following; $C_{60}OH_x$, NAC and TTA at 37 °C in 5% CO_2. FCCP [carbonyl cyanide 4-(trifluoromethoxy)phenylhydrazone]) was used at 1 μM concentration as an inhibitor of the mitochondria functionality which is demonstrated by a reduction in TMRE fluorescence. After washing, cells were immediately observed by confocal microscope with an acquisition at red channel to visualize TMRE fluorescent changes. A change in TMRE intensity is proportional to a change in the mitochondria membrane potential (ΔΨm).

Reactive oxygen species (ROS) formation was analyzed by measuring the conversion of the non-fluorescent dye H2DCFDA (2',7'- Dichlorofluoresceine, $C_{24}H_{16}C_{12}O_7$ Sigma, D6883-50MG, LOT# 092M4004V, CAS: 4091-99-0) to the highly fluorescent 2,7-dichlorofluorescein (DCF) upon oxidization by radicals. MDCK cells were seeded at a density of $2x10^5$cells/ml in 96 well black plates. After 24 hours, cells were loaded with 5μM H2DCFDA for 10 minutes. Thereafter, cells were treated with 40 or 100 μM of TBHP, NAC and fullerenes ($C_{60}OH_x$, TGA, TTA and C_3). TBHP was used

as positive control for ROS production at 40 and 100 µM. The fluorescent DCF was measured spectroscopically after 90 minutes incubation with fullerenes at 480/529 nm. The protective role of fullerenes against TBHP toxicity was studied by incubating cells with fullerenes 24 hours before TBHP treatment.

Western blot analysis of NF-κB activity. For the analysis of NF-κB activation, cells were seeded at a density of 3 $x10^5$ cells/ml for each well in a 6 well plate and incubated for 24 hours at 37 °C, thereafter 40 µM of $C_{60}OH_x$ was added and after 24 hours of incubation, PMA was added to induce nuclear translocation at a concentration of 25 µM. After 5 hours of incubation, cells were lysed using NF-κB extraction kit (NFKB-2, Fivephoton biochemical, San Diego, California). Cell lysates were fractionated by 4–20% SDS-PAGE gel (mini- Protean TGX, Bio-Rad. Cat. 456-1093), 30 µl of protein was loaded on and the gel was run for 15 minutes at 300 volts. The gel was subsequently transferred onto a nitrocellulose membrane using Trans-Blot Turbo Transfer system. Primary antibody P65 (No. p65Ab, Rab IgG, Lot 388, Fivephoton Biochemicals) was used at a dilution of 1:400 and Secondary antibody Goat Anti – Rab IgG- HRP was used at 1:3000. Proteins were detected by an enhanced chemiluminescence (ECL) reagent using a commercial kit (see appendix C, p.149 for more details).

Results

Cell Cytotoxicity. Our study showed the biocompatibility of different fullerene derivatives, there was no cytotoxic effect observed using either the MTT or MTS cell proliferation assays (Figures 17 & 18). There was no inhibition of cell growth or

induction of morphological changes compared to the untreated cells at any tested concentration.

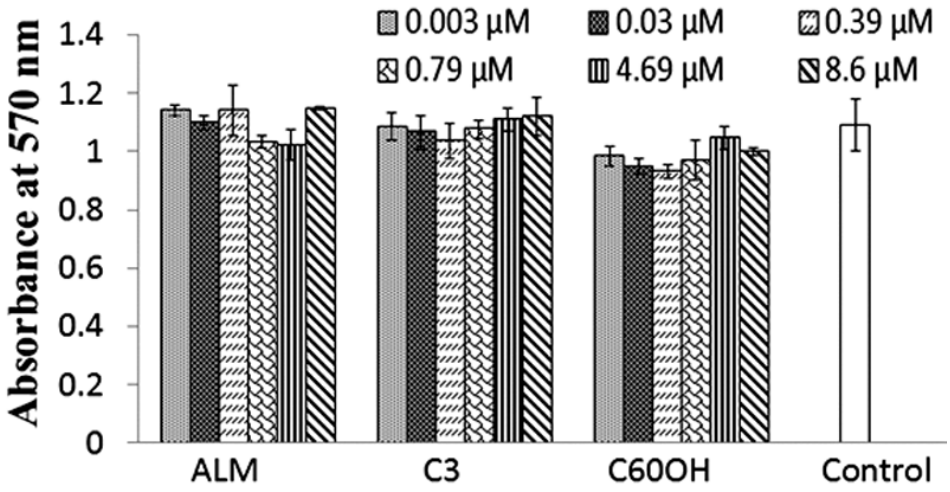

Figure 17. The colorimetric MTT proliferation assay was used to test cell viability after incubation with $C_{60}OH_x$, C_3 and ALM. MDCK Cells were seeded at a density of 2.0 $x10^5$ cells/ml in a 96 well plate and incubated for 24 hours at 37 °C in 5% CO_2. Cells were further incubated at the absence (control) or presence of various concentrations of fullerene derivatives, 0.003, 0.03, 0.39, 0.79, 4.69 and 8.6 µM of ALM, $C_{60}OH_x$ and C_3. The resulted colored solution was detected at 570 nm using a spectrometer. The absorbance values represent the mean of four readings and the corresponding standard errors of the means (s.e.m.). T-test was conducted and there were no significant differences between the means.

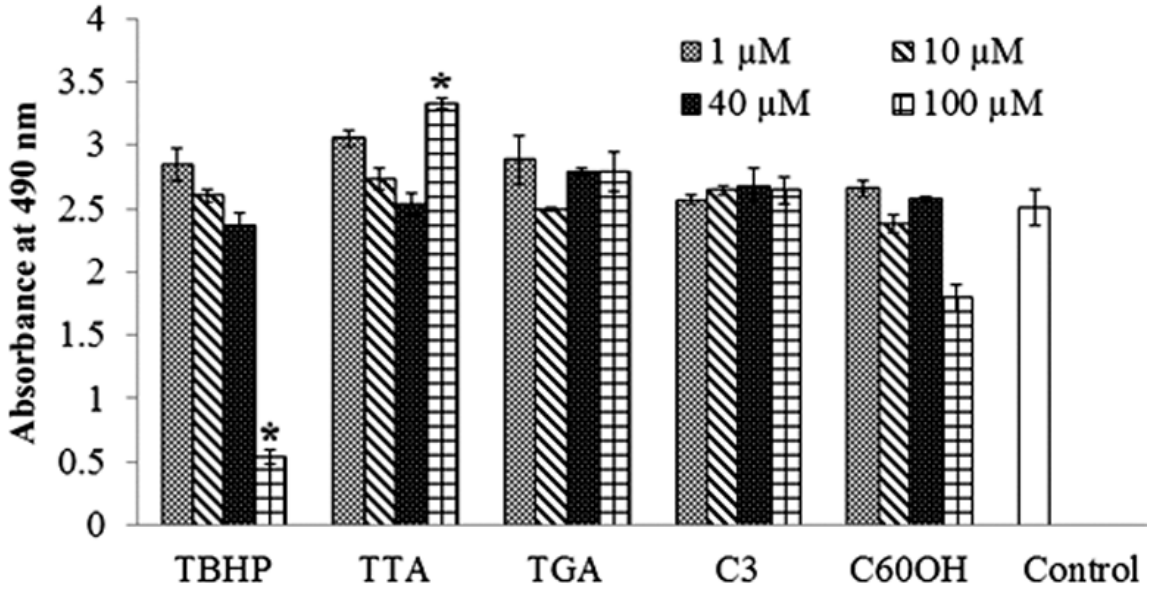

Figure 18. The colorimetric MTS proliferation assay (CellTiter 96®AQ_{ueous} one solution reagent) was used to test the viability of cells incubated with water soluble FULLERENES. MDCK cells were seeded at a density of 2.0 x 10^5 cells/ml in 96 well plates and incubated for 24 hours at 37 °C in 5% CO_2, cells were incubated for further 24 hours at the absence (control) or presence of various concentrations of fullerene derivatives; 1, 10, 40 and 100 µM of $C_{60}OH_x$, TGA, TTA and C_3. TBHP was used as positive control. The resulted colored solution was detected at 490 nm using a spectrometer. The absorbance values represent the mean of four readings and the corresponding standard errors of the means (s.e.m.). T-test was conducted and there was a significant reduction in cell growth in the case of 100 µM TBHP. TTA at 100 µM concentration resulted in a significant increase in cell growth.

Measurement of NF-κB inhibition in 5KBpHIVLacZ transfected cells by β-galactosidase reporter gene activity. NF-κB activity assay was plotted as log values of fullerene concentrations (x axis) versus absorbance (relative β-gal activity) as % of control. Fullerol ($C_{60}OH_x$) and C_3 inhibited the activity of NF-κB at concentration 8.6 μM (Figure 19) supporting their role as a free radical sponge. The sigmoid curve (dose response curve) shows that low concentrations of fullerol increased the NF-κB response above 100%. It should be noted that the observed inhibitory effect was recorded for fullerol and C_3, while ALM showed no inhibitory reaction. The inhibition of the expression of genes under the regulation of NF-κB suggested that fullerenes suppress signaling downstream, penultimate to the DNA binding step.

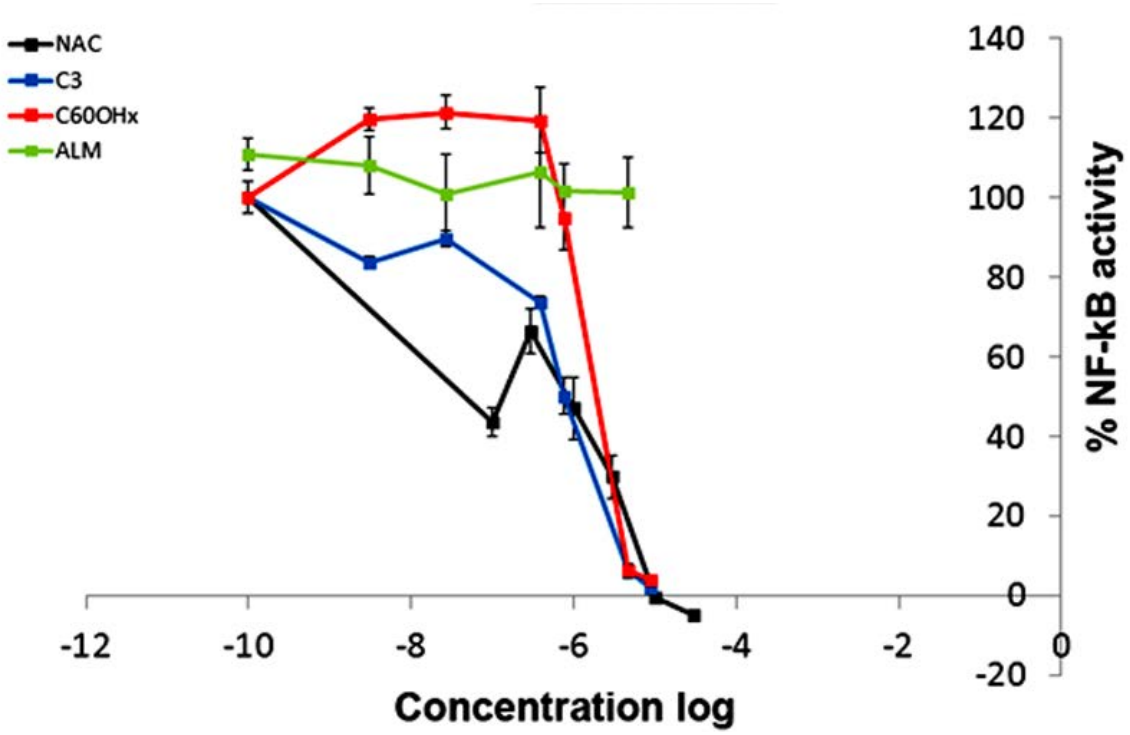

Figure 19. The curve (log-dose response curve, sigmoidal in shape) shows the INHIBITORY effect of $C_{60}OH_x$, C_3 and ALM on the activity of NF-κB. The following concentrations were tested; 8.6 $x10^{-6}$, 4.69 $x10^{-6}$, 7.85 $x10^{-7}$, 3.9 $x10^{-7}$, 2.74 $x10^{-8}$ and 3.04 $x10^{-9}$ M. High concentrations (8.6 $x10^{-6}$ and 4.69 $x10^{-6}$) of $C_{60}OH_x$ and C_3 resulted almost in a complete inhibition. Low concentrations of $C_{60}OH_x$ (3.9 $x10^{-7}$, 2.74 $x10^{-8}$ and 3.04 $x10^{-9}$ M) increased the NF-κB response (Hormesis). The absorbance as % of the control values represents the mean of four readings and the corresponding standard errors of the means (s.e.m.).

A visual intracellular localization study for the determination of fullerene effects on PMA induced NF-κB nuclear translocation. For visualizing the translocation of NF-κB from the cytosol to nucleus, a GFP-p65 construct was used for the transfection of cells and its localization in the cells was monitored by fluorescence microscopy. In PMA stimulated cells, the expressed p65 was translocated to the nucleus within three hours (Figure 20.A), TBHP induced NF-κB translocation as well (Figure 20.B). The presence of antioxidant NAC (Figure 20.C) did not inhibit the translocation whereas antioxidant LA did (Figure 20.D). Fullerene derivatives did not inhibit NF-κB translocation (Figure 21).

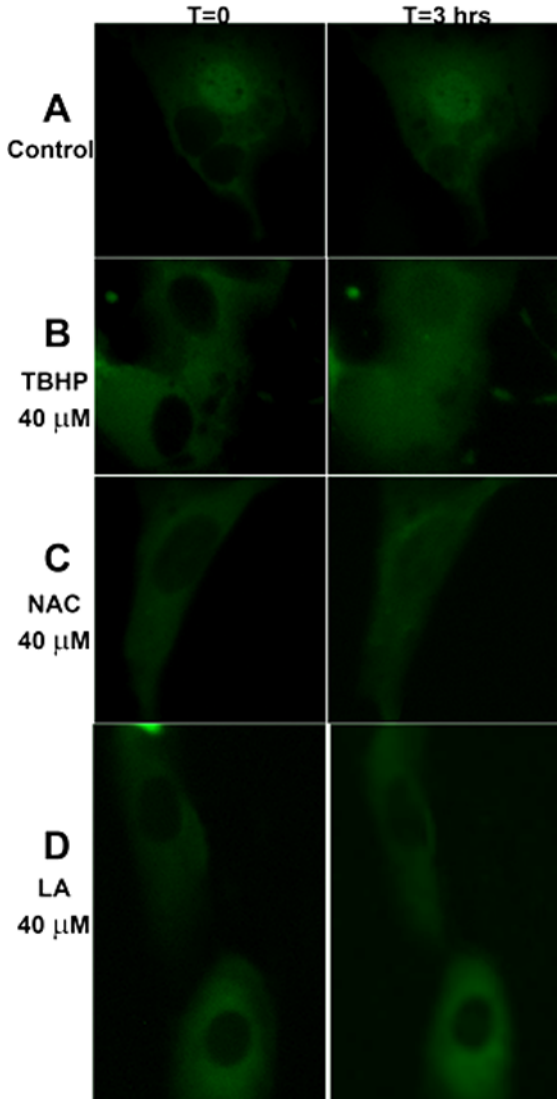

Figure 20. PMA induced nuclear translocation of NF-κB. MDCK Cells were transfected with GFP-RelA plasmid encoding p65. After 24 hours of transfection, cells were incubated only with 25 μM PMA (A), cells incubated only with 40 μM TBHP (B) and cells were simultaneously incubated with 25 μM PMA and either 40 μM NAC (C) or 40 μM lipoic acid, LA (D). Time lapse imaging of PMA induced NF-κB nuclear translocation was done using the EVOS FL microscope (AMG Micro, Bothell, WA, USA, at 20× magnification). Nuclear translocation occurred within 3 hours of PMA incubation.

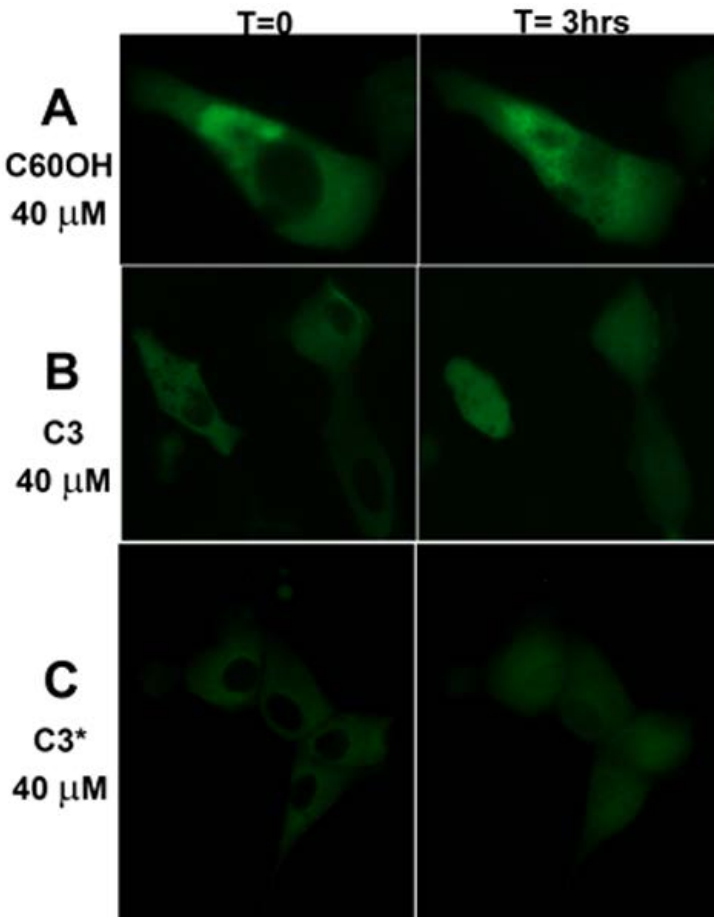

Figure 21. Fullerene treatment causes NO inhibitory effect on PMA induced nuclear translocation of NF-κB. MDCK Cells were transfected with GIF-RelA plasmid encoding p65. After 24 hours of transfection, cells were incubated simultaneously with 25 μM PMA and 40 μM of either $C_{60}OH_x$ (A) or C_3 (B). Another group of cells were incubated with 40 μM C_3 for 24 hours prior to PMA addition (C). Time lapse imaging of PMA induced NF-κB nuclear translocation was done using the EVOS FL microscope (AMG Micro, Bothell, WA, USA, at 20× magnification). Nuclear translocation occurred within 3 hours of PMA incubation.

Determination of mitochondrial membrane potential (ΔΨm) and ROS level

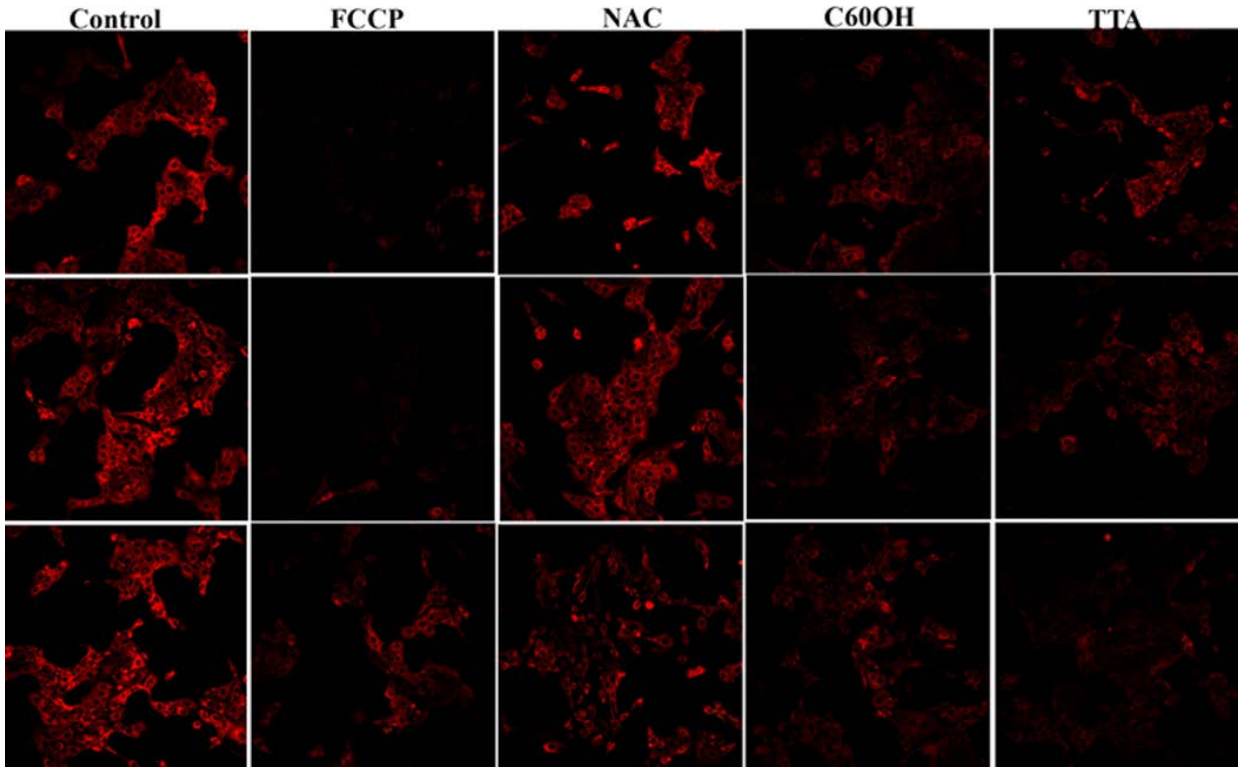

Figure 22. Detection of mitochondrial membrane potential (ΔΨm) of MDCK cells. MDCK cells were labelled with 100 nM of the fluorescent dye TMRE (tetramethylrhodamine methyl ester) for 5-10 minutes followed by incubation with the absence (control) or presence of 40 µM of the following; $C_{60}OH_x$, NAC and TTA for an hour and a half at 37 °C in 5% CO_2. FCCP [carbonyl cyanide 4-(trifluoromethoxy)phenylhydrazone]) was used at 1 µM concentration as an inhibitor of the mitochondria functionality which is demonstrated by a reduction in TMRE fluorescence. A change in TMRE intensity is proportional to a change in the mitochondrial membrane potential (ΔΨm). Notice the reduction of intensity upon using fullerenes.

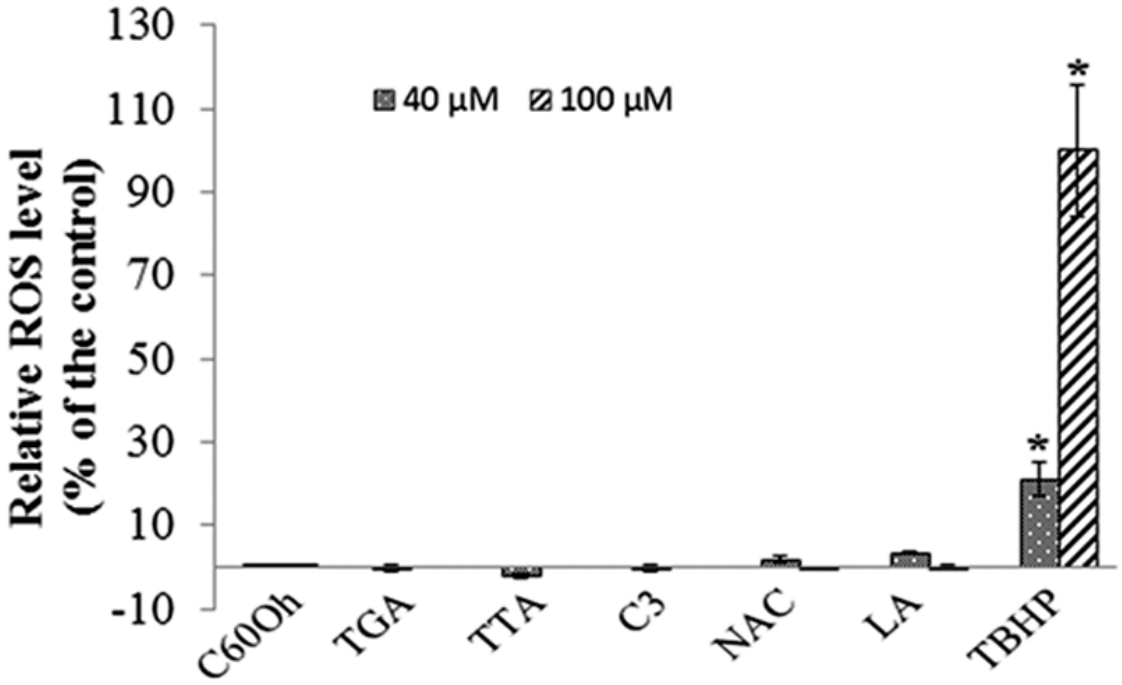

Figure 23. Investigation of the generation of reactive oxygen species (ROS) in the presence of fullerene derivatives. For the detection of ROS generation, (ROS) formation was analyzed by measuring the conversion of the non-fluorescent dye H2DCFDA (2',7'-Dichlorofluorescence, $C_{24}H_{16}C_{12}O_7$) to the highly fluorescent 2,7-dichlorofluorescein (DCF). After 24 hours of seeding MDCK cells, they were loaded with 5µM H2DCFDA for 10 minutes. Thereafter, cells were treated with 40 or 100 µM of one of the following; tertyl butyl hydrogen peroxide (TBHP), NAC, LA and fullerenes ($C_{60}OH_x$, TGA, TTA and C_3). Tertyl butyl hydrogen peroxide (TBHP) was used as positive control for ROS production at 40 and 100 µM, The radical mediated oxidation converts the non-fluorescent form of the dye to the fluorescent DCF which was measured spectroscopically after 90 minutes at 480/529 nm. Relative values compared to TBHP treated cells (Control 100%) are shown which represent the mean of four readings and the corresponding standard errors of the means (s.e.m.). * Significantly different from zero. Fullerenes did not result in free radical generation.

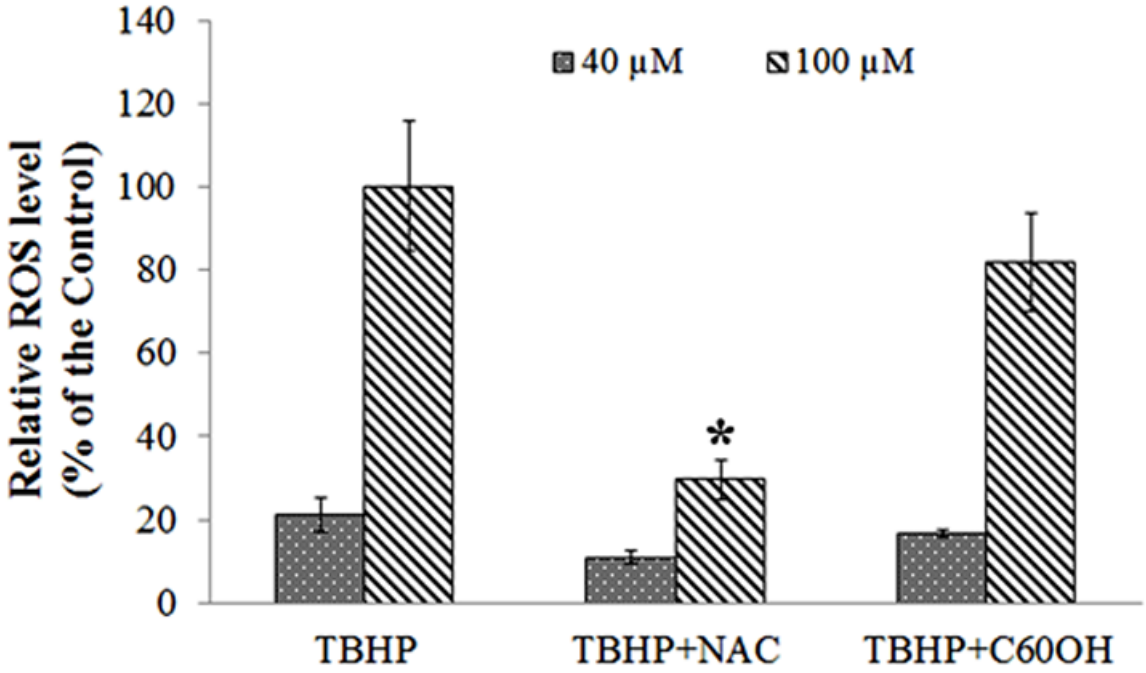

Figure 24. Detection of the PROTECTIVE roles of fullerene derivatives against TBHP toxicity. Reactive oxygen species (ROS) formation was analyzed by measuring the conversion of the non-fluorescent dye H2DCFDA (2',7'-Dichlorofluorescin, $C_{24}H_{16}C_{12}O_7$) to the highly fluorescent 2,7-dichlorofluorescein (DCF). After 24 hours of seeding MDCK cells, they were loaded with 5µM H2DCFDA for 10 minutes. Thereafter, cells were simultaneously incubated with 40 or 100 µM of TBHP and either $C_{60}OH_x$ or NAC. Tertyl butyl hydrogen peroxide (TBHP) alone was used as positive control for ROS production at 40 and 100 µM, The radical mediated oxidation converts the non-fluorescent form of the dye to the fluorescent DCF which was measured spectroscopically after 90 minutes at 480/529 nm. Relative values compared to TBHP treated cells (Control 100%) are shown which represent the mean of four readings and the corresponding standard error of the mean (s.e.m.). * Significantly different than the control. NAC significantly decreased radical generation and protected against TBHP toxicity at 100 µM. $C_{60}OH_x$ did not provide significant protect against TBHP induced toxicity.

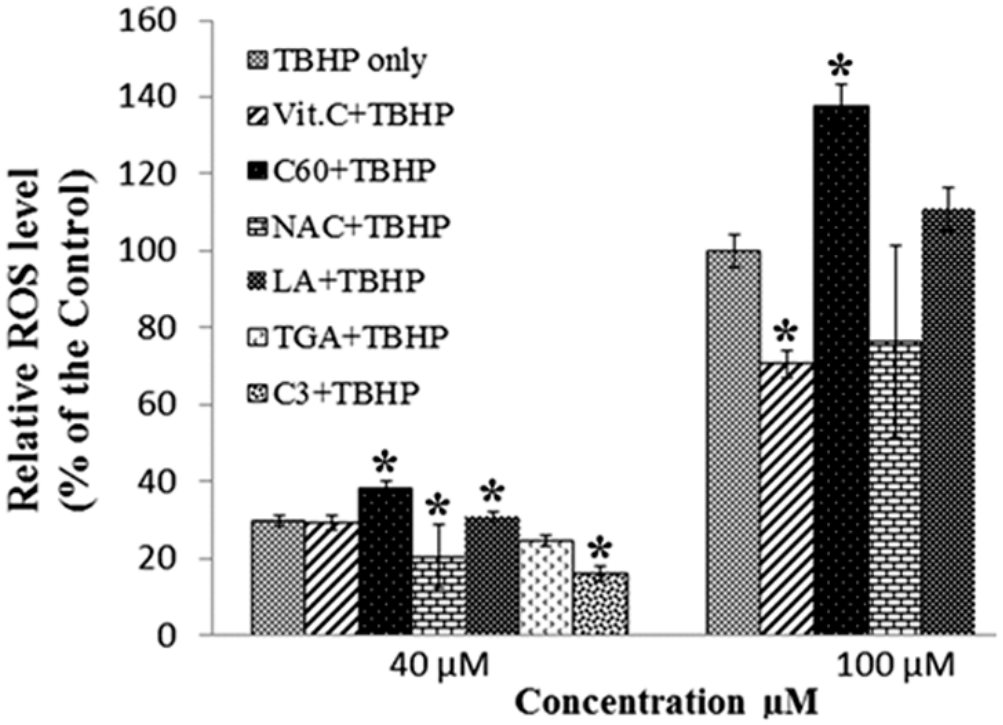

Figure 25. Determination of the PROTECTIVE roles of fullerene derivatives against TBHP toxicity. Reactive oxygen species (ROS) formation was analyzed by measuring the conversion of the non-fluorescent dye H2DCFDA to the fluorescent (DCF) in cells preincubated with fullerenes and treated with TBHP thereafter. MDCK were incubated for 24 hours with 40 or 100 µM of one of the antioxidants; NAC, Vitamin C and LA and one of fullerene derivatives ($C_{60}OH_x$, TGA, TTA and C_3). Following the incubation, cells were incubated for 5-10 minutes with 5 µM of H2DCFDA fluorescent and 40 or 100 µM of tertyl butyl hydrogen peroxide (TBHP) was added to cells to induce ROS production. After 90 minutes incubation, the fluorescent DCF was measured spectroscopically at 480/529 nm. Relative values compared to TBHP treated cells (Control 100%) are shown which represent the mean of four readings and the corresponding standard errors of the means (s.e.m.). * Significantly different. Preincubation of cells with C_3 resulted in a significantly reduced radical generation induced by TBHP. Vitamin C significantly reduced ROS level and protected against TBHP toxicity.

Western blot analysis of NF-κB activity. Nuclear translocation of NF-κB is a critical step in NF-κB activation. Immunofluorescence analyses using anti-p65 antibody for the cytosol extract have revealed that PMA induced translocation of NF-κB in the nucleus was stimulated more in $C_{60}OH_x$ treated cells.

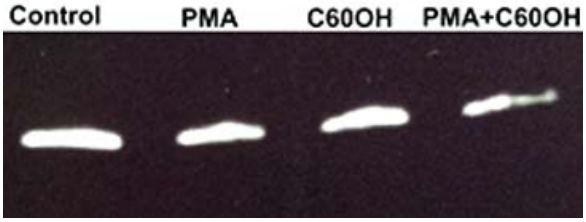

Figure 26. WESTERN BLOT analysis of MDCK cells stimulated with 25 μM PMA for 5 hours, the result shows a detectable decrease in expression in the cytosol corresponding to an activity stimulation of p65 in nucleus. $C_{60}OH_x$ resulted in lower p65 protein level in the cytosol extracts as well.

Discussion

As a pro-inflammatory mediator in the immune system, NF-κB is activated upon exposure to various noxious stimuli such as cytokines, pathogens, free radicals and other ROS like peroxides. Once activated in the cytosol, NF-κB translocates to the nucleus, where it binds to its cognate DNA sequences and activates target genes. Because ROS, particularly H_2O_2, activate the NF-κB pathway, the widely observed inhibition of NF-κB by many antioxidants is not surprising. However, there is a growing appreciation of the complexity of NF-κB activation and regulation by ROS, and the inhibitory mechanisms of antioxidants [128, 129]. One study showed that overexpression of exogenous catalase did not inhibit NF-κB activation stimulated by TNF/PMA, leading the authors to question

the role of H_2O_2 as a second messenger for TNF/PMA induction of NF-κB activation [71]. Another study found that NF-κB activation by H_2O_2 depends on cell type; EL4.NOB-1 T and KB epidermal cells were not activated by H_2O_2. Moreover, antioxidants such as NAC failed to inhibit activation of those cells after stimulation with TNF.

On the other hand, H_2O_2 has been widely used to activate NF-κB in many studies, and NAC has an inhibitory effect on NF-κB in Jurkat cells after TNF treatment [69]. The natural thiol antioxidant α-lipoic acid (LA) has been studied as a potential anti-inflammatory drug for blocking the NF-κB pathway; it was found that LA inhibited NF-κB activation stimulated by TNF or PMA in Jurkat cells [130]. LA is significantly more potent than NAC, and, like NAC, has been used as a "complementary" therapy for HIV/ AIDS. Both Pyrrolidine dithiocarbamate (PDTC) and NAC block NF-κB activation via a pathway independent of their activity as antioxidants; NAC was found to act by lowering the affinity of TNF receptor to TNF, while PDTC suppresses the IκB–ubiquitin ligase activity [131].

The modulation of NF-κB activity by fullerenes has not been very well studied. One of the few relevant previous studies showed that fullerene derivatives act as potent inhibitors against PMA-induced inflammatory response. However, their mechanism of inhibition was not clear; it was suggested that fullerenes act by decreasing levels of ROS responsible for inducing inflammation after treatment with PMA [75]. Another study used polymer wrapped fullerenes, Polyvinylpyrrolidone (PVP) fullerene, to protect against UVA-induced cell death by the inhibition of NF-κB activation [132].

We report here for the first time direct evidence that some fullerene derivatives are effective inhibitors of NF-κB-driven gene expression. Specifically, a representative carboxy (tris-malonyl) fullerene derivative (C_3) and a hydroxy fullerene ($C_{60}OH_x$) were tested and found to be active; both fully inhibited NF-κB driven β-gal expression at micromolar concentrations (Figure 19) that are non-toxic to cells (Figures 17 & 18). In contrast, the highly lipophilic fullerene ALM was inactive as an NF-κB inhibitor (Figure 19), perhaps because it cannot easily pass through the cytosol to the cell nucleus. However, unlike some antioxidants such as α-lipoic acid, the active fullerenes were found to have no effect on PMA-induced nuclear translocation of NF-κB, even at high concentration (40 μM).

Regarding the effects of different oxidants (TBHP), antioxidants (NAC and LA) and fullerenes on PMA induced nuclear translocation in our experiments, it should be noted that exogenous (transfected) NF-κB as an NF-κB-GFP fusion protein expression construct was introduced to cells to monitor nuclear translation in response to PMA treatment. Our results are in agreement with a previous study that found that the thiol antioxidant NAC did not inhibit the nuclear translocation of NF-κB in cells overexpressing (transfected) p65 [133]. NAC was used to detect the role of redox response in NF-κB signaling pathway induced by TNF alpha. The same study found that NAC inhibited endogenous NF-κB activation through the suppression of phosphorylation by kinases, however, NAC failed to inhibit kinase activity in vitro, indicating that NAC mediates the suppression of the kinases IKKα and IKKβ through an unknown redox mechanism. In contrast to vitamin C or glutathione, LA was found to inhibit IκB/NF-κB

signaling pathway at the level, or upstream, of IκB kinase [134], blocking nuclear translocation of NF-κB. LA acid is the most potent of the common thiol antioxidants, and in our hands, it was the most potent translocation blocker, with no GFP fluorescence visible in the cell nuclei three hours after combined PMA and LA treatment; in comparison, NAC at best gave only a minor reduction in translocation (Figure 20).

Thus, the fullerenes that were effective inhibitors of NF-κB-driven gene expression (C_3 and $C_{60}OH_x$) had no effect at all on NF-κB nuclear translocation (Figure 21), suggesting that their mechanism of action is distinct from that of a potent antioxidant like LA, which inhibits NF-κB signaling by blocking its nuclear translocation. Taken together, these results strongly suggest that the active fullerene derivatives block NF-κB signaling downstream of the cytosolic activation pathway (the site of action of many antioxidants), possibly inhibiting NF-κB activation at a step penultimate to DNA binding. One such step is the reductive activation of NF-κB by Trx in the nucleus, which is essential for any effect of NF-κB on gene transcription, because the oxidized disulfide form of NF-κB is sterically blocked from binding to DNA [135]. This suggests a need for further studies of the interactions of fullerenes with the Trx system.

Tert-butyl hydroperoxide (TBHP) is an amphiphilic peroxide that is structurally similar to hydroperoxides that result from lipid peroxidation, which contributes to cellular dysfunction and disease. TBHP is a highly reactive strong oxidant with a long half-life which can pass with ease through the membrane and migrate in the cell. TBHP activates the NF-κB pathway by inducing the phosphorylation of inhibitor of kB (IkB) through the IkB kinase (IKK) pathway, which involves p38 MAPK and ERK. For these reasons,

TBHP was used in our experiments as a positive control to enhance NF-κB nuclear translocation (Figure 20), as well as ROS formation and toxicity in cells (Figures 23, 24 & 25), wherein the ability of fullerenes to antagonize TBHP-induced toxicity in cells was investigated by analyzing ROS level using a fluorescent probe. Fullerenes were not significantly effective in protecting against TBHP toxicity (Figures 24 & 25), which may primarily reflect the potency of THBP as an oxidant, because TBHP cytotoxicity was also not very effectively prevented using common antioxidants such as vitamin C and NAC at a concentration of 40μM; however vitamin C at 100 μM significantly reduced TBHP cytotoxicity. The previous results indicate that higher drug concentrations are needed to prevent cytotoxicity induced by TBHP in MDCH cells. NAC was previously reported to require very high concentrations (millimolar) to protect against cytotoxicity induced in cells [136].

It is important to note that none of the 4 carboxy or hydroxy fullerenes tested was found to increase ROS levels when exposed to cells as a mono therapy (Figure 23). Thus, despite their paradoxical role of scavenging free radicals by oxidation [126], the carboxy and hydroxyl fullerenes under study apparently do not indiscriminately oxidize other cell components other than free radicals. This probably contributes to their low toxicity, which is of considerable importance, because, for fullerene derivatives to be clinical useful as anti-inflammatory agents, they must have acceptably low toxicity.

The fullerene derivatives tested here were not toxic in MDCK cells at concentrations up to high micromolar (Figures 17 & 18), which is in agreement with previous literature. Several previous in vivo and in vitro studies have shown that

fullerenes have no acute or subacute toxicity [137, 138]. However, some aqueous dispersion of fullerenes have been reported to induce oxidative damage in bacteria, algae and fish. Fullerene cytotoxicity is highly variable and depends on factors such as: particle size, aggregation state, shape, the degree of cage derivatization, chemical composition, surface charge and chemistry, water solubility, light exposure as well as dispersion [91, 139]. Therefore the literature contains some contradictory findings. The toxicity of aggregated fullerene particles in aqueous solution was reported at very low concentration part per billion (ppb) against human cell lines, the toxicity was exhibited by cell membrane peroxidation resulted from reactive oxygen species (ROS) [91]. In all studies which showed the toxicity of nC_{60} used tetrahydrofuran (THF) or dimethyl sulfoxide (DMSO) as solvent for the preparation of nC_{60} or other fullerene derivatives [15, 64, 140-142]. It was also claimed that some colorimetric methods used to detect ROS production [31, 91] were found to interfere with nC_{60} and produce false positive results [143-145]. Because different fullerene structures have distinct cytotoxic mechanisms, fullerene derivatives must be evaluated individually [140]. Fullerenes have been shown to suppress production of ROS in a number of studies, e.g.[146-148].

Finally, our results do show that fullerenes may cause some perturbation of mitochondrial function (Figure 22), which is in agreement with previous in vivo and in vitro studies of liver cells [136, 149], where hydroxylated fullerenes caused hydrogen ion depletion in cells, possibly due to their disruption of ATP synthesis in the mitochondria [150]. This could be interesting in the light of evidence of anti-aging effects of some fullerenes like C_3 [74], if slowing down of mitochondrial function could mimic

the effects of dietary caloric restriction. However, this effect on mitochondria is apparently not sufficient to decrease cell viability (Figures 17 & 18). Despite this caveat, taken as a whole, our results suggest that fullerenes are a promising class for the development of NF-κB inhibitors. NF-κB [120] and fullerenes [4] were discovered just one year apart, so it will be an interesting coincidence if fullerenes prove to be an important chemical class for the development of potential anti-inflammatory drugs that act by inhibition of NF-κB signaling.

CHAPTER IV

PHYSICAL CHARACTERIZATION OF FULLERENES

The structure of fullerene C_{60} consists of 60 vertices and 32 faces, comprising 12 pentagons and 20 hexagons folded into a sphere of 1 nm diameter [4]. The atoms are connected by sp2 hybridized bonds in which every carbon atom forms bonds to three other adjacent atoms, resulting in its pseudo-aromatic structure due to its conjugated double bonds and the delocalization of π-electrons over its carbon core. There are two types of bonds in fullerene: C5–C5 single bonds in the pentagons and C5–C6 double bonds in the hexagons [148]. There are 12 pentagon rings in fullerenes regardless their size, thus each fullerene Cn, n=any even number, is constructed of 12 pentagonal rings, and any number of hexagonal ones, m such that m= (n-20)/2 (Euler's rule).

There is a large gap between the energy of the highest occupied molecular orbital (HOMO) and the lowest unoccupied molecular orbital (LUMO) [151]. The energy separation between HOMO and LUMO have been roughly used as an indicator of kinetic stability for fullerenes, specifically, susceptibility to chemical reactions and decomposition. However as fullerene size increases, the HOMO-LUMO energy difference becomes smaller [152].

Early spectroscopic studies for the existence of fullerenes assumed that C_{60} would be an extremely stable aromatic molecule. This view was supported by the calculation that there are 12,500 resonance structures possible for C_{60}. But this overlooks an

important feature, C_{60} has the tendency to avoid having double bond character in the pentagonal ring. The presence of double bonds shortens bonds in the already strained ring, producing the Mills-Nixon effect. There is thus only one structure for C_{60} that avoids having any double bonds in pentagonal rings, and this has two important consequences; first, the delocalization of electrons is poor, so C_{60} is much more reactive than originally expected, otherwise C_{60} would have all the chemical excitement of brick dust. Second, C_{60} is not so much an aromatic molecule as a giant closed cage alkene. The same applies to other fullerenes. The stability of fullerene derivatives is largely controlled by avoiding double bonds in the pentagonal rings, which is also important in determining which fullerene isomers are stable.

Unlike aromatics, fullerenes have no hydrogen atoms or other groups attached and so are unable to undergo substitution reactions. Substitution reactions can take place on derivatives once these have been formed by addition. As the cage consists entirely of sp2 hybridized carbon, which have electron withdrawing inductive effects, the fullerenes are strongly electron attracting. This affects their chemical behavior; for example, they react readily with nucleophiles. In general, the molecules appear to undergo all the reactions associated with poorly conjugated and electron deficient alkenes. But their unique feature is the vast number of products that may arise from addition of just one reagent [153]. The thirty conjugated double bonds attribute to C_{60} a propensity to addition reactions. In order to enhance their water solubility and their interaction with the biological systems, fullerenes are commonly modified chemically by directly binding moieties to the carbon

cage. Such fullerene compounds includes polyhydroxylated C_{60} (fullerenol), and tris malonyl C_{60} or C_3 (carboxylated fullerenes).

The behavior of fullerene derivatives in aqueous solution is complex and as a consequence their interaction with the biological system is far from well understood. Both derivatization and preparation can change the physical properties resulting in nanoscale aggregates with distinctly different properties from the parental molecule. Therefore, it is essential to study fullerene physical properties, including agglomeration state, size distribution of agglomerates, solubility in terms of the biological media, indeed the variable nanomaterials activity or responses is based on characterization in media rather than drawing a general conclusion for the whole class of nanomaterials. The type, number and placement of substituents can dramatically impact the physiochemical properties of fullerenes and subsequently their activities and interaction with biological systems and uptake by cells. For further development of their medical applications, more understanding is needed for their behavior in different conditions.

In addition to the relatively expensive prices, low availability of derivatized fullerenes restricts their chemical structure characterization; although nanogram to microgram quantities is enough to induce biological activities, milligrams of fullerenes are needed for chemical and structural analysis. Another challenge is that most fullerene derivatives fail to maintain their structure upon characterization, particularly in a mass spectrometer; most C_{60} derivatives gave only one peak at 720 a.m.u corresponding to the core (C_{60}).

Despite the recorded biological activities of polyhydroxylated fullerenes in vivo and in vitro[64, 98, 105], the number of hydroxyl groups attached is difficult to determine and can vary from 2-30 or higher than 30, depending on production conditions; this results in molecules with different solubility and activity. However most of the biological research on hydroxylated fullerenes has focused on fullerenols with a number of hydroxyl groups below 30. Little is known about the bioactivity of highly hydroxylated fullerenes (over 30 OH groups).

Along with hydroxyl groups, other groups such as salt and oxygen Cn(OH)xOy might be present in fullerenol solution, therefore it is not possible to describe fullerenol solution as highly pure >99% while they might be (>95%). As a result, heterogeneous fullerenol solutions (mixed solutions) are cheaper, so typically there are other types of chemical groups in mixed fullerenol solutions and they might also have traces of heavier fullerene cores, C_{70}, to C_{96} [154].

It is important to consider while preparing fullerenol solutions for pharmacological purposes that pH value changes with concentration for fullerenol solution as a result of proton dissociation. A concentration of 0.1 mM of fullerenol solution yields a pH change of about 0.1, while for about 2 mM, this change is about 1, which results in a pH of 6.[155]. Because hydrogen dissociation of fullerenol solution changes the pH of aqueous solutions, fullerenol solution acts as a weak acid. A similar effect is expected for the dissociation of K^+ in the other fullerene derivative solutions.

Fullerene derivatives have a high propensity to form aggregates in solution; hydroxylated fullerenes tend to form aggregates in polar solution with a size range of 20–100 nm [14, 137, 156] while TGA was found to form 20-50 nm aggregates [137].

Materials and Methods

Mass spectrometry, optical spectroscopy, zeta potential and size were used in this study for characterization of fullerene derivatives. Mass spectrometry (Figure 27) is used commonly to check the purity and to detect the chemical composition of fullerenes, however the ionization process may result in generation of new carbon species from the pure sample. Another consideration is the extensive fragmentation of C_{60}, which leads to peaks less than m/z 720 (peak at 720 m/z corresponds to C_{60}) indicating unreliable impurities in the sample. For these reasons, mass spectra do not reflect purity higher than 99%.

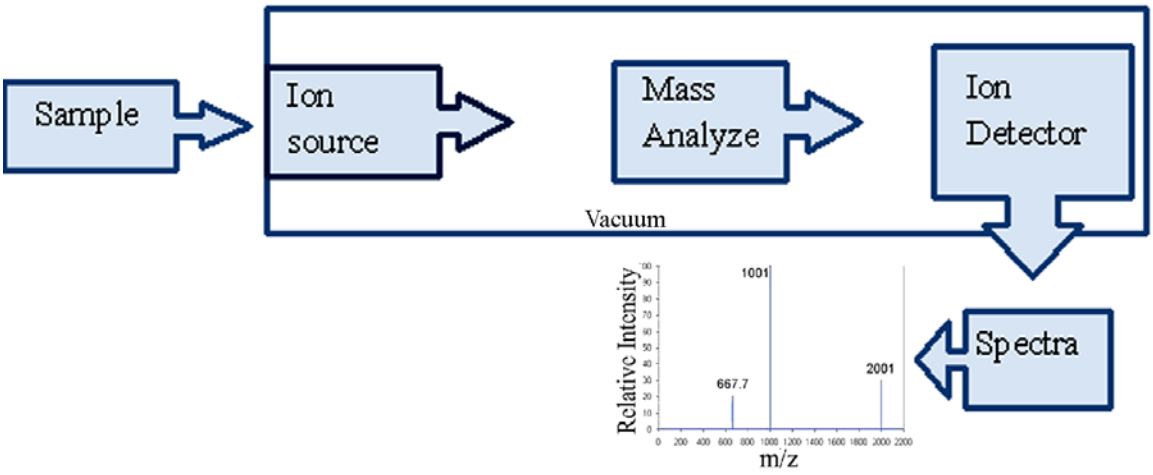

Figure 27. MASS SPECTROMETRY scheme process. The molecules must be charged (converted into ions) before measuring in MS. The accelerated charged particles are deflected by a magnetic field according to their masses and charges. Mass analyzer separates travelled ions based on mass to charge ratio (m/z). Detector counts number of ions for each m/z, amplifies the ion signal and transfers it to data system, which displays the analysis to a spectrum (m/z values of the ions vs. their intensities). MS process is under the control of data system.

MALDI/TOF, Matrix Assisted Laser Desorption/Ionization Time of Flight Mass Spectroscopy. MALDI/TOF technique was used in this study to identify cross contamination of fullerenes in solution, and not for quantitation purposes. MALDI, matrix assisted laser desorption ionization, is the ion source, considered as soft ionization method and TOF, time of flight is the mass analyzer. Some advantages of using MALDI/TOF include the tolerance of salts and buffers, fast data acquisition and sensitivity for small quantities. The acidic matrix (α-CHCA; cyano-4-hydroxycinnamic acid) was selected, and 1-3 µl of fullerene solution was loaded into a plate (Figure 28). The mix ratio is 10,000:1 matrix to sample, the mixture was dried for 5 minutes to allow co-crystallization of matrix with the sample.

Figure 28. Sample preparation on a standard plate for MALDI with multiple wells. Sources: [157] and www.ms-textbook.com).

The MALDI plate was placed into the MALDI plate holder. The sample is then irradiated with a laser (positive mode) (Figure 29) and the generated analyte ions pass through a flight tube based on their mass to charge ratio. Mass analyzer TOF detects the analytes at different times.

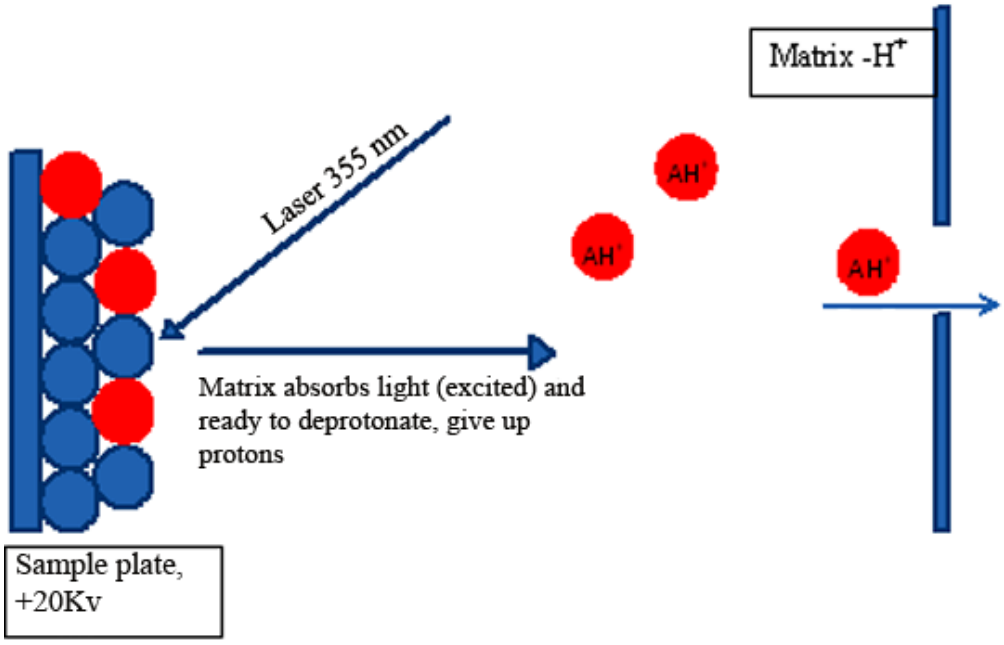

Figure 29. A representative scheme of MALDI. Sample A (analyte) is mixed with excess matrix (M) and allowed to dry on plate to form crystals. Irradiation of the mixture by laser causes ionization of the matrix molecules (MH^+), the ionized matrix transfer a proton to the analyte thus ionizing the analyte. $MH^+ + A \longrightarrow M + AH^+$. Accelerated ions enter the time of flight tube, where lighter ions travel faster than heavy ones, reflecting their mass, so smaller ions reach the detector first [158].

Optical Spectroscopy. Despite the paucity of information that can be obtained from optical spectra of fullerenes, they still can be used to determine heterogeneity of fullerenes in solution. The optical absorption spectra obtained depend on the size and structure of fullerenes. As the LUMO HOMO gap becomes smaller with increasing size of the fullerene, less energy is needed for electron transition, thus larger fullerenes absorb light at longer wavelength. For that particular reason, the presence of certain peaks in solution can provide a method for detecting C_{70} impurities in C_{60} solution. A Biotek Synergy™ Mx microplate reader was used for the measurement using Gen5 software, version 1.09.8 (BioTek Instruments, Inc., Highland Park, Winooski, VT). In this study we

used spectrophotometry to measure the optical absorption of fullerene derivatives in the range 280-880 nm. A UV-Visible absorbance spectrophotometer was also used for characterization of C_3, $C_{60}OH_x$ and ALM. Quartz cuvette (1 cm) was used and phosphate buffer saline was used as the background solution. Absorbance was collected between 202-802 nm.

Zeta potential and Zeta size. We used Malvern Zetasizer Nano Z ZS90 (Malvern Instruments Ltd), which uses both techniques of Dynamic Light Scattering, DLS and Laser Doppler micro-electrophoresis for the measurement of size and charge respectively of carbon nanoparticles. DLS measures the diffusion of moving particles which have been dissolved in a liquid, particles movement due to Brownian motion (which is the movement of particles due to random collision) causes laser light to be scattered at different intensities. DLS analyses these intensities by converting them to velocity of Brownian motion and hence, size and size distribution, by using the Stokes-Einstein relationship.

The Zeta potential technique uses laser Doppler electrophoresis to measure the velocity of particles in solution when electric field is applied (known as electrophoretic mobility), then zeta potential is calculated by using viscosity and dielectric constant based on Henry's equation. Zeta potential is important for the determination of the tendency of particles to flocculate in solution, indicating the stability of particles. Zeta potential values larger than +30 mV or -30 mV represent stable particles with no tendency to flocculate.

By using the software, we created a SOP (Standard operating procedure) for measuring fullerenes. Physical properties of sample were set including the refractive index, viscosity cP and dispersant dielectric. The refractive index values were 1.9, 1.332, 1.33 and 1.365 for fullerenes, PBS, water and DMEM respectively. Viscosity (cP) values of PBS, water and DMEM were; 0.891, 0.8872, 1.054 respectively and the dispersant dielectric constants of PBS, water and DMEM were; 78.6, 78.5 and 80.0 respectively.

The size analysis result are shown as a size distribution graph represented in two ways, the descriptive values (cumulant analysis) which includes both Z-average (intensity mean) and polydispersity (PDI) and the distribution results. Peaks display the size and percentage by either intensity, number for up to three peaks within the results. The demonstration of one peak of the distribution in some dispersants, coupled with small PDI, is called monomodal or monodisperse. The Z-average is used to compare samples dissolved in the same dispersant when polydispersity (PDI) is < 0.5. However for broader distributions, with high PDI > 0.5, the distribution graph and analysis and not Z-average should be used to determine the size. Zeta potential results are represented in a graph with statistics including the mean and standard deviation. Samples were diluted to: 0.01- 0.05 mg/ml in a total volume of 1 ml in PBS for Zeta measurements. Cell type was chosen as disposable polystyrene cuvettes and folded capillary cells for measuring size and zeta respectively.

Results

MALDI/TOF, Matrix Assisted Laser Desorption/Ionization Time of Flight Mass Spectroscopy. The mass-spectrometric peaks generated, and the most abundant fragment at m/z 720 for C_{60} derivatives ($C_{60}OH_x$ and C_3) (Figures 30, 31 & 32). The mass spectra of fullerenol contain peaks m/z: 720 (C_{60}^+), 721 ($C_{60}H^+$), 722 ($C_{60}H_2^+$), 737 ($C_{60}(OH)^+$) (Figures 31 & 32), other minor peaks can be detected which are attributed to oxyfullerenols and sodium salts. The most abundant peak for C_{70} fullerene derivatives is at m/z 840 (Figures 31 & 32). The parent ion is missing from the spectra for all fullerene derivatives, indicating changes in the structure of molecules in solution or, more likely, upon ionization.

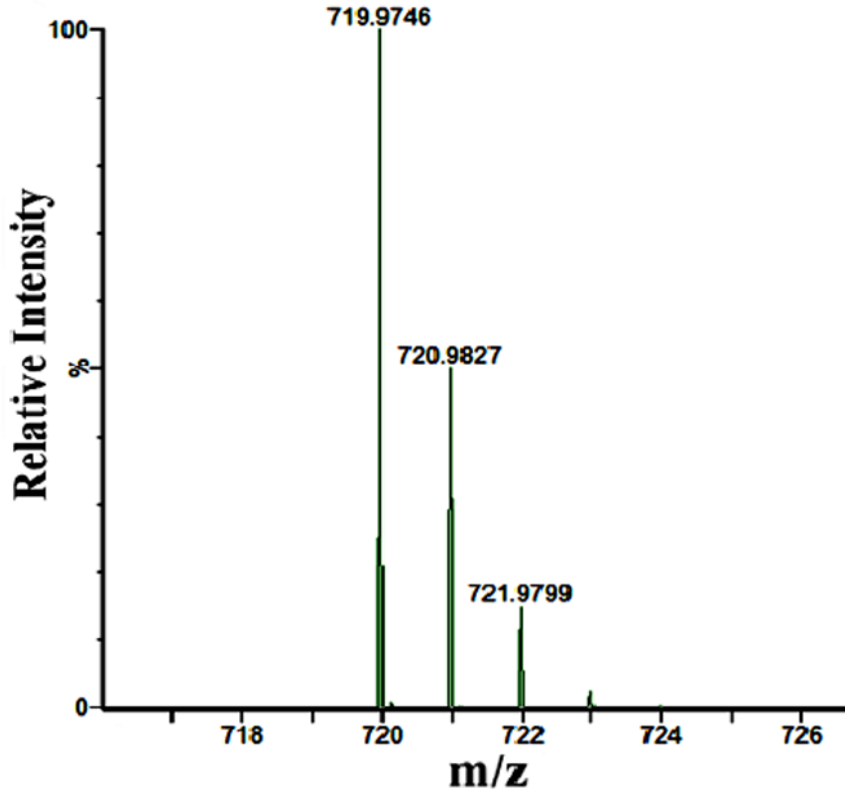

Figure 30. MALDI/TOF spectrum shows the most abundant peak for the analysis of C_3 is 720 m/z, fullerane $C_{60}H_2$ was detected at 722 m/z, the presence of fulleranes in C_{60} mass has been detected before.

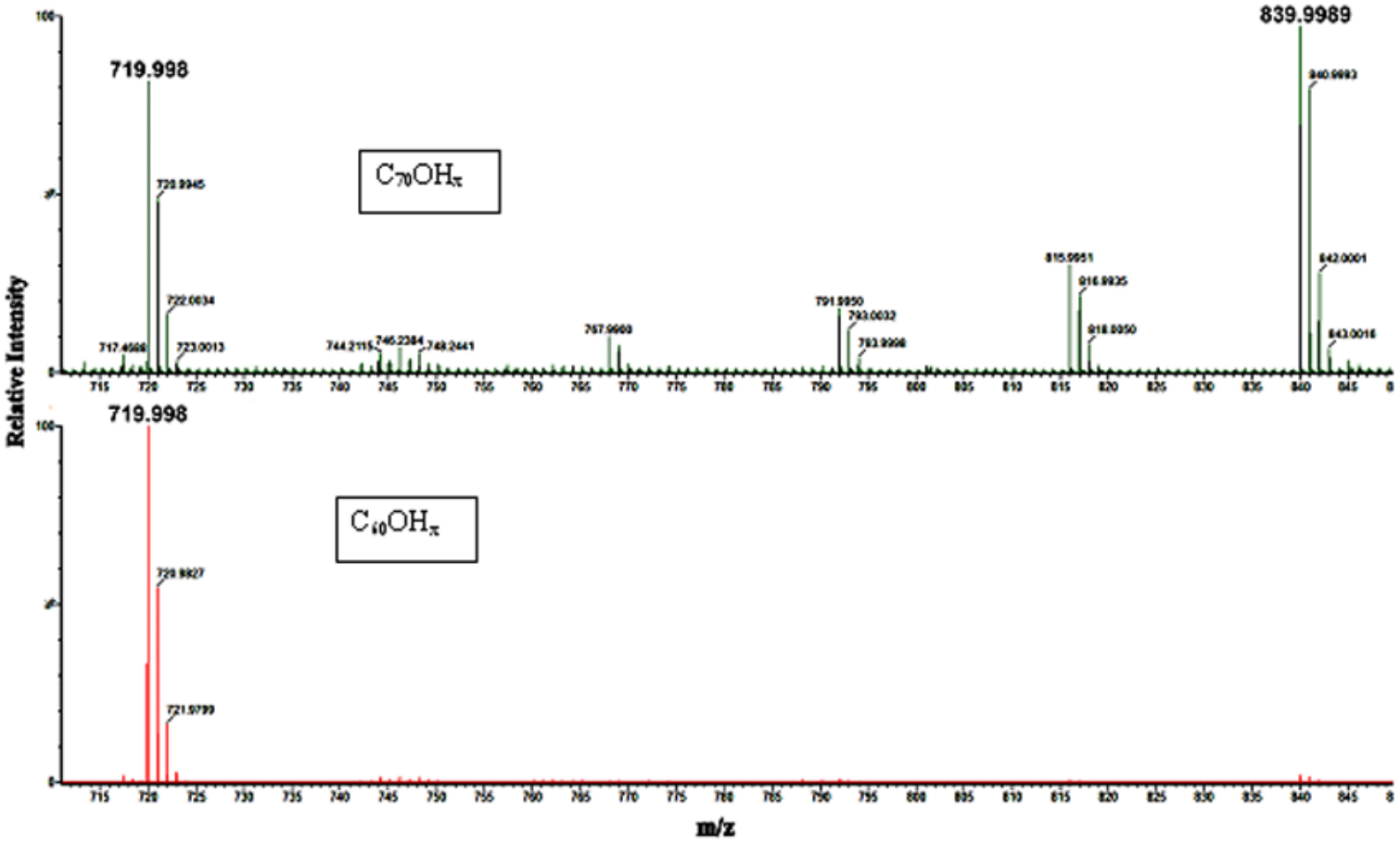

Figure 31. MALDI/TOF spectrum shows the purity of hydroxylated fullerenes ($C_{70}OH_x$ and $C_{60}OH_x$). The C_{70}/C_{60} ratio in $C_{70}OH_x$ is almost 50:50, while the abundant peak at 720 m/z in $C_{60}OH_x$ reflects their purity from C_{70}. Fullerane $C_{60}H_2$ was detected at 722 m/z; the presence of fulleranes in C_{60} mass has been detected before.

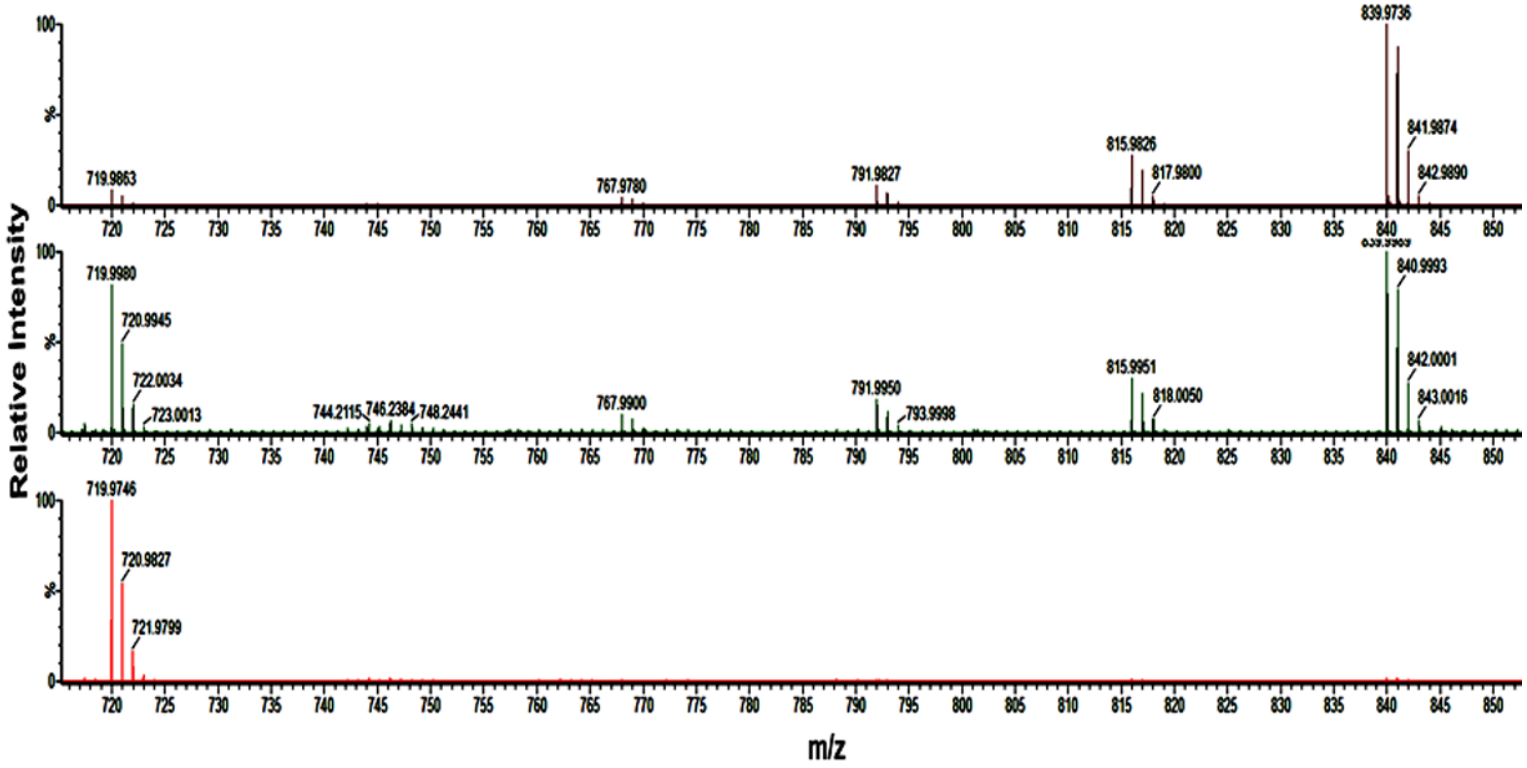

Figure 32. MALDI/TOF spectrum shows the purity of fullerene derivatives (TGA, $C_{70}OH_x$ and $C_{60}OH_x$). The C_{70}/C_{60} ratio in $C_{70}OH_x$ is almost 50:50, while the abundant peak at 720 m/z in $C_{60}OH_x$ reflects their purity of C_{70}. Fullerane $C_{60}H_2$ was detected at 722 m/z, the presence of fulleranes in C_{60} mass has been detected before.

Optical Spectroscopy. The electron spectrum of fullerene derivatives has no observable typical absorption bands. While both C_{60} and C_{70} derivatives absorb at 280-330 nm, C_{70} derivatives have distinct absorption peaks at ~468-500 nm while fullerenol absorption is featureless above 300 nm (Figure 33). The absorption of TTA in water is much higher than on other solvents (PBS or DMEM) (Figure 34), indicating its high solubility in water. TGA has better solubility in DMEM than TTA (Figure 35).

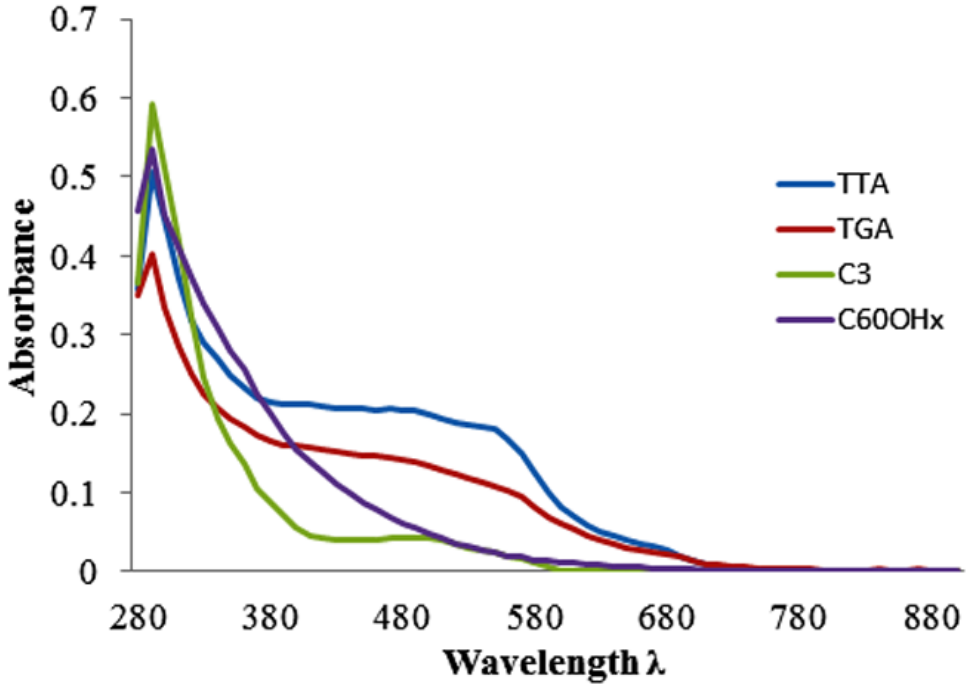

Figure 33. Optical absorption spectra of fullerene derivatives in PBS ($C_{60}OH_x$, C_3, TGA and TTA). The difference in spectra can be used to detect heterogeneity in fullerene solution, and C_{70} contamination in C_{60} samples. Absorption at 468-500 nm is a feature of C_{70} content in solution.

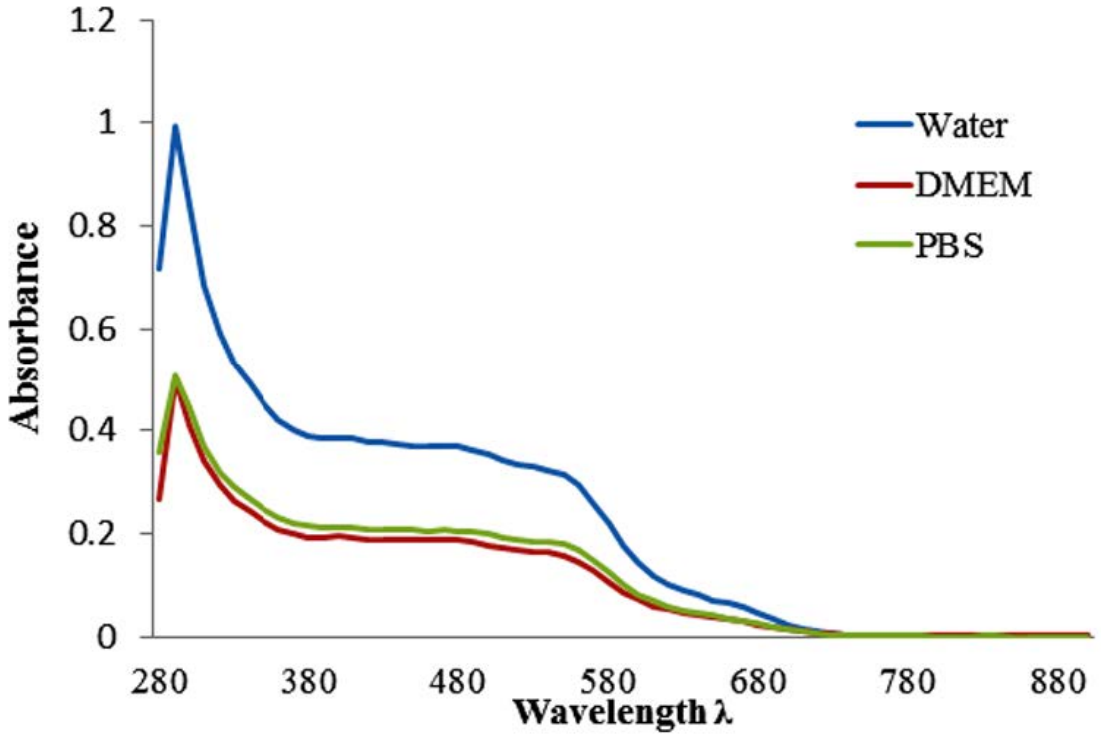

Figure 34. Optical absorption spectra of TTA in different solvents (Water, DMEM and PBS). These spectra illustrate the difference in optical density in different solvents, the difference can be used to assess the solubility of the sample. Absorption of TTA in different solvents is shown in a descending order: water (1) > PBS (0.5) > DMEM (0.49). Absorption at 468-500 nm is a feature of C_{70} content in solution.

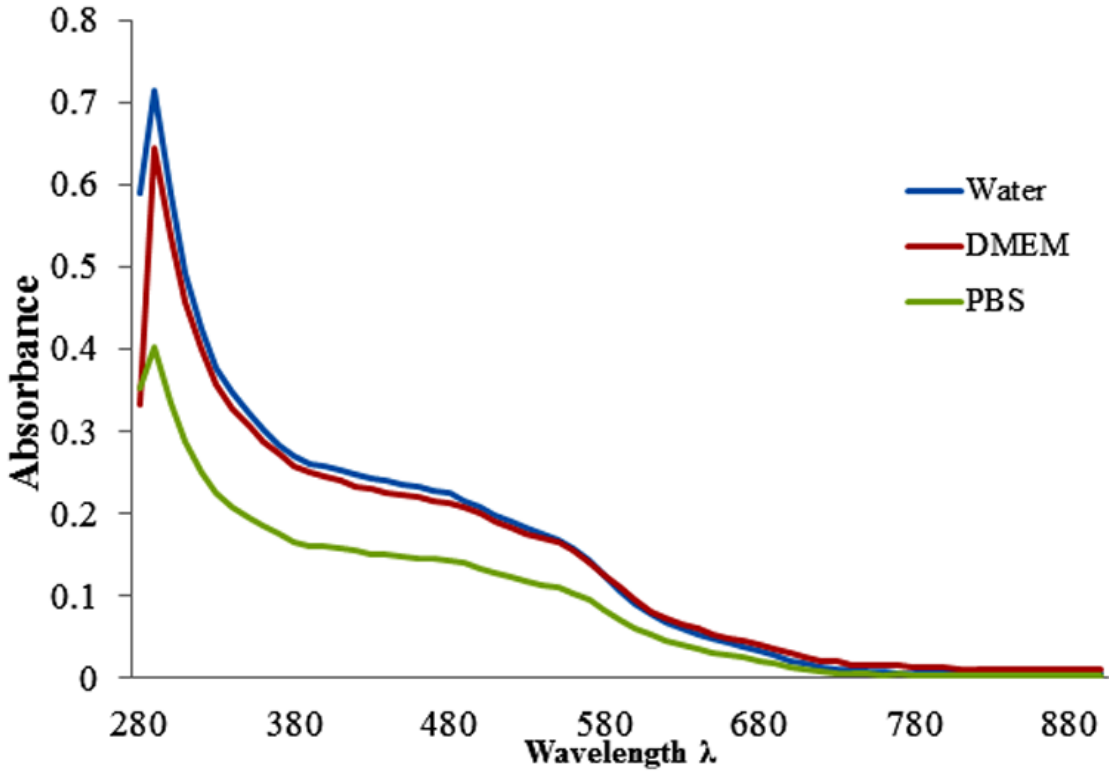

Figure 35. Absorbance spectra of TGA in different solvents (Water, DMEM and PBS). These spectra illustrate the difference in optical density in different solvents. Absorption of TGA in different solvents is shown in a descending order; water (0.71) > DMEM (0.64)> PBS (0.4). Absorption at 468-500 nm is a feature of C70 content in solution.

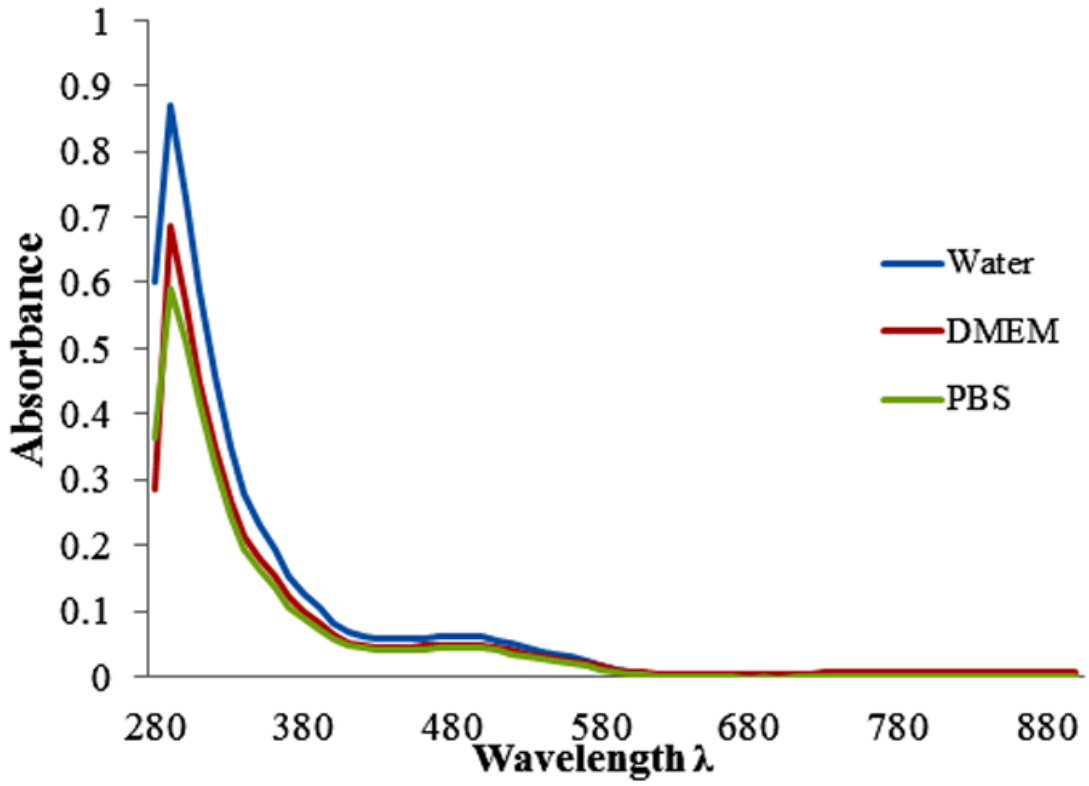

Figure 36. Absorbance spectra of C_3 in different solvents (Water, DMEM and PBS). These spectra illustrate the difference in optical density in different solvents. Absorption of C_3 in different solvents is shown in a descending order; water (0.88) > DMEM (0.69) > PBS (0.59).

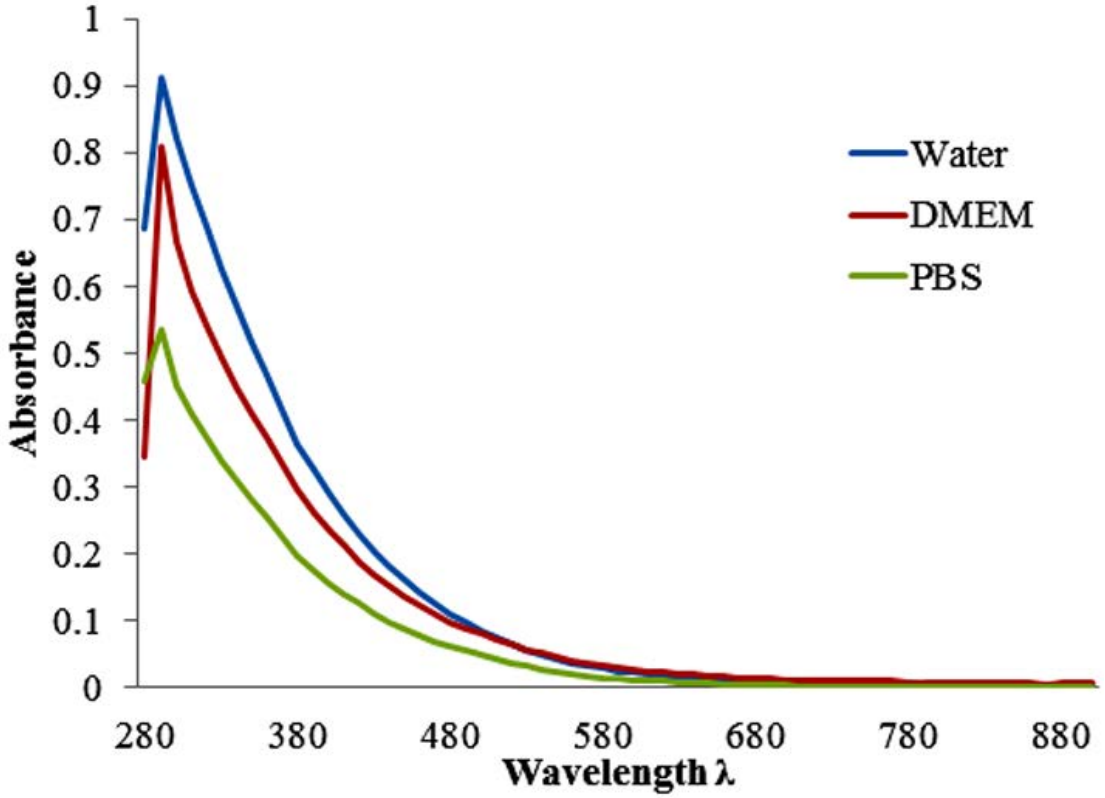

Figure 37. Absorbance spectra of $C_{60}OH_x$ in different solvents (Water, DMEM and PBS). These spectra illustrate the difference in optical density in different solvents. Absorption of $C_{60}OH_x$ in different solvents is shown in a descending order; water (0.91) > DMEM (0.81) > PBS (0.53).

Figure 38 shows that fullerene derivatives have different absorption bands in the UV region, indicating the differences in electronic structure. C_3 has a highly intense absorption and sharp peaks in UV region at 270 nm and a shoulder at 235 nm. However $C_{60}OH_x$ and ALM showed much lower absorption, whereas $C_{60}OH_x$ has the lowest intense absorption (fullerol has no absorption bands in UV region). Although C_3 and $C_{60}OH_x$ both have the same core C_{60} they showed different absorption patterns, indicating different behavior in solution and probably different electrochemical structure.

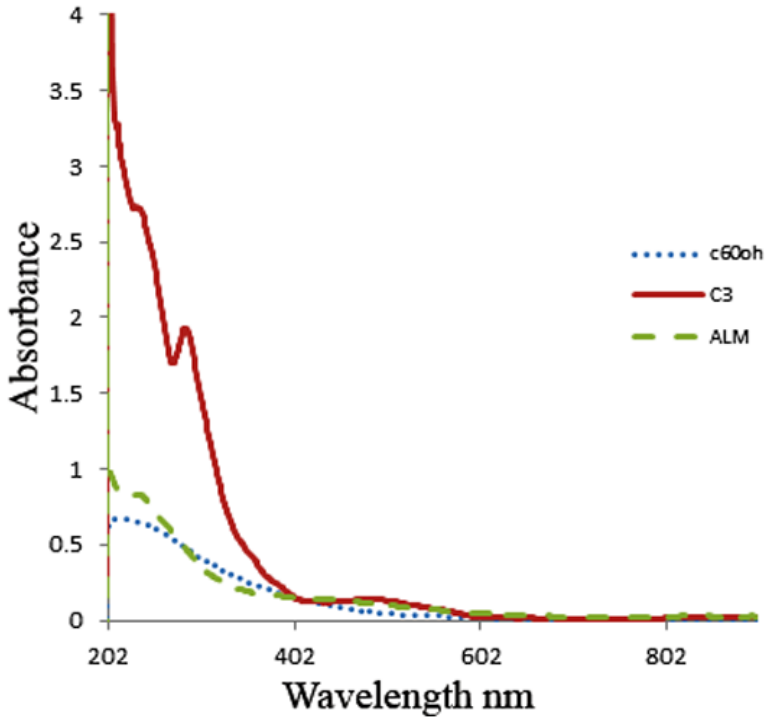

Figure 38. UV/Vis absorbance spectra of $C_{60}OH_x$, C_3 and ALM dissolved in PBS.

Zeta potential and Zeta size. The zeta potential graphs for the particles are shown in figures (39, 41, 43 & 45). The zeta-potential readings show that all of the fullerene particles are negatively charged under the assay conditions, probably due to the presence of ionizable OH and COOH groups. The distribution curves of the particle size of TTA, TGA, C_3 and $C_{70}OH_x$ are shown in figures (40, 42, 44 & 46), the x axis represents diameter (nm) while y axis shows the relative intensity of the scattered light. All of fullerenes form aggregates in solution (polydisperse distribution) indicated by high to moderate PDI values (broad monomodal distribution or the presence of multiple peaks within a distribution, heterogeneous distribution of particles) (Table 2). The mean diameter of fullerenes in this study ranges from 54.6 nm (C_3) to 145 nm (TGA). Most of the fullerenes are low charged particles <-30 mV except TGA having a high zeta potential, which indicates electrically stabilized colloids, however all fullerenes exhibit a tendency to aggregate in solution regardless of zeta potential values. Fullerenes were sonicated in a water bath sonicator for 30 minutes to deagglomerate and disperse the particles; however the size of aggregates did not become smaller (Table 2). A previous study showed an average size of 268 nm of fullerenol in water [159].

Table 2. Zeta potential values (mV) and average size and size distribution (nm) of fullerene derivatives.

Sample	**Zeta (mV)**	**Size (nm)**	**Size (nm) after 30 minutes sonication**
TTA	-2.23	Z-Average= 119.3, PDI= 0.17	Z-Average= 112.8, PDI= 0.192
TGA	-39.1	Z-Average= 145, PDI= 0.427	Z-Average= 273.6, PDI= 0.318
C_3	-1.27	54.65 (94.6%) and 0.781 (5.4%), high PDI	117.2 (100%), high PDI
$C_{70}OH_X$	-17.8	92.81 (94.8%), 6.551 (5.4%), high PDI	36.06 (100%), high PDI
$C_{60}OH_X$	-	Z-Average= 100	-
ALM	-	Z-Average= 120	-

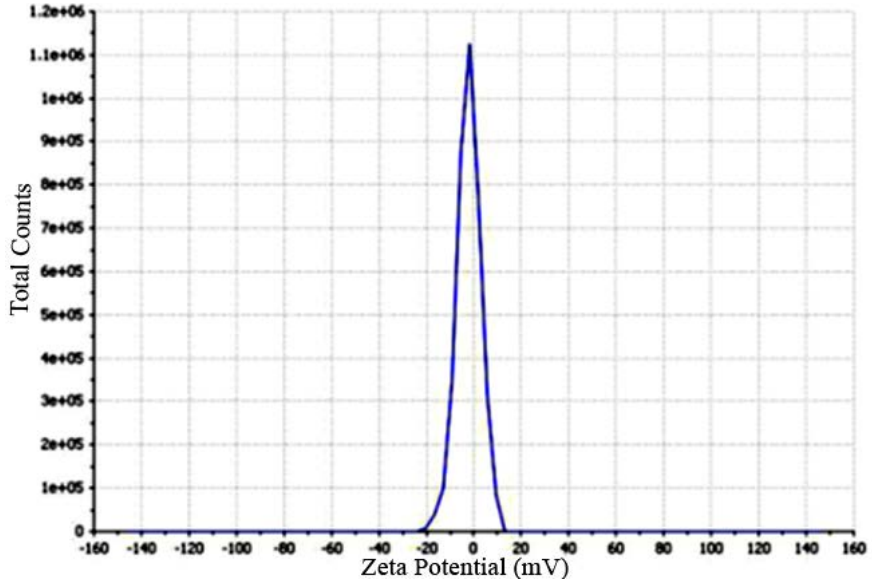

Figure 39. ZETA potential of TTA was -2.23 mV.

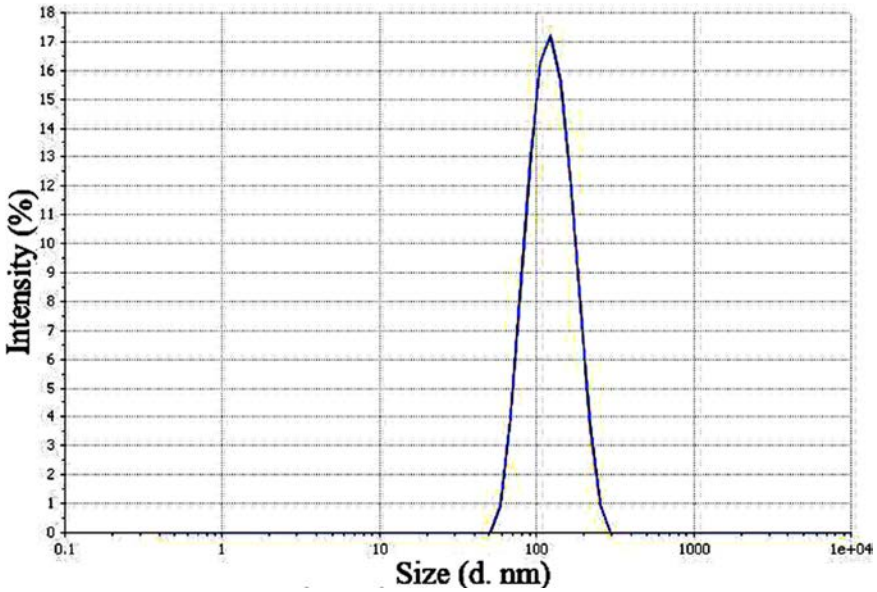

Figure 40. SIZE distribution of TTA. The average size was 119.3 nm.

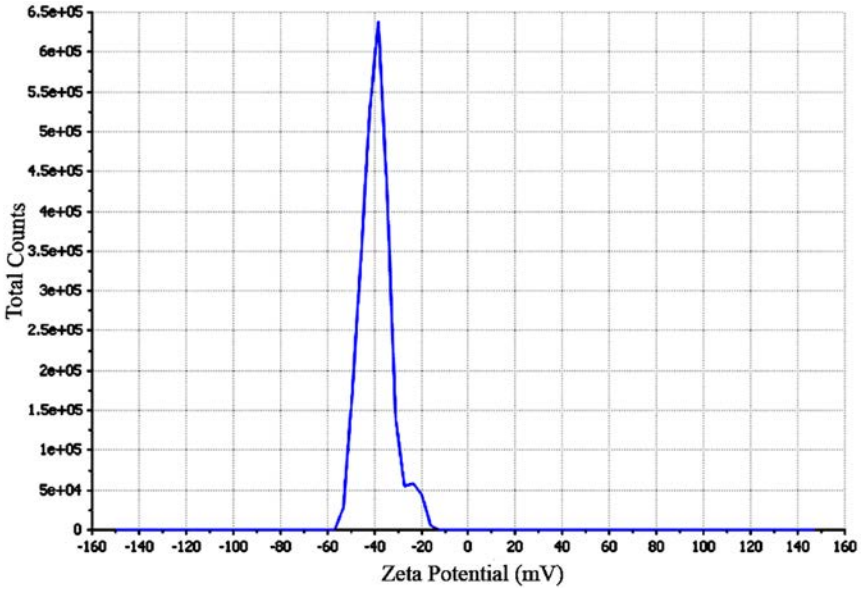

Figure 41. ZETA potential of TGA. The average zeta potential was -39.1 mV.

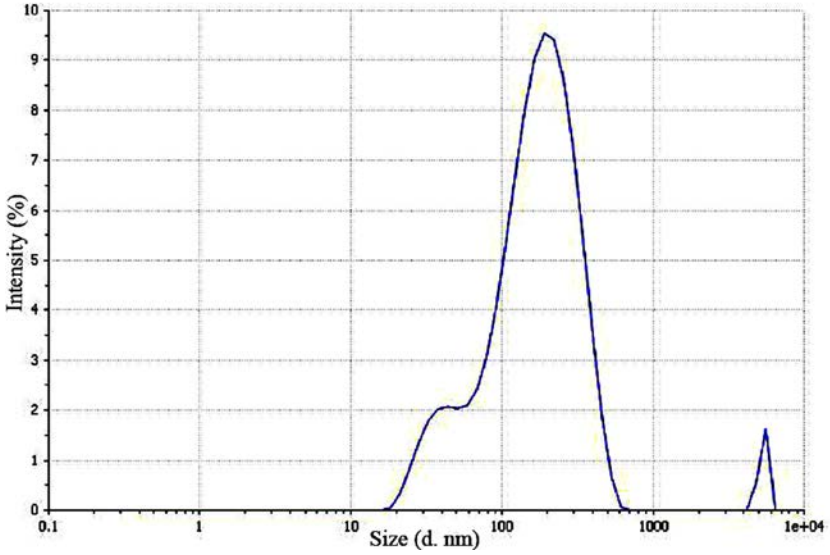

Figure 42. SIZE distribution of TGA. Z- average size= 145 nm (Broad size distribution).

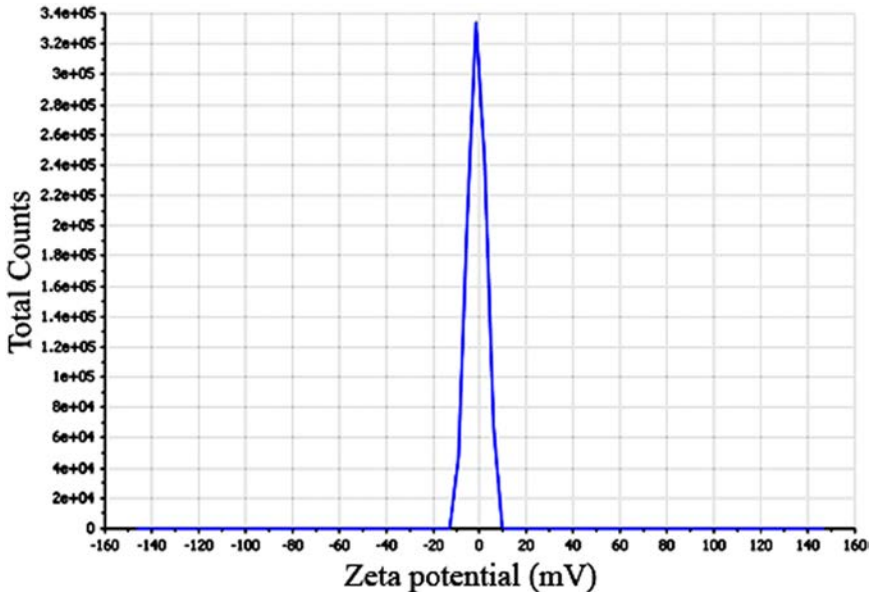

Figure 43. ZETA potential of C_3 was -1.27 mV.

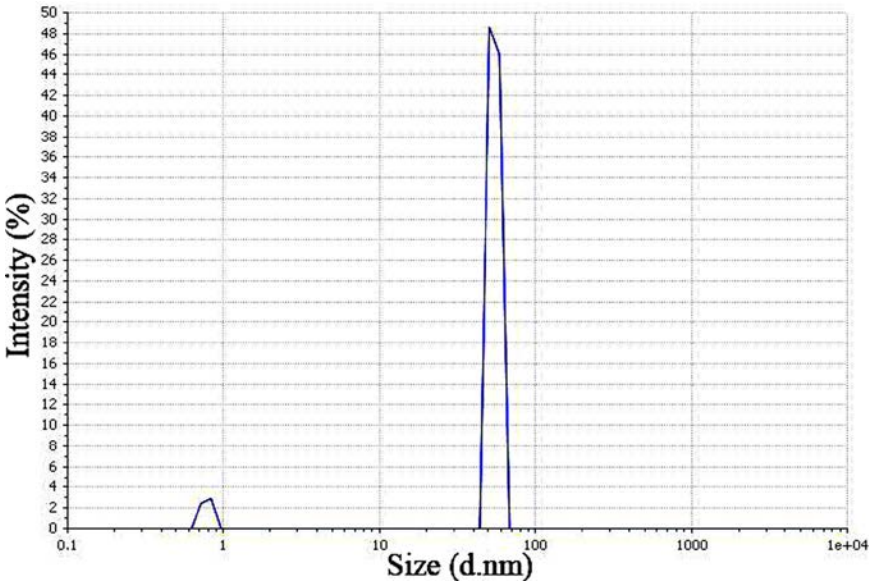

Figure 44. SIZE distribution of C_3.

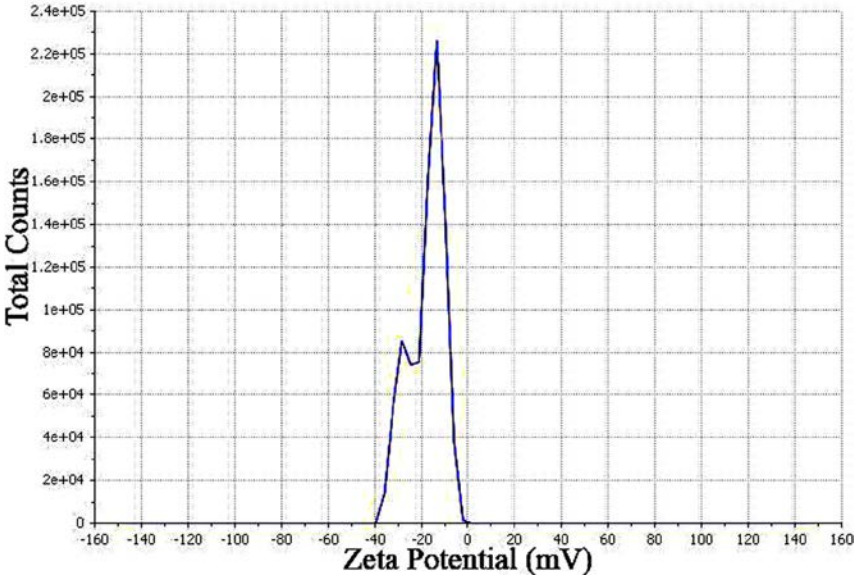

Figure 45. ZETA potential of $C_{70}OH_x$ was -17.8 mV.

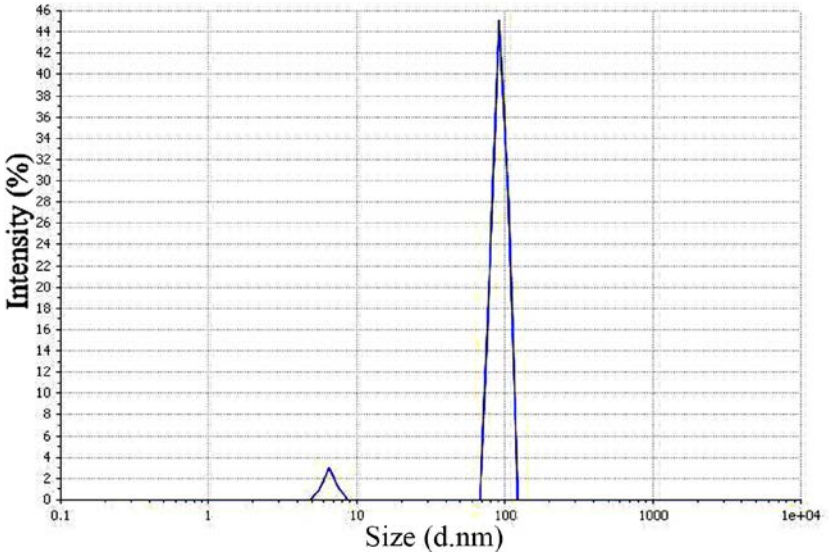

Figure 46. SIZE distribution of $C_{70}OH_x$.

CHAPTER V

CONCLUSION AND FUTURE STUDIES

The mechanism of antioxidant activity of fullerene derivatives was investigated for the first time (to our knowledge) using a non cellular assay, FRAP assay. The results showed that different fullerene derivatives ($C_{60}OH_x$, C_3, TTA and TGA) did not act as antioxidants by donating electrons, compared to primary antioxidant such as Vitamin C, however their free radical scavenging activity was detected using EPR spectroscopy (Electron paramagnetic resonance), which demonstrated the radical scavenging ability of fullerenes C_3 is similar to that of vitamin C. The previous results of both assays (FRAP and EPR) brings a new dimension to the definition of antioxidant and emphasis the distinction between antioxidant and antiradical activity of fullerene derivatives. We proposed a redox cycle of fullerenes similar to thioredoxin, showing that the reduced form of fullerene can acts as an actual reducing agent by donating its electron to neutralize ROS. This conclusion is very original and supports the identification of fullerenes as selective prooxidant toward ROS but not towards biological macromolecules.

Evaluating fullerenes activity in regard to primary antioxidants was considered very critical in drawing our conclusion regarding their activity. Based on this context, the radical quenching ability of fullerenes C_3 was less efficient than that of vitamin C as

shown by EPR spectroscopy results, this is similar to previous documented result indicating the less scavenging activity of fullerenes compared to natural enzymatic scavenging system, implying the effect of the experimental conditions (e.g. ambient light, storage) on their reaction.

The exposure of cells to either fullerenol or C_3 significantly suppressed functional NF-κB-driven gene expression in our model. By visualizing the nuclear translocation of exogenous NF-κB in cells stimulated with PMA and incubated with fullerenes, along with Western blot analysis, we concluded that fullerenes do not inhibit the cytoplasmic events of the NF-κB activation pathway. Indeed, they more likely inhibit closer to the downstream DNA binding step in the NF-κB pathway. This was revealed by monitoring the expression of an NF-κB targeted gene, detected by measuring PMA stimulated NF-κB gene expression in cells transfected with a NF-κB binding sequence vector, followed by fullerene treatment.

It is not clear how fullerenes inhibit NF-κB binding to DNA, but by considering the redox environment for NF-κB activity which is mediated by thioredoxin (Trx, a redox regulator of NF-κB which is translocated to the nucleus in response to PMA inducing NF-κB activation), fullerenes might inhibit the reducing enzyme (Trx reductase) resulting in an inhibition of NF-κB reduction and subsequently prevent its DNA binding. The previous prediction is based on our established knowledge about the role of Trx in reducing NF-κB in order to bind to DNA, and in relation to previous studies that

demonstrated the ability of fullerenes to bind to HIV-1 protease, showing their potential to act as enzyme inhibitors.

Based on the cytotoxicity tests conducted in this study, exposure to fullerene derivatives for 24 hours and up to 100 μM concentration produced negligible toxicity (detected by cell proliferation tests), moreover they did not produce ROS in cells.

However fullerenes derivatives caused a reduction in mitochondrial membrane potential. This effect might be cell type specific and or reversible over time, implying the need to test their effect on other cells. This affect does not seem to lead to reduced cell viability, based on our results from cell proliferation assays, therefore we conclude that at least in the short term, these fullerenes may be safe for use in biological system. However, the water soluble fullerenes did not demonstrate potent ROS antioxidant activity against oxidation induced by TBHP (product of lipid peroxidation).

There is a considerable challenge in studying the physical and chemical properties of water soluble fullerenes. Fullerenes derivatives with multiple moieties are often a mixture of many compounds. The high cost and low availability of fullerenes necessitates working on a very small scale. The tendency to form aggregates in aqueous media with a broad range of diameters is a general limitation for the elucidation and prediction of their activities. Because the behavior of fullerenes in solution is complicated, extensive studies are needed to investigate their electronic properties in solution in order to be able to determine their biological properties according to the surrounding biological environment.

Overall, this study contributes to the development of pharmacological uses of water soluble fullerenes, specifically as anti-inflammatory drugs. This has been confirmed (Chapter III) by showing their ability to modulate the activity of the redox transcription factor NF-κB. Based on our model, the ability to inhibit NF-κB activation pathway is most likely due to a direct or indirect action in the nucleus penultimate to DNA binding, since the active fullerene inhibitors of NF-κB fail to block its translocation into the nucleus. No inhibition of NF-κB cytoplasmic steps of the pathway was reported in this study.

Future Studies

This study highlights the need to conduct a combination of experimental and computational studies to confirm our results and to further enhance our understanding of the interactions of fullerene derivatives with the NF-κB activation pathway;

- Real time PCR (Polymerase Chain Reaction) and proteomics approaches can be used to present quantitative measurements of NF-κB activity stimulated by PMA under the influence of fullerene derivatives, by assessing the changes in gene expression of target genes. It is important to test the molecular events involved of the interaction of fullerene derivatives with NF-κB pathway.
- Other cellular and non-cellular antioxidant tests can be conducted such as: oxygen radical absorbance capacity (ORAC) assay, superoxide dismutase (SOD) assay, thioredoxin, thioredoxin reductase and catalase activity.

- Conduction of a more relevant system involving the use of human cells coupled with the detection of the endogenous NF-κB level under the influence of water soluble fullerenes.
- Computational modeling and simulation methods to study the effect of fullerene derivatives on the redox structure of NF-κB and the bound conformation of NF-κB with IκB inhibitor and DNA.
- Quantum mechanics calculation studies to detect the variation of the electronic structure among different fullerene derivatives and under the influence of the biological environment.

REFERENCES

1. *Nano and the top 10 big cosmetic companies: L'Oreal, Procter and Gamble and Henkel on the podium for patents*. 2009; Last cited 2/27/2014]. Available from: http://nanocolors.wordpress.com/2009/10/29/nano-the-top-10-big-cosmetics-companies-loreal-procter-gamble-and-henkel/.

2. *Nano and the top 10 big pharmaceutical companies: Merk, Pfizer, Johnson&Johnson and Novartis on the podium for patents*. 2009; Last cited 2/27/2014]. Available from: http://nanocolors.wordpress.com/2009/08/10/nano-the-top-10-big-pharmaceutical-companies-a-cautious-involvement/

3. Togashi, H., et al., *Analysis of hepatic oxidative stress status by electron spin resonance spectroscopy and imaging.* Free Radic Biol Med, 2000. **28**(6): p. 846-53.

4. Kroto, H.W., et al., *C60: Buckminsterfullerene.* Nature, 1985. **318**(6042): p. 162-163.

5. Kratschmer, W., et al., *Solid C60: a new form of carbon.* Nature, 1990. **347**(6291): p. 354-358.

6. Diederich, F., et al., *The Higher Fullerenes: Isolation and Characterization of C76, C84, C90, C94, and C70O, an Oxide of D5h-C70.* Science, 1991. **252**(5005): p. 548-551.

7. Piskoti, C., J. Yarger, and A. Zettl, *C36, a new carbon solid.* Nature, 1998. **393**(6687): p. 771-774.

8. Kroto, H.W., A.W. Allaf, and S.P. Balm, *C60: Buckminsterfullerene.* Chemical Reviews, 1991. **91**(6): p. 1213-1235.

9. Zhou, Z., et al., *Liposomal formulation of amphiphilic fullerene antioxidants.* Bioconjug Chem, 2010. **21**(9): p. 1656-1661.

10. Taylor, R. and D.R.M. Walton, *The chemistry of fullerenes.* Nature, 1993. **363**(6431): p. 685-693.

11. Buseck, P.R., S.J. Tsipursky, and R. Hettich, *Fullerenes from the Geological Environment.* Science, 1992. **257**(5067): p. 215-217.

12. Pizzarello, S., et al., *The Organic Content of the Tagish Lake Meteorite.* Science, 2001. **293**(5538): p. 2236-2239.

13. Milanez, D.H., et al., *Development of carbon-based nanomaterials indicators using the analytical tools and data provided by the web of science database.* Materials Research, 2013. **16**: p. 1282-1293.

14. Brant JF, L.J., Labille JF, Bottero JY, Bottero JF, Wiesner MR., *Characterizing the impact of preparation method on fullerene cluster structure and chemistry.* Langmuir, 2006. **22**(8): p. 3878-3885.

15. Deguchi S, A.R., Tsujii K,, *Stable dispersions of fullerenes, C60 and C70, in water, preparation and characterization.* Langmuir 2001. **17**: p. 6013-6017.

16. Makha, M., Purich, A., Raston, C. L. and Sobolev, A. N, *Structural Diversity of Host–Guest and Intercalation Complexes of Fullerene C60.* Eur. J. Inorg. Chem, 2005. **2006**: p. 507-517.

17. Bosi, S., et al., *Fullerene derivatives: an attractive tool for biological applications.* European Journal of Medicinal Chemistry, 2003. **38**(11–12): p. 913-923.

18. Da Ros, T. and M. Prato, *Medicinal chemistry with fullerenes and fullerene derivatives.* Chemical Communications, 1999(8): p. 663-669.

19. Nakamura, E. and H. Isobe, *Functionalized Fullerenes in Water. The First 10 Years of Their Chemistry, Biology, and Nanoscience.* Accounts of Chemical Research, 2003. **36**(11): p. 807-815.

20. Dugan, L.L., et al., *Buckminsterfullerenol free radical scavengers reduce excitotoxic and apoptotic death of cultured cortical neurons.* Neurobiol Dis, 1996. **3**(2): p. 129-35.

21. Dugan LL, T.D., Du C, Lobner D, Wheeler M, Almli CR, Shen CK, Luh TY, Choi DW, Lin TS, *Carboxyfullerenes as neuroprotective agents. .* Proc Natl Acad Sci U S A 1997. **94**: p. 9434–9439.

22. Badireddy AF, H.E., Chellam S, Alvarez P, Wiesner MR, *Inactivation of bacteriophages via photosensitization of fullerol nanoparticles.* Environ Sci Technol 2007. **41**: p. 6627–6632.

23. Friedman SH, D.D., Sijbesma R, Srdanov G, Wudl F, Kenyon GL, *Inhibition of the HIV-1 protease by fullerene derivatives: model building studies and experimental verification.* J. Am. Chem. Soc., 1993. **115**: p. 6506–6509.

24. Schinazi RF, et al., *Synthesis and virucidal activity of a water-soluble, configurationally stable, derivatized C60 fullerene.* Antimicrob. Agents Chemother, 1993. **37**(8): p. 1707-1710.

25. Tang, Y., et al., *Charge-associated effects of fullerene derivatives on microbial structural integrity and central metabolism.* Nano Lett, 2007. **7**(3): p. 754-760.

26. Huang, Y., et al., *Blockage of apoptotic signaling of transforming growth factor-beta in human hepatoma cells by carboxyfullerene.* Eur J Biochem., 1998. **254**(1): p. 38-43.

27. Tokuyama, H., et al., *Photoinduced biochemical activity of fullerene carboxylic acid.* Journal of the American Chemical Society, 1993. **115**(17): p. 7918-7919.

28. Bosi, S., et al., *Synthesis and anti-HIV properties of new water-soluble bis-functionalized[60]fullerene derivatives.* Bioorg Med Chem Lett, 2003. **13**(24): p. 4437-4440.

29. Liu, J., et al., *Preparation of PEG-conjugated fullerene containing Gd3+ ions for photodynamic therapy.* J Control Release, 2007. **117**(1): p. 104-110.

30. Bolskar, R., et al., *First soluble M@C60 derivatives provide enhanced access to metallofullerenes and permit in vivo evaluation of Gd@C60[C(COOH)2]10 as a MRI contrast agent.* J Am Chem Soc, 2003. **125**(18): p. 5471-5478.

31. Sayes, C., et al., *The Differential Cytotoxicity of Water-Soluble Fullerenes.* Nano Letters, 2004. **4**(10): p. 1881-1887.

32. Chiang, L.Y., et al., *Multi-hydroxy additions onto C60 fullerene molecules.* Journal of the Chemical Society, Chemical Communications, 1992(24): p. 1791-1793.

33. Chiang, L.Y., R.B. Upasani, and J.W. Swirczewski, *Versatile nitronium chemistry for C60 fullerene functionalization.* Journal of the American Chemical Society, 1992. **114**(26): p. 10154-10157.

34. Tsai, M., Chen YH, and L. Chiang, *Polyhydroxylated C60, fullerenol, a novel free-radical trapper, prevented hydrogen peroxide- and cumene hydroperoxide-elicited changes in rat hippocampus in-vitro.* J Pharm Pharmacol, 1997. **49**(4): p. 438-445.

35. Dalle-Donne, I., et al., *Biomarkers of oxidative damage in human disease.* Clin Chem, 2006. **52**(4): p. 601-623.

36. Dhalla, N., R. Temsah, and T. Netticadan, *Role of oxidative stress in cardiovascular diseases.* J Hypertens, 2000. **18**(6): p. 655-673.

37. Jenner, P., *Oxidative stress in Parkinson's disease.* Ann Neurol, 2003. **53**.

38. Sayre, L., M. Smith, and G. Perry, *Chemistry and biochemistry of oxidative stress in neurodegenerative disease.* Curr Med Chem, 2001. **8**(7): p. 721-738.

39. Halliwell, B. and J.M. Gutteridge, *The definition and measurement of antioxidants in biological systems.* Free Radic Biol Med, 1995. **18**: p. 125-6.

40. Harman, D., *Aging: a theory based on free radical and radiation chemistry.* J Gerontol, 1956. **11**(3): p. 298-300.

41. Blagosklonny, M. and M. Hall, *Growth and aging: a common molecular mechanism.* Aging (Albany NY), 2009. **1**(4): p. 357-362.

42. Dillin, A., et al., *Rates of behavior and aging specified by mitochondrial function during development.* Science, 2002. **298**(5602): p. 2398-2401.

43. Hamilton, B., et al., *A systematic RNAi screen for longevity genes in C. elegans.* Genes Dev., 2005. **19**(13): p. 1544-1555.

44. Lee, S., et al., *A systematic RNAi screen identifies a critical role for mitochondria in C. elegans longevity.* Nat. Genet., 2003. **33**(1): p. 40-48.

45. Heidler, T., et al., *Caenorhabditis elegans lifespan extension caused by treatment with an orally active ROS-generator is dependent on DAF-16 and SIR-2.1.* Biogerontology, 2010. **11**(2): p. 183-195.

46. Yang, W. and S. Hekimi, *A mitochondrial superoxide signal triggers increased longevity in Caenorhabditis elegans.* 2010(1545-7885 (Electronic)).

47. Olshansky, S.J., B.A. Hayflick L Fau - Carnes, and B.A. Carnes, *Position statement on human aging.* J Gerontol A Biol Sci Med Sci, 2002. **57**(8): p. 292-297.

48. Dizdaroglu, M., et al., *Free radical-induced damage to DNA: mechanisms and measurement.* Free Radic Biol Med, 2002. **32**(11): p. 1102-15.

49. Kohen, R. and A. Nyska, *Oxidation of biological systems: oxidative stress phenomena, antioxidants, redox reactions, and methods for their quantification.* Toxicol Pathol, 2002. **30**(6): p. 620-50.

50. Conte, M. and K. Carroll, *THE CHEMISTRY OF THIOL OXIDATION AND DETECTION* in *Oxidative Stress and Redox Regulation*. 2013, Dordrecht ; New York : Springer The Scripps Research Institute, Jupiter, FL 33458, United States. p. 1-42.

51. Kabe, Y., et al., *Redox regulation of NF-kappaB activation: distinct redox regulation between the cytoplasm and the nucleus.* Antioxid Redox Signal, 2005. **7**((3-4)): p. 395-403.

52. Mates, J.M., C. Perez-Gomez, and I. Nunez de Castro, *Antioxidant enzymes and human diseases.* Clin Biochem, 1999. **32**(8): p. 595-603.

53. Thomas, J., B. Poland, and R. Honzatko, *Protein sulfhydryls and their role in the antioxidant function of protein S-thiolation.* Arch Biochem Biophys, 1995. **319**(1): p. 1-9.

54. Winterbourn, C.C., *Reconciling the chemistry and biology of reactive oxygen species.* Nat Chem Biol, 2008. **4**(5): p. 278-286.

55. Heyland, D., et al., *Antioxidant nutrients: a systematic review of trace elements and vitamins in the critically ill patient.* Intensive Care Med., 2005. **31**(3): p. 327-337.

56. McCall, M.R. and B. Frei, *Can antioxidant vitamins materially reduce oxidative damage in humans?* Free Radic Biol Med, 1999. **26**(7-8): p. 1034-53.

57. Meyer, F., et al., *Antioxidant vitamin and mineral supplementation and prostate cancer prevention in the SU.VI.MAX trial.* Int. J. Cancer, 2005. **116**(2): p. 182-186.

58. Packer, L. and Y.J. Suzuki, *Vitamin E and alpha-lipoate: role in antioxidant recycling and activation of the NF-kappa B transcription factor.* Mol Aspects Med, 1993. **14**(3): p. 229-39.

59. Kasparova, S., et al., *Study of the oxidative stress in a rat model of chronic brain hypoperfusion.* Neurochem Int, 2005. **46**(8): p. 601-11.

60. Stadtman, E.R., *Protein oxidation and aging.* Free Radic Res, 2006. **40**(12): p. 1250-8.

61. Valko, M., et al., *Free radicals, metals and antioxidants in oxidative stress-induced cancer.* Chem Biol Interct., 2006. **160**(1): p. 1-40.

62. Krusic, P.J., et al., *Radical Reactions of C60.* Science, 1991. **254**(5035): p. 1183-1185.

63. McEwen, C., R. McKay, and B. Larsen, *C60 as a radical sponge.* Journal of the American Chemical Society, 1992. **114**(11): p. 4412-4414.

64. Andrievsky, G., et al., *Peculiarities of the antioxidant and radioprotective effects of hydrated C60 fullerene nanostuctures in vitro and in vivo.* Free Radic Biol Med, 2009. **47**(6): p. 786-793.

65. Ali, S.S., et al., *A biologically effective fullerene (C60) derivative with superoxide dismutase mimetic properties.* Free Radic Biol Med, 2004. **37**(8): p. 1191-202.

66. Dugan, L.L., et al., *Fullerene-based antioxidants and neurodegenerative disorders.* Parkinsonism Relat Disord, 2001. **7**(3): p. 243-246.

67. Liu, G.-F., et al., *High Catalytic Activity of Dendritic C60 Monoadducts in Metal-Free Superoxide Dismutation.* Angewandte Chemie International Edition, 2008. **47**(21): p. 3991-3994.

68. Baeuerle, P. and T. Henkel, *Function and activation of NF-kappa B in the immune system.* Annu Rev Immunol., 1994. **12**: p. 141-179.

69. Brennan, P. and L.A.J. O'Neill, *Effects of oxidants and antioxidants on nuclear factor κB activation in three different cell lines: evidence against a universal hypothesis involving oxygen radicals.* Biochimica et Biophysica Acta (BBA) - Gene Structure and Expression, 1995. **1260**(2): p. 167-175.

70. Schmidt, K.N., et al., *The roles of hydrogen peroxide and superoxide as messengers in the activation of transcription factor NF-kappa B.* Chem Biol., 1995. **2**(1): p. 13-22.

71. Suzuki, Y., Mizuno M, and L. Packer, *Transient overexpression of catalase does not inhibit TNF- or PMA-induced NF-kappa B activation.* Biochem Biophys Res Commun, 1995. **210**(2): p. 537-541.

72. Ito, K., et al., *Cigarette smoking reduces histone deacetylase 2 expression, enhances cytokine expression, and inhibits glucocorticoid actions in alveolar macrophages.* FASEB J., 2001. **15**(6): p. 1110-1112.

73. Rouse JG, Y.J., Ryman-Rasmussen JP, Barron AR, Monteiro-Riviere NA, *Effects of mechanical flexion on the penetration of fullerene amino acid-derivatized peptide nanoparticles through skin.* Nano Lett 2007. **7**(1): p. 155-160.

74. Quick, K.L., et al., *A carboxyfullerene SOD mimetic improves cognition and extends the lifespan of mice.* Neurobiol Aging, 2008. **29**(1): p. 117-28.

75. Dellinger, A., et al., *Fullerene nanomaterials inhibit phorbol myristate acetate-induced inflammation.* Exp Dermatol, 2009. **18**(12): p. 1079-81.

76. Norton, S.K., et al., *Epoxyeicosatrienoic acids are involved in the C(70) fullerene derivative-induced control of allergic asthma.* J Allergy Clin Immunol, 2012. **130**(3): p. 761-769.

77. Xiao, L., et al., *Antioxidant effects of water-soluble fullerene derivatives against ultraviolet ray or peroxylipid through their action of scavenging the reactive oxygen species in human skin keratinocytes.* Biomed Pharmacother, 2005. **59**(7): p. 351-358.

78. Lin, A.M., et al., *Carboxyfullerene prevents iron-induced oxidative stress in rat brain.* J Neurochem, 1999. **72**(4): p. 1634-40.

79. Liu, Q., et al., *C-Carboxyfullerenes as Efficient Antioxidants to Protect Cells against Oxidative-Induced Stress.* ACS Appl Mater Interfaces, 2013.

80. Holmgren, A. and J. Lu, *Thioredoxin and thioredoxin reductase: current research with special reference to human disease.* Biochem Biophys Res Commun, 2010. **396**: p. 120-4.

81. Inoue, M., et al., *Mitochondrial generation of reactive oxygen species and its role in aerobic life.* Curr Med Chem, 2003. **10**: p. 2495-505.

82. Lubos, E., J. Loscalzo, and D.E. Handy, *Glutathione peroxidase-1 in health and disease: from molecular mechanisms to therapeutic opportunities.* Antioxid Redox Signal, 2011. **15**: p. 1957-97.

83. Herrera, E., et al., *Aspects of antioxidant foods and supplements in health and disease.* Nutr Rev, 2009. **67 Suppl 1**: p. S140-4.

84. Lovat, R. and J. Preiser, *Antioxidant therapy in intensive care.* Curr Opin Crit Care, 2003. **9**(4): p. 266-270.

85. Wang, I., et al., *C(60) and water-soluble fullerene derivatives as antioxidants against radical-initiated lipid peroxidation.* J Med Chem, 1999. **42**(22): p. 4614-4620.

86. Seifert G, Vietze K, and Schmidt R, *Ionization energies of fullerenes—size and charge dependence.* J. Phys. B: At. Mol. Opt. Phys., 1996. **29**: p. 5183–5192.

87. Buhl, M. and A. Hirsch, *Spherical aromaticity of fullerenes.* Chem Rev, 2001. **101**(5): p. 1153-83.

88. Hamamoto, N., J. Jitsukawa, and C. Satoko, *Geometric Properties of Alkali-C60 Molecules.* Eur. Phys. J. D. , 2002. **19**: p. 211–221.

89. Ferguson, A.J., J.L. Blackburn, and N. Kopidakis, *Fullerenes and carbon nanotubes as acceptor materials in organic photovoltaics.* Materials Lett., 2013. **90**: p. 115-125.

90. Horie, M., et al., *In vitro evaluation of cellular influences induced by stable fullerene C70 medium dispersion: Induction of cellular oxidative stress.* Chemosphere, 2013. **93**(6): p. 1182-8.

91. Sayes, C.M., et al., *Nano-C60 cytotoxicity is due to lipid peroxidation.* Biomaterials, 2005. **26**(36): p. 7587-95.

92. Trpkovic, A., et al., *Oxidative stress-mediated hemolytic activity of solvent exchange-prepared fullerene (C60) nanoparticles.* Nanotechnology, 2010. **21**(37): p. 375102.

93. Usenko, C., S. Harper, and R. Tanguay, *Fullerene C60 exposure elicits an oxidative stress response in embryonic zebrafish.* Toxicol Appl Pharmacol, 2008. **229**(1): p. 44-55.

94. Zhou, Z., *Liposome formulation of fullerene-based molecular diagnostic and therapeutic agents.* Pharmaceutics, 2013. **5**(4): p. 525-41.

95. Benzie, I.F.F. and J.J. Strain, *The ferric reducing ability of plasma (FRAP) as a measure of "antioxidant power": the FRAP assay.* Analytical Biochemistry 1996. **239**: p. 70-76.

96. Thaipong K, B.U., Crosby K, Zevallos LC, Byrne DH, *Comparison of ABTS, DPPH, FRAP, and ORAC assays for estimating antioxidant activity from guava fruit extracts.* Journal of Food Composition and Analysis, 2006. **19**(6–7): p. 669-675.

97. Lin TS, D.L., Luh TY, *EPR studies of free radical reactions of carboxyfullerenes.* Appl. Magn. Reson., 2000. **18**: p. 321-331.

98. Yin JL, L.F., Fu PP, Wamer WG, Zhao YL, Wang PC, Qiu Y, Sun B, Xing G, Dong J, Liang XJ, Chen C., *The scavenging of reactive oxygen species and the potential for cell protection by functionalized fullerene materials.* Biomaterials 2009. **30**(4): p. 611-621.

99. Martínez, A., et al., *Donator acceptor map for carotenoids, melatonin and vitamins.* J Phys Chem 2008. **112** (38): p. 9037–9042.

100. Germany, A.s.f. *(C60-Fulleren 2 Uploaded by Diaa_abdelmoneim)*. Available from: http://commons.wikimedia.org/wiki/File%3AC60_Fullerene_solution.jpg.

101. Halliwell, B. and J. Gutteridge, *Free Radicals in Biology and Medicine*. 2007, Oxford University Press. p. 888.

102. Mroz, P., et al., *Functionalized fullerenes mediate photodynamic killing of cancer cells: Type I versus Type II photochemical mechanism.* Free Radic Biol Med, 2007. **43**(5): p. 711-719.

103. Yang, J., et al., *Fullerene-derivatized amino acids: synthesis, characterization, antioxidant properties, and solid-phase peptide synthesis. .* Chemistry, 2007. **13**(9): p. 2530-2545.

104. Chiang, L.Y., F.-J. Lu, and J.-T. Lin, *Free radical scavenging activity of water-soluble fullerenols.* Journal of the Chemical Society, Chemical Communications, 1995(12): p. 1283-1284.

105. Djordjević A, C.B., Vojinovic MM, Bogdanovic G *Antioxidant properties and hypothetical radical mechanism of fullerenol C60(OH)24. .* Oxidation Communications 2004. **27**(4): p. 806-812.

106. Enes, R., et al., *Synthesis and antioxidant activity of [60]fullerene–flavonoid conjugates. .* Tetrahedron, 2009. **65**(1): p. 253-262.

107. Enes, R.F., et al., *Synthesis and antioxidant activity of [60]fullerene-BHT conjugates.* Chemistry, 2006. **12**(17): p. 4646-53.

108. Mirkov, S.M., et al., *Nitric oxide-scavenging activity of polyhydroxylated fullerenol, C60(OH)24.* Nitric Oxide, 2004. **11**(2): p. 201-7.

109. Shi, Z., et al., *Synthesis and antioxidant properties of polyphenol-fullerenes.* Chinese Science Bulletin, 2001. **46**(21): p. 1790-1792.

110. SUN Dayong, Z.Y., LIU Ziyang, LIU Guizhen, GUO Xinghua, ZHAN Ruiyun, LIU Shuying, *Active oxygen radical scavenging ability of water-soluble fullerenols.* Chinese Science Bulletin, 1997. **42**(9): p. 748-752.

111. Koppenol, W.H., *The Haber-Weiss cycle--70 years later.* Redox Rep, 2001. **6**(4): p. 229-34.

112. Harman, D., *The free radical theory of aging.* Antioxid Redox Signal, 2003. **5**(5): p. 557-61.

113. Harman, D., *Free radical theory of aging: an update: increasing the functional life span.* Ann N Y Acad Sci, 2006. **1067**: p. 10-21.

114. Kabe, Y., et al., *Redox regulation of NF-kappaB activation: distinct redox regulation between the cytoplasm and the nucleus.* Antioxidants & Redox Signaling 2005. **7**: p. 395-403.

115. Winterbourn, C., *Reconciling the chemistry and biology of reactive oxygen species.* Nat Chem Biol, 2008. **4**(5): p. 278-286.

116. Di Simplicio, P., et al., *Role of protein -SH groups in redox homeostasis--the erythrocyte as a model system.* Arch Biochem Biophys, 1998. **355**(2): p. 145-52.

117. Hansen, R.E., D. Roth, and J.R. Winther, *Quantifying the global cellular thiol-disulfide status.* Proc Natl Acad Sci U S A, 2009. **106**(2): p. 422-7.

118. Requejo, R., et al., *Cysteine residues exposed on protein surfaces are the dominant intramitochondrial thiol and may protect against oxidative damage.* FEBS J, 2010. **277**(6): p. 1465-80.

119. Schroder, K., et al., *Nox1 mediates basic fibroblast growth factor-induced migration of vascular smooth muscle cells.* Arterioscler Thromb Vasc Biol, 2007. **27**(8): p. 1736-43.

120. Sen, R. and D. Baltimore, *Multiple nuclear factors interact with the immunoglobulin enhancer sequences.* Cell, 1986. **46**(5): p. 705-16.

121. Perkins, N.D., *The Rel/NF-kappa B family: friend and foe.* Trends Biochem Sci, 2000. **25**(9): p. 434-40.

122. Scheidereit, C., *IkappaB kinase complexes: gateways to NF-kappaB activation and transcription.* Oncogene, 2006. **25**(51): p. 6685-705.

123. Baud, V., et al., *Signaling by proinflammatory cytokines: oligomerization of TRAF2 and TRAF6 is sufficient for JNK and IKK activation and target gene induction via an amino-terminal effector domain.* Genes Dev, 1999. **13**(10): p. 1297-308.

124. Oeckinghaus, A. and S. Ghosh, *The NF-kappaB family of transcription factors and its regulation.* Cold Spring Harb Perspect Biol, 2009. **1**(4): p. 1-14.

125. Rade, I., et al., *Bioapplication and activity of fullerenol C60(OH)24.* African Journal of Biotechnology, 2008. **7**(25): p. 4940-4050.

126. Rawashdeh, R., et al., *The fullerene paradox: biological antioxidants with low inherent reducing ability.* Submitted for publication, 2014.

127. Xiao, L., et al., *Activity of the dietary antioxidant ergothioneine in a virus gene-based assay for inhibitors of HIV transcription.* Biofactors, 2006. **27**(1-4): p. 157-65.

128. Gloire, G., S. Legrand-Poels, and J. Piette, *NF-kappaB activation by reactive oxygen species: fifteen years later.* Biochem Pharmacol, 2006. **72**(11): p. 1493-505.

129. Siomek, A., *NF-kappaB signaling pathway and free radical impact.* Acta Biochim Pol, 2012. **59**(3): p. 323-331.

130. Suzuki, Y., B. Aggarwal, and L. Packer, *Alpha-lipoic acid is a potent inhibitor of NF-kappa B activation in human T cells.* Biochem Biophys Res Commun, 1992. **189**(3): p. 1709-1715.

131. Hayakawa, M., et al., *Evidence that reactive oxygen species do not mediate NF-κB activation.* EMBO J. , 2003. **22**(13): p. 3356–3366.

132. Xiao, L., et al., *Fullerene-polyvinylpyrrolidone clathrate localizes in the cytoplasm to prevent Ultraviolet-A ray-induced DNA-fragmentation and activation of the transcriptional factor NF-kappaB.* J Cell Biochem, 2010. **111**(4): p. 955-66.

133. Oka, S., et al., *N-acetylcysteine suppresses TNF-induced NF-kappaB activation through inhibition of IkappaB kinases.* FEBS Lett, 2000. **472**(2-3): p. 196-202.

134. Zhang, W. and B. Frei, *α-Lipoic acid inhibits TNF-α-induced NF-κB activation and adhesion molecule expression in human aortic endothelial cells.* The FASEB Journal, 2001. **15**(13): p. 2423-2432.

135. Chandrasekaran, V. and E. Taylor, *Molecular modeling of the oxidized form of nuclear factor-kappa B suggests a mechanism for redox regulation of DNA binding and transcriptional activation.* J Mol Graph Model, 2008. **26**(5): p. 861-7.

136. Nakagawa, Y., et al., *Effects of N-acetyl-L-cysteine on target sites of hydroxylated fullerene-induced cytotoxicity in isolated rat hepatocytes.* Arch Toxicol, 2014. **88**(1): p. 115-26.

137. Ehrich, M., et al., *Fullerene antioxidants decrease organophosphate-induced acetylcholinesterase inhibition in vitro.* Toxicol In Vitro, 2011. **25**(1): p. 301-7.

138. Fujita, K., et al., *Gene expression profiles in rat lung after inhalation exposure to C60 fullerene particles.* Toxicology, 2009. **258**(1): p. 47-55.

139. Rancan, F., et al., *Fullerene-pyropheophorbide a complexes as sensitizer for photodynamic therapy: uptake and photo-induced cytotoxicity on Jurkat cells.* J Photochem Photobiol B, 2005. **80**(1): p. 1-7.

140. Isakovic, A., et al., *Distinct cytotoxic mechanisms of pristine versus hydroxylated fullerene.* Toxicol Sci, 2006. **91**(1): p. 173-83.

141. Levi, N., et al., *C60-fullerenes: detection of intracellular photoluminescence and lack of cytotoxic effects.* J Nanobiotechnology, 2006. **4**(14): p. 11.

142. Zhu, S., E. Oberdorster, and M.L. Haasch, *Toxicity of an engineered nanoparticle (fullerene, C60) in two aquatic species, Daphnia and fathead minnow.* Mar Environ Res, 2006. **62 Suppl**: p. S5-9.

143. Lyon, D., et al., *Antibacterial Activity of Fullerene Water Suspensions (nC60) Is Not Due to ROS-Mediated Damage.* Nano Letters, 2008. **8**(5): p. 1539-1543.

144. Monteiro-Riviere, N.A. and A.O. Inman, *Challenges for assessing carbon nanomaterial toxicity to the skin.* Carbon, 2006. **44**(6): p. 1070-1078.

145. Monteiro-Riviere, N.A., A.O. Inman, and L.W. Zhang, *Limitations and relative utility of screening assays to assess engineered nanoparticle toxicity in a human cell line.* Toxicol Appl Pharmacol, 2009. **234**(2): p. 222-35.

146. Cai, X., et al., *Polyhydroxylated fullerene derivative C(60)(OH)(24) prevents mitochondrial dysfunction and oxidative damage in an MPP(+) -induced cellular model of Parkinson's disease.* J Neurosci Res, 2008. **86**(16): p. 3622-34.

147. Dobrovolskaia, M.A. and S.E. McNeil, *Immunological properties of engineered nanomaterials.* Nat Nanotechnol, 2007. **2**(8): p. 469-78.

148. Markovic, Z. and V. Trajkovic, *Biomedical potential of the reactive oxygen species generation and quenching by fullerenes (C60).* Biomaterials, 2008. **29**(26): p. 3561-73.

149. K, S., et al., *Cytotoxic Effects of Hydroxylated Fullerenes in Three Types of Liver Cells.* Materials 2013. **6**: p. 2713-2722.

150. Sergio M, et al., *Fullerenes Toxicity and Electronic Properties. .* Environ. Chem. Lett., 2013. **11**: p. 105–118.

151. Michael D. Diener and J.M. Alford., *Isolation and properties of small-bandgap fullerenes.* Nature, 1998. **393**: p. 668-671.

152. Yang, Y., et al., *Reversible Fullerene Electrochemistry: Correlation with the HOMO-LUMO Energy Difference for C60, C70, C76, C78, and C84.* Journal of the American Chemical Society, 1995. **117**(29): p. 7801-7804.

153. Taylor, R. and D. Walton, *The chemistry of fullerenes.* Nature, 1993. **363**(6431): p. 685-693.

154. Semenov, K.N., et al., *The synthesis and identification of mixed fullerenol prepared by the direct one-stage oxidation of fullerene black.* Russian Journal of Physical Chemistry A, 2011. **85**(6): p. 1009-1015.

155. Sardenberg, R.B., et al., *Nonlinear conductivity of fullerenol aqueous solutions.* ACS Nano, 2011. **5**(4): p. 2681-6.

156. Vileno, B., et al., *Cover Picture: Spectroscopic and Photophysical Properties of a Highly Derivatized C60 Fullerol (Adv. Funct. Mater. 1/2006).* Advanced Functional Materials, 2006. **16**(1): p. n/a-n/a.

157. http://en.wikipedia.org/wiki/Matrix-assisted_laser_desorption/ionization. [cited 2014].

158. Marvin, L., M. Roberts, and Fay LB, *Matrix-assisted laser desoprtion/ionization time-of-flight mass spectrometry in clinical chemistry.* Clinica Chimica Acta, 2003. **337**: p. 11-21.

159. Monteiro-Riviere, N.A., et al., *Lack of hydroxylated fullerene toxicity after intravenous administration to female Sprague-Dawley rats.* J Toxicol Environ Health A, 2012. **75**(7): p. 367-73.

160. Togashi H, S.H., Matsuo T, Takeda Y, Takahashi T, Aoyama M, Oikawa K, Kamada H., *Analysis of hepatic oxidative stress status by electron spin resonance spectroscopy and imaging.* Free Radical Bio. Med, 2000. **28**(6): p. 846-853.

161. E, F., R. GM, and R. EJ, *Spin Trapping. Kinetics of the Reaction of Superoxide and Hydroxyl Radicals with Nitrones.* J. Am. Chem. SOC., 1980. **102**: p. 4994-4999.

APPENDIX A

EPR AND FRAP ASSAYS

An electron paramagnetic resonance EPR is often called electron spin resonance ESR, it is analogous to nuclear magnetic resonance spectroscopy NMR but instead of the measurement of the nuclear transition, EPR is specific for the detection of unpaired electron of chemical species such as free radicals and transition metal ions. EPR spectroscopy detects the unpaired electron in an applied magnetic field and is sensitive to reaction condition of the unpaired electron.

EPR machine consists of a microwave radiation source known as klystron which is a stable vacuum tube, the majority of EPR works at 9.5 GHz, the sample is placed in a cavity where it being subjected to a microwave radiation, the weak signal is amplified by an amplifier, absorption lines are detected by a detector when separation of energy level is equal to the frequency of the incident microwave photons. EPR spectrometer measures the absorption of electromagnetic radiation and by using a phase sensitive detector the absorption spectrum is converted to its first derivative in the spectrum. EPR spectrum results by applying a constant frequency of radiation and varying the magnetic field which is represented on the axis of EPR spectrum using the unit gauss (G). The center of the EPR signal at zero corresponds to the absorption peak of the absorption spectrum (Figure 4).

EPR spectroscopy is based on an intrinsic spin property of an electron that gives rise to the magnetic moment of the electron. S is the spin quantum number, and under the application of a magnetic field B_0, two spin states of electron, M_S, results with different

energies or what is called Zeeman effect. The unpaired electron has either parallel orientation at the lower energy level, the alignment of the electron magnetic moment with the magnetic field represented by M_S= -1/2, or antiparallel orientation at the higher energy level, the alignment of the electron magnetic moment against the magnetic field represented by M_S= +1/2. The energy status of the unpaired electron is represented by the following equation;

$$E = \pm 1/\ 2g\beta B_0$$

Where g (g-factor) equals~2.0, β = the Bohr magneto, and B_0 is the applied magnetic field. For measuring the separation between two spin levels of energy, the frequency of microwave irradiation is typically held constant while sweeping the external magnetic field. The absorption spectrum results from the transition of an electron from the lower state to the higher state (Figure 47. A). The spectroscopy is represented with different line shapes and characteristics depending on different factors including the local environment of the unpaired electron.

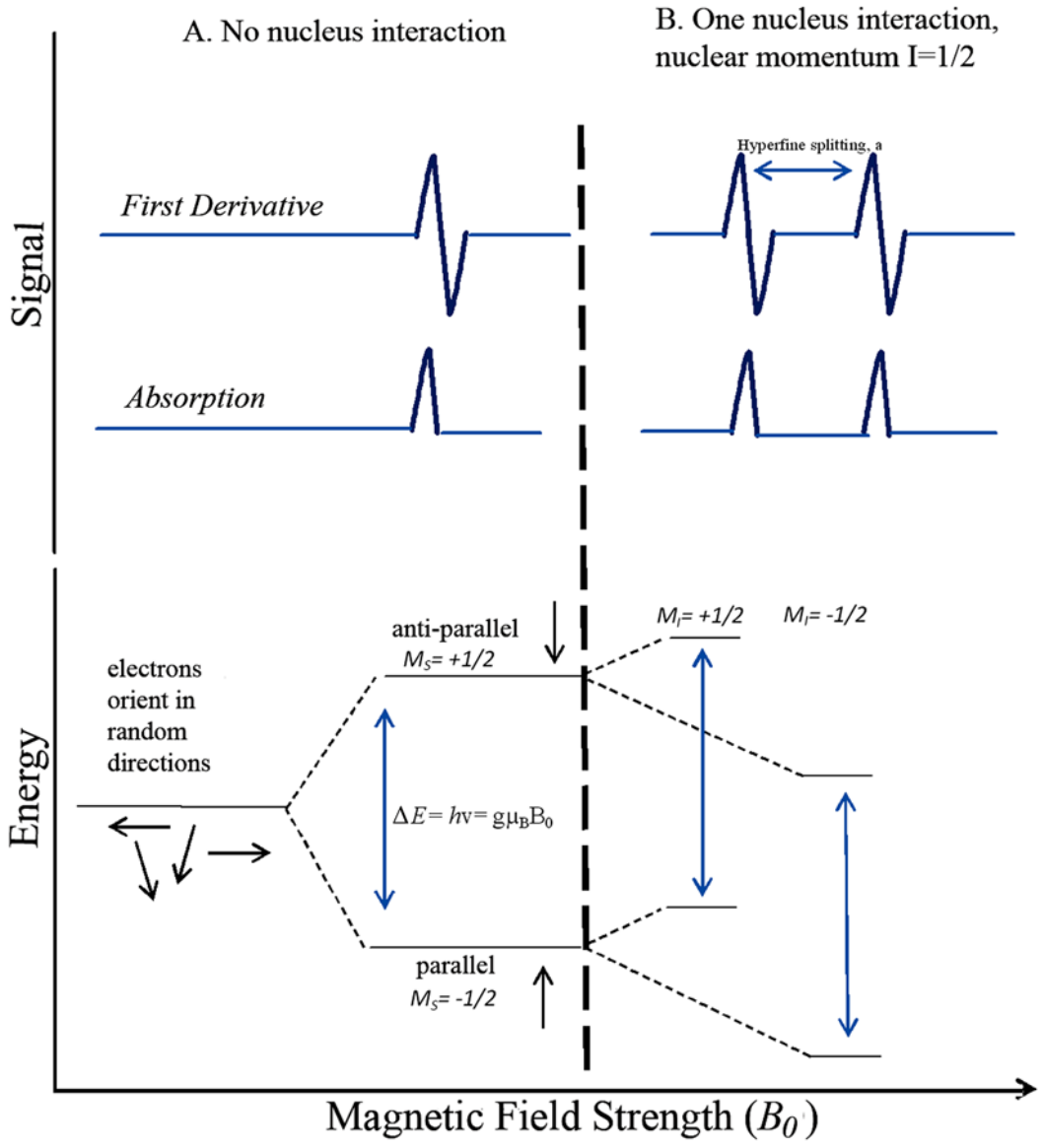

Figure 47. Generation of EPR spectra.

Because of the hyperfine interaction which is the interaction between the electron and the nucleus. The electron is under the effect of the magnetic field of the applied field and of the nucleus causing the Zeeman level to split as a result of hyperfine splitting by the value of the nuclear spin quantum number. So the equation is extended further as a result of hyperfine interaction, this gives information about the identity and number of nuclei and their distance from the unpaired electron.

$$E = \pm 1/\ 2g\beta B + aM_S M_I$$

where *a* is the hyperfine coupling constant, the distance between the centers of two signals and M_I is the nuclear spin quantum number for the neighboring nucleus. EPR spectrum of the free electron changes and split additionally. The nuclear spin and the number of lines in the spectrum is determined by 2NI+1, N= number of equivalent nuclei interacting and I is the spin, so for a single nucleus with I = ½ will split each energy level into two, giving 2 absorption lines (representing two transitions) for one nucleus interaction (Figure 47. B). Certain atomic nuclei have certain values of I but the common spin is 1/2. The determination of the relative intensities of lines in the spectra depends on the number of interacting nuclei. In a case of multiple nuclei interacting with a spin ½, the intensities follow binomial distribution.

The enzyme/substrate system xanthine/xanthine oxidase was used to determine the ROS generation by fullerene derivatives. As most of radical species are difficult to detect because of their short life span, DMPO (5,5-dimethyl-1-pyrolline-N-oxide) spin trapping reagent is used for radicals detection by forming a persistent aminoxyl spin

adduct which have longer life-span. Xanthine oxidase (XO) oxidizes xanthine to uric acid [160]. In the presence of spin trapping agent DMPO, DMPO-·OOH adduct formed and the detection of this adduct corresponds to superoxide production (Figure 12).

Hydroxyl adduct DMPO-·OH which originates from hyperfine intereaction of an electron spin with a 15N nucleus spin and a 1H nucleus spin with similar coupling results in the formation of 1:2:2:1 quartet peaks indicating hydroxyl adduct formation, while the hyperfine interaction results in different coupling in superoxide addut DMPO-·OOH represented by a different spectrum intensity (Figure 12). Because DETAPAC (diethylenetriaminepentaacetic acid) inhibits the formation of hydroxyl adduct DMPO-·OH [161], it is used to verify the detection of superoxide adducts rather than hydroxyl ones.

The use of 40 μM concentration of different fullerene derivatives did not result in reducing radical signal as demosntrated by EPR spectra in figures: 48, 49, 50, 51 & 52.

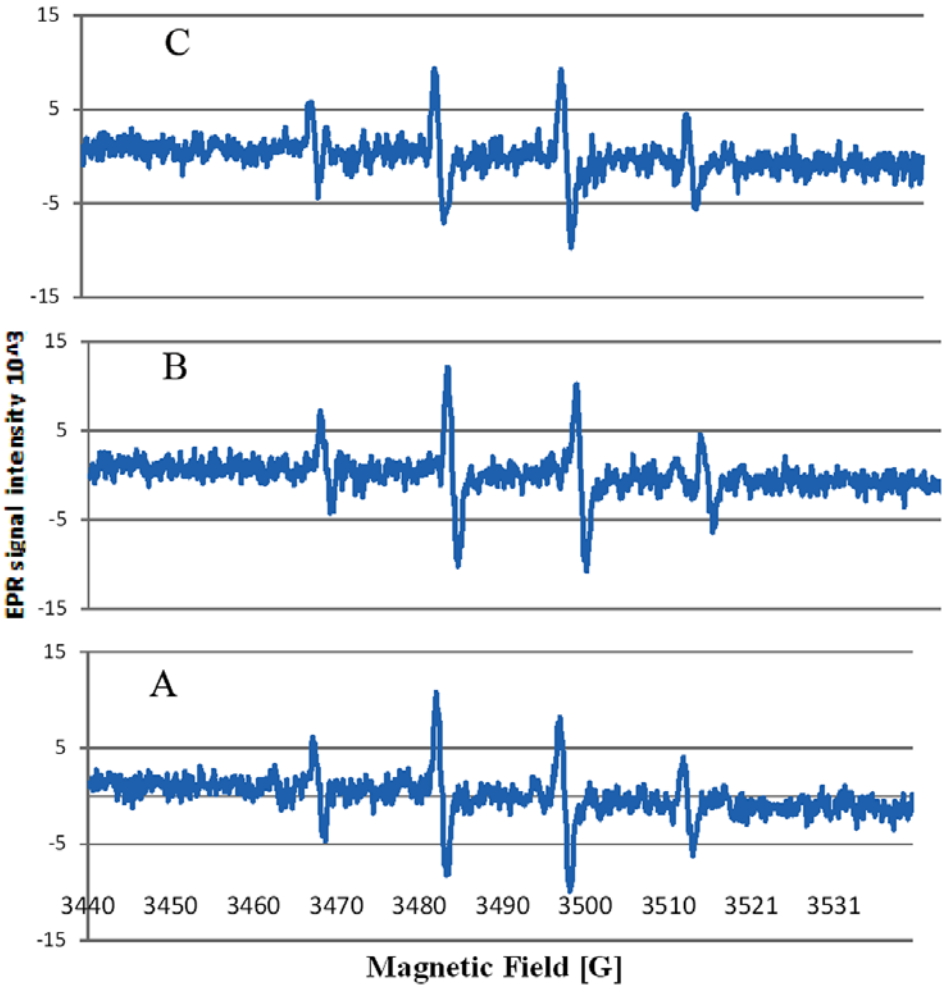

Figure 48. EPR spectra of DMPO-·OOH (Hydroxyl adduct) generated by the decomposition of superoxide adduct from xanthine/xanthine oxidase in the presence of DMPO only in PBS as the control (A), with the addition of 40 µM of TTA (B) and TGA (C) fullerenes derivatives.

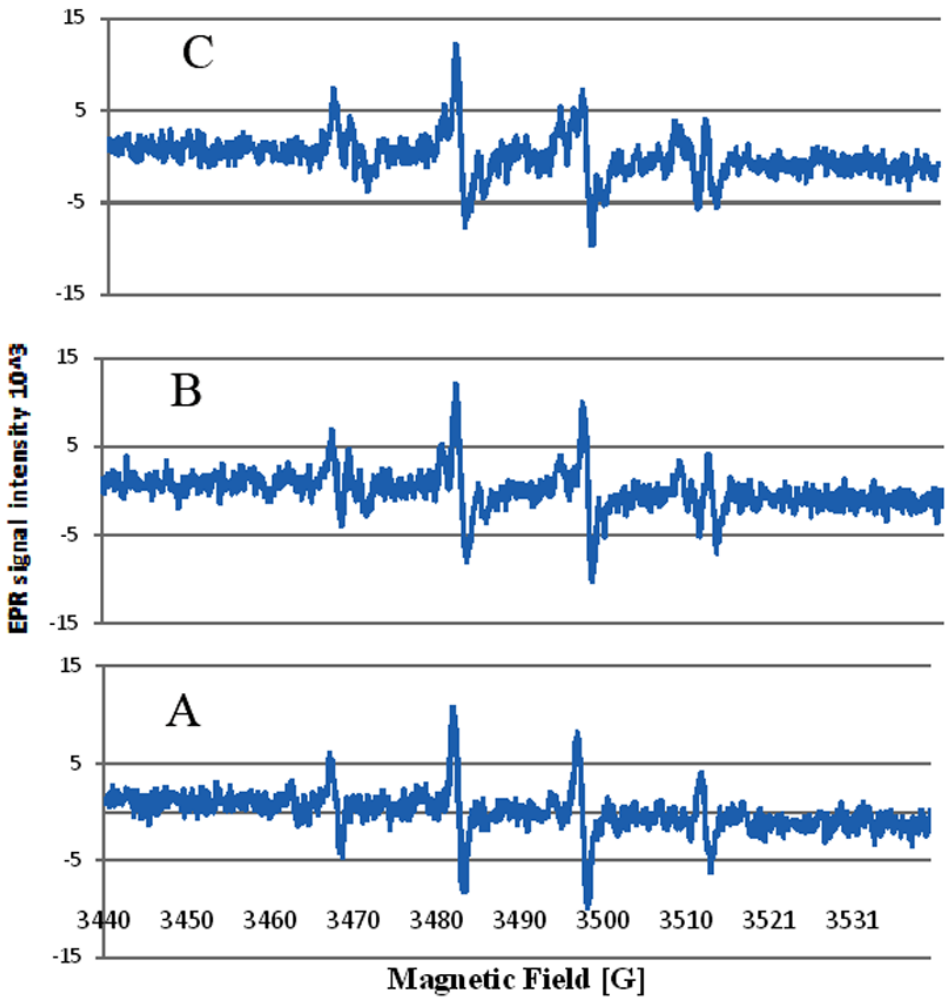

Figure 49. EPR spectra of DMPO-·OOH (Hydroxyl adduct) generated by the decomposition of superoxide adduct from xanthine/xanthine oxidase in the presence of DMPO only in PBS as the control (A), with the addition of 40 µM of C_3 (B) and $C_{60}OH_x$ (C) fullerene derivatives.

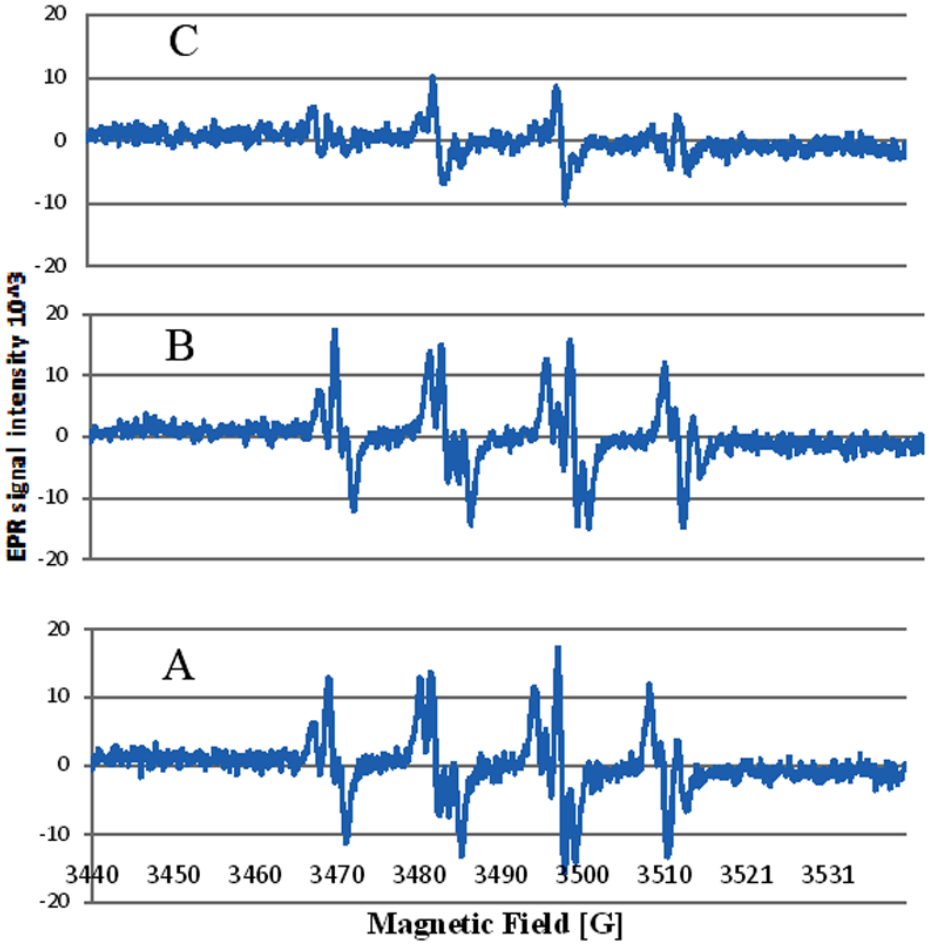

Figure 50. EPR spectra of DMPO-·OH (superoxide adduct) generated from xanthine/xanthine oxidase in the presence of 1mM DETAPAC and DMPO in PBS as the control (A) and in the presence of 40 µM NAC (B) and 10 mM NAC (C).

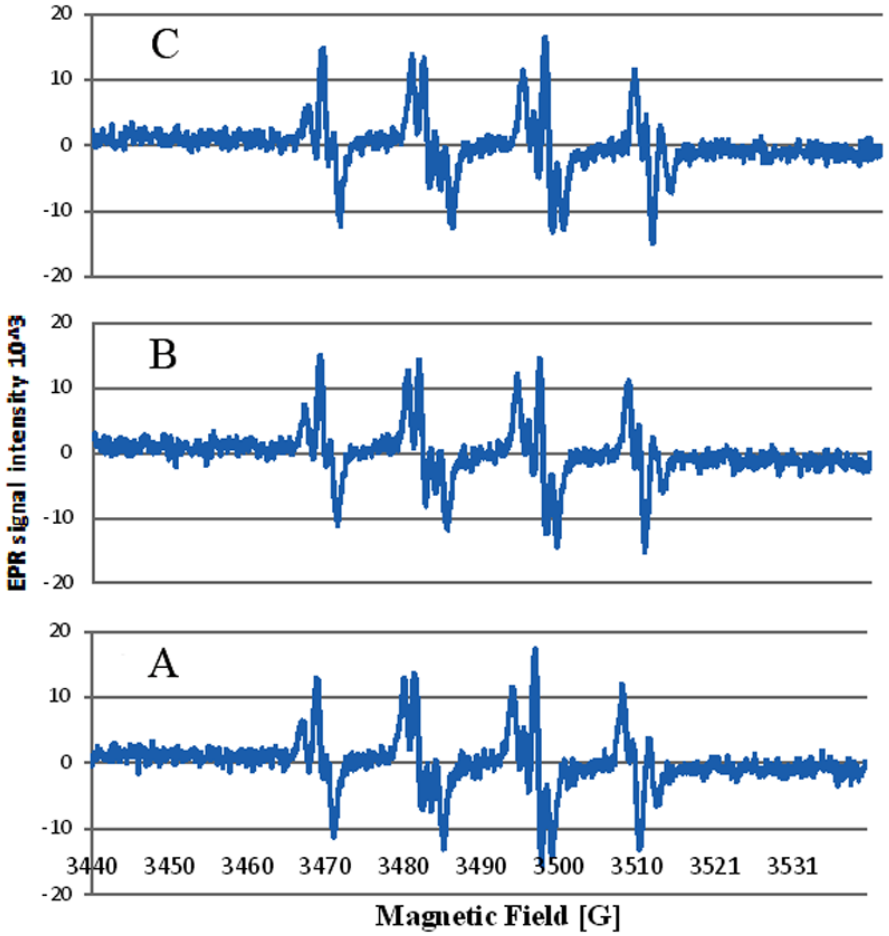

Figure 51. EPR spectra of DMPO-·OH (superoxide adduct) generated from xanthine/xanthine oxidase in the presence of 1mM DETAPAC and DMPO in PBS as the control (A) and in the presence of 40 µM of TTA (B) and TGA (C) fullerenes derivatives.

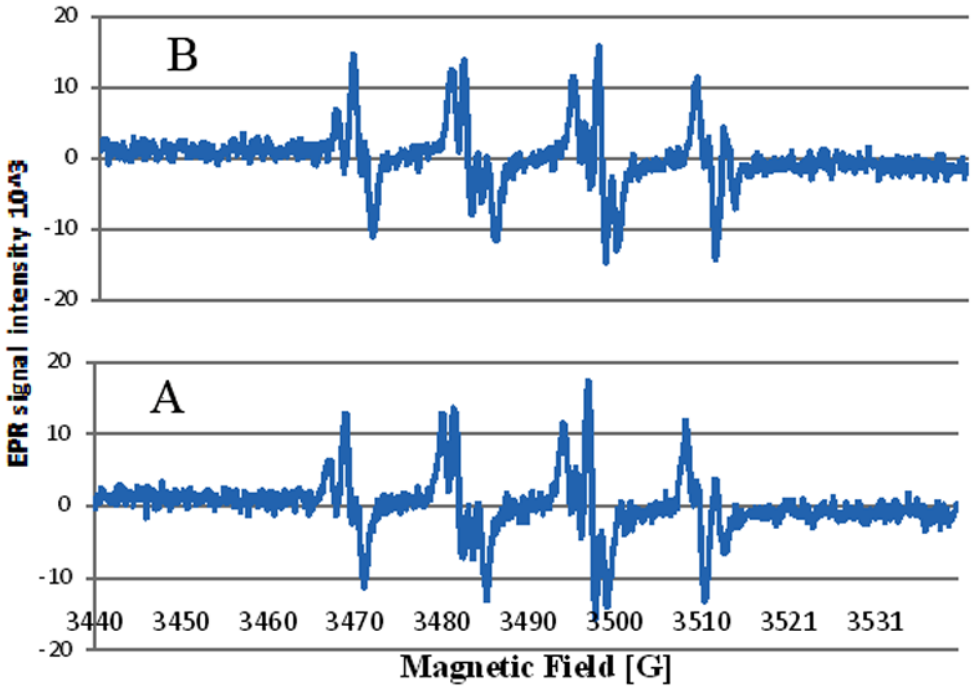

Figure 52. EPR spectra of DMPO-·OH (superoxide adduct) generated from xanthine/xanthine oxidase in the presence of 1mM DETAPAC and DMPO in PBS as the control (A) and in the presence of 40 µM of $C_{60}OH_x$ (B).

Table 3. EPR reaction mixtures of hydroxyl generation; volumes and concentrations

Reagent, stock solution	**Concentration required**	**Volume (µl)**				
		Control	$C_{60}OH_x$ (872.7 µM)	C_3 (784 µM)	TGA (784 µM)	TTA (538 µM)
PBS, 0.1 M (pH 7.4)		8.75	8.635	7.48	7.47	6.9
Xanthine solution in PBS (1 mM)	0.5 mM	12.5	12.5	12.5	12.5	12.5
DMPO, 1 M in PBS	100 mM	2.5	2.5	2.5	2.5	2.5
Xanthine oxidase (1 units/ml)	0.05 units/ml	1.25	1.25	1.25	1.25	1.25
Water soluble fullerenes	40 µM	0.0	0.115	1.27	1.275	1.858
Total volume reaction*		25 µl				

* The total volume was set to 35 µl for some reactions of EPR spectroscopy

Table 4. EPR reaction mixtures of superoxide generation: volumes and concentrations

Reagent, stock solution	**Concentration required**	**Volume (µl)**				
		Control	$C_{60}OH_x$ (872.7 µM)	C_3 (784 µM)	TGA (784 µM)	TTA (538 µM)
PBS, 0.1 M (pH 7.4)		8.75	6.635	5.48	5.47	4.9
Xanthine solution in PBS (1 mM)	0.5 mM	12.5	12.5	12.5	12.5	12.5
DMPO, 1 M in PBS	100 mM	2.5	2.5	2.5	2.5	2.5
Xanthine oxidase (1 units/ml)	0.05 units/ml	1.25	1.25	1.25	1.25	1.25
DETAPAC in PBS (12.5 M)	1mM	2.0	2.0	2.0	2.0	2.0
Water soluble fullerenes	40 µM	0.0	0.115	1.27	1.275	1.858
Total volume reaction*		25 µl				

* The total volume was set to 35 µl for some reactions of EPR spectroscopy

Preparation of Fullerenes:

The concentration of stock solution of water soluble fullerenes was 1 mg/ml. Molecular weight for hydroxylated fullerenes was calculated based on predicting the number of OH group, in case of C_{60} hydroxylated fullerenes, (C_{60}-OH LnW-0564, C-

nanomaterials) with 25 OH groups, the molecular weight ≈ 1145.8312 g/mol. Thus the molarity is;

$M = (0.001\ g)/(1145.8312\ g/mole)/(.001\ L) = 8.727 \times 10^{-4}\ M$

FRAP of Fullerenes:

Figure 53. FRAP assay result showing the color change in a plate. Vitamin C turns yellow to blue as a result of reduction of ferric to ferrous, while TTA, TGA and $C_{70}OH_x$ did not turn the color into blue indicating that there is no reduction activity occurred.

APPENDIX B

CELL CULTURE AND CYTOTOXICITY OF FULLERENE DERIVATIVES

MDCK Cell culture and passaging

Madin Darby Canine Kidney, MDCK cells were purchased from American Type Cell Culture ATCC (Catalog No. CCL-34, CCL-34). MDCK cells are epithelial cells (Figure 54) obtained from kidney tissue from *Canis familiaris* (adult female). Common property of MDCK is the exhibition of high transfection efficiency, so it useful for studying the expression of exogenous genes and virus propagation.

MDCK cells were grown in Minimum Essential Medium (MEM) or Dulbecco's Modification of Eagle's Medium, DMEM, 1X (4.5 g/L glucose & sodium pyruvate without L-glutamine & phenol red) (catalogue no. 17-205-CV, Cellgro, Mediatech, Inc, Manassas, VA 20109), this media was supplemented with 2 mM of L-Glutamine 200mM (100x) solution (Hyclone), 0.1 mM non-essential amino acid solution 100x (Sigma M7145) and 10% Fetal Bovine Serum. Cell culture was maintained using aseptic technique and without the use of antibiotics.

Cells were routinely passaged when cell confluence is 80% (mid log phase) and subcultured every 3 days (72 hours ± 6 hours) at a seeding density of 5×10^4 to 1×10^5 cells/cm^2 in 25 cm^2 vent cap T- flasks (Corning), total volume of media was 5 mL per flask . Cells were split at a ratio of 1:50 or higher ratio 1:20 because they were growing at a fast rate, therefor the low split ratio is to keep the same amount of confluence. Cells were incubated at 37 °C ± 3 °C and 5% CO_2 in a humidified environment. Cell counts

were determined by counting technique using TC10 automated cell counter (Bio-Rad) and cell dilution was typically 1:1 in 0.04% Trypan Blue.

During the course of this work, different cell batches of the same cell line were frozen and kept at liquid nitrogen. For cryopreservation; cells were diluted to get a concentration of 1.0 x 10^6 cells/ ml in cold mixture of 90% DMEM+10% DMSO. Cells were transferred to refrigerator for 1-2 hours followed by overnight incubation at -80 °C and eventually stored in liquid nitrogen.

Frozen cells were recovered by placing them immediately in 37 °C water bath to rapidly thaw the cells (2 minutes). After spraying with 70% ethanol and then wiping with clean paper, the vial content was transferred to 15 ml tube with culture media (2- 4 ml). Centrifugation was done at 2000 g (125 xg) for 10 minutes. The supernatant was discarded and the pellet was suspended in 1 ml of warm medium that was placed in the incubator for at least 15 minutes. Based on cell count, cells are diluted and the calculated volume transferred to a 25 cm^2 flask, the total volume is brought to 5 ml cell culture. Pipetting was done to mix the cells well. Cells were examined under the microscope and after that incubated at 37 °C and 5% CO_2.

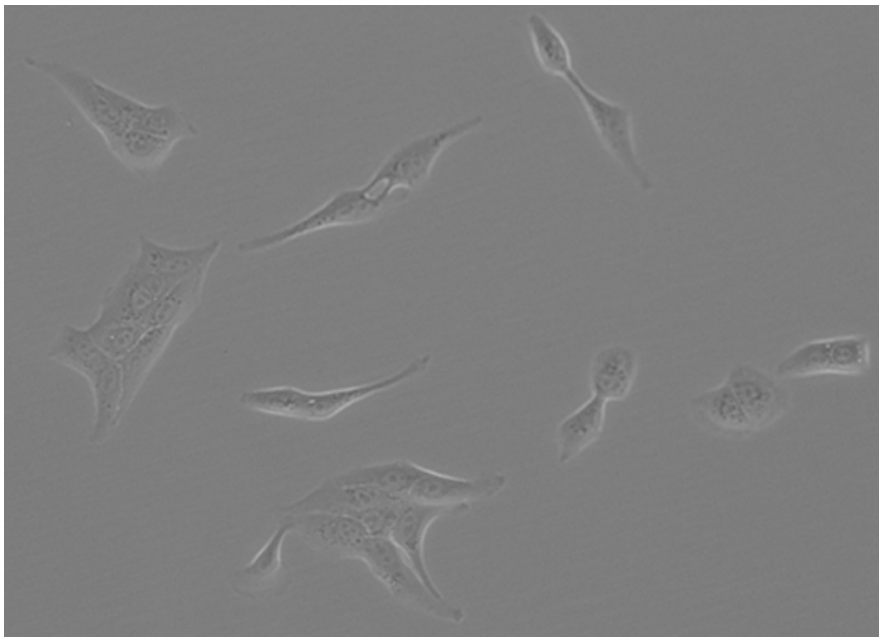

Figure 54. MDCK cells after 24 hours incubation (low density). Cells were incubated in DMEM with 2 mM of L-Glutamine, 0.1 mM non-essential amino acid solution and 10% Fetal Bovine Serum. Picture taken by EVOS FL microscope (AMG Micro, Bothell, WA, USA, at 20× magnification). Cells start in calm shape and then develop their epithelial morphology over time.

The medium is removed and cells are washed with 2-4 ml of 1X PBS (Phosphate Buffer Saline) to remove the residual medium. Cells are then incubated with Trypsin EDTA solution (Thermo Fisher Scientific Inc. Catalog no. NC0043665) at 37 °C for 15 to 21 minutes. When cells are almost completely detached, 1-2 ml of medium is added to stop trypsinization and pipetting is done to detach all cells. Cell suspension is transferred to falcon 15 ml tube (Falcon™ 15mL conical centrifuge tube) and centrifuged for 7-10 minutes. After discarding the supernatant, the pellet is suspended with 1 ml of warmed medium. Cells are diluted and counted as described previously.

MDCK cells doubling time was calculated based on the formula;

$$1 \div \left[\frac{[\log(\text{Final cell number}) - \log(\text{Initial cell number})] \times 3.32}{[T_2 - T_1]} \right]$$

T_2-T_1 time difference between cell numbers

The doubling time was found to vary according to initial cell number and time difference between initial and final number of cells. Cells used in assays were passaged at a regular basis after 2-3 days, when confluency is 80%, however they were passaged after 4 days for a couple of times. The doubling time was found to be around 22 hours (Figure 55).

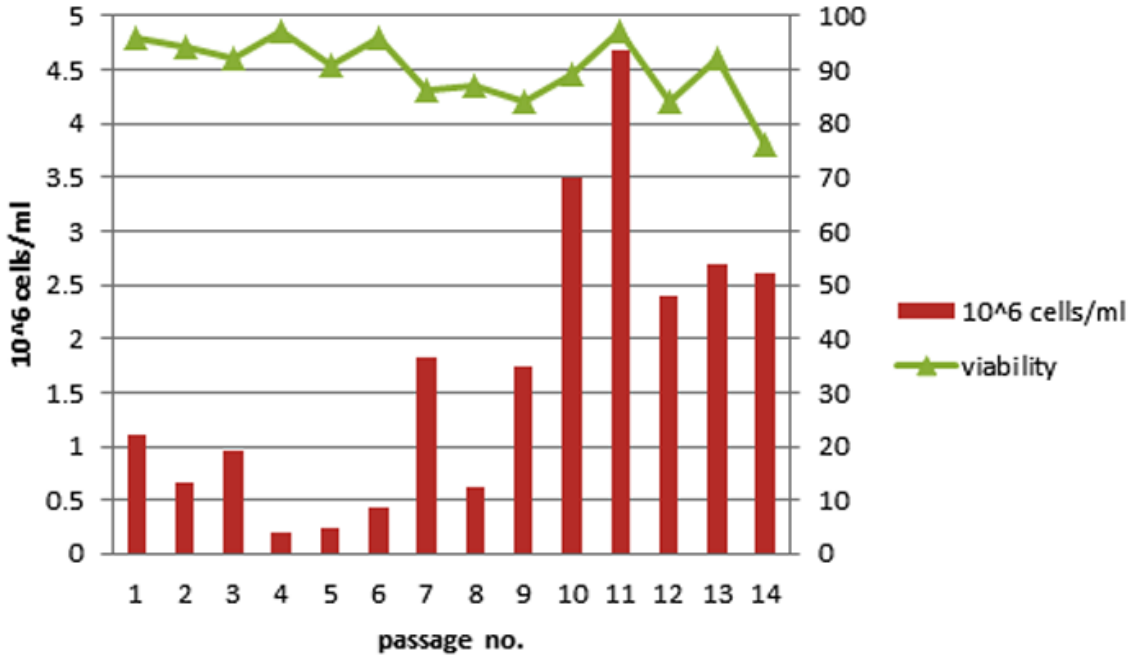

Figure 55. MDCK cells were maintained in DMEM for less than 20 passaging. Cell counts gradually increased over the course of the study. Cells were passaged every three to two days.

Cytotoxicity Assays

The reduction of tetrazolium salt is widely used as indication of metabolic activity of cells. MTT (3-(4,5-dimethylthiazol-2-yl)-2,5-diphenyltetrazolium bromide, a yellow tetrazole) is a very common proliferation assay used for the investigation of the reactivity of oxi-reductase enzymes.

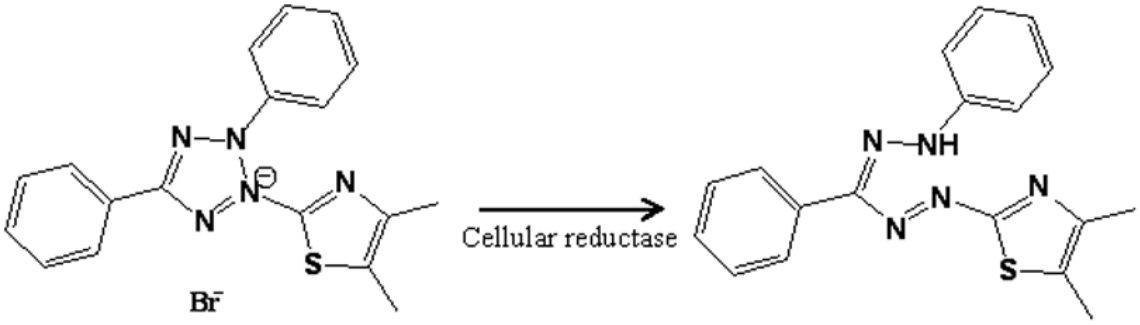

Figure 56. A comment tetrazole used in MTT is the diphenyl-tertrazolium bromide (water soluble yellow tetrazole) which turns into insoluble purple formazan upon reduction.

Another form of tetrazole is used in MTS cell proliferation one step assay, the reagent is composed of solutions of a novel tetrazolium compound [3-(4,5-dimethylthiazol-2-yl)-5-(3-carboxymethoxyphenyl)-2-(4-sulfophenyl)-2H-tetrazolium] in the presence of electron coupling reagent, phenazine methosulfate (PMS). MTS is close to MTT but it is one solution instead of two. MTS creates a soluble reaction product, thereby eliminating the solubilization step required with MTT. MTS is reduced by certain intracellular enzymes into a soluble formazan product that can be detected at absorbance at 490-500 nm. Cells were observed by the optical microscope to detect any morphological changes after fullerene derivatives treatment.

The last cell proliferation and cytotoxicity assay used is Alamar Blue, Resazorin ($C_{12}H_7NO_4$), also known as Diazoresorcinol or Azoresorcin (Figure 57). One advantage of using alamar blue along simplicity and sensitivity is biocompatibility to cells.

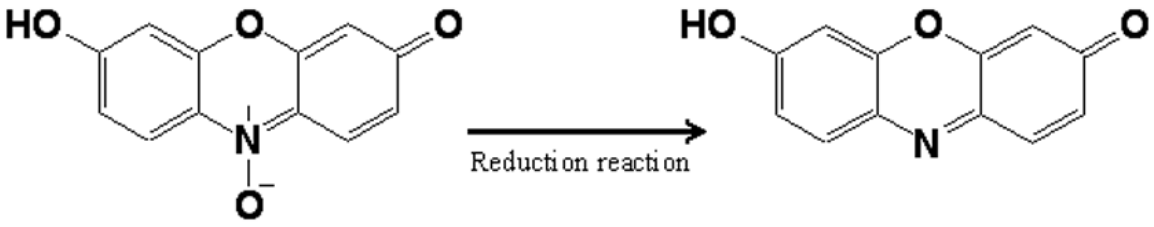

Figure 57. Resazurin assay or Alamar Blue assay is a cell redox indicator, a non-fluorescent blue dye, resazurin, is converted to bright red fluorescent resorufin by the reduction process of live cells. The resulted fluorescent amount is proportional to number of cells. The product is measured quantitatively by measuring the fluorescence (560EX nm/590EM nm) or absorbance (570 nm), the amount produced is proportional to the number of living cells.

However, this fluorometric test is not suitable to our model, the observed false results, as shown by figure 58, might be due to interference with carbon nanoparticles (fullerene derivatives), or probably due to interference with mitochondrial reductase activity considering the contribution of mitochondrial reductase to the reduction of Alamar Blue.

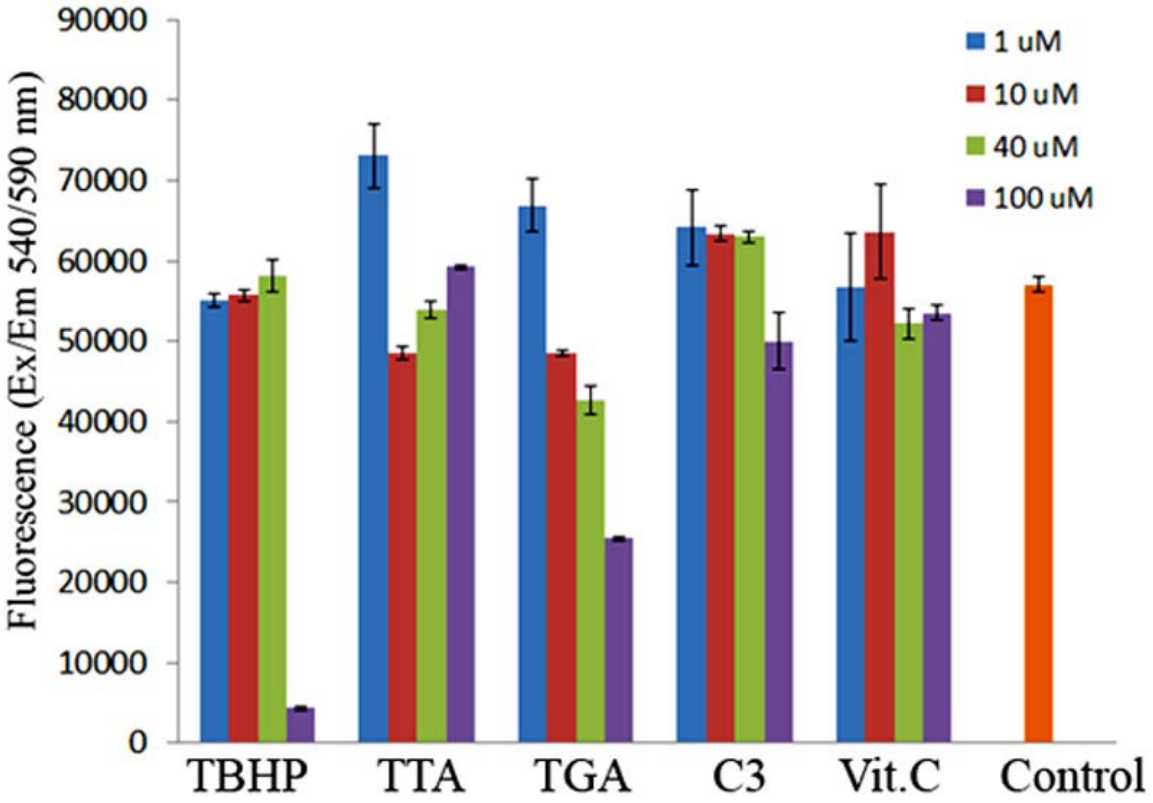

Figure 58. The colorimetric Alamar Blue proliferation assay was used to test the viability of cells incubated with water soluble fullerenes. MDCK cells were seeded at a density of 2.0 x 10^5 cells/ml in 96 well black plates and incubated for 24 hours at 37 °C in 5% CO_2, cells were incubated for further 24 hours at the absence (control) or presence of various concentrations of fullerene derivatives; 1, 10, 40 and 100 µM of TGA, TTA and C_3 as well as Vitamin C. TBHP was used as positive control. Fluorescence was detected at excitation/emission 540/590 nm. The Fluorescence values represent the mean of four readings and the corresponding standard errors of the means (s.e.m.).

APPENDIX C

PROTOCOLS OF PLASMID TRANSFECTION AND WESTERN BLOT

The plasmid construct

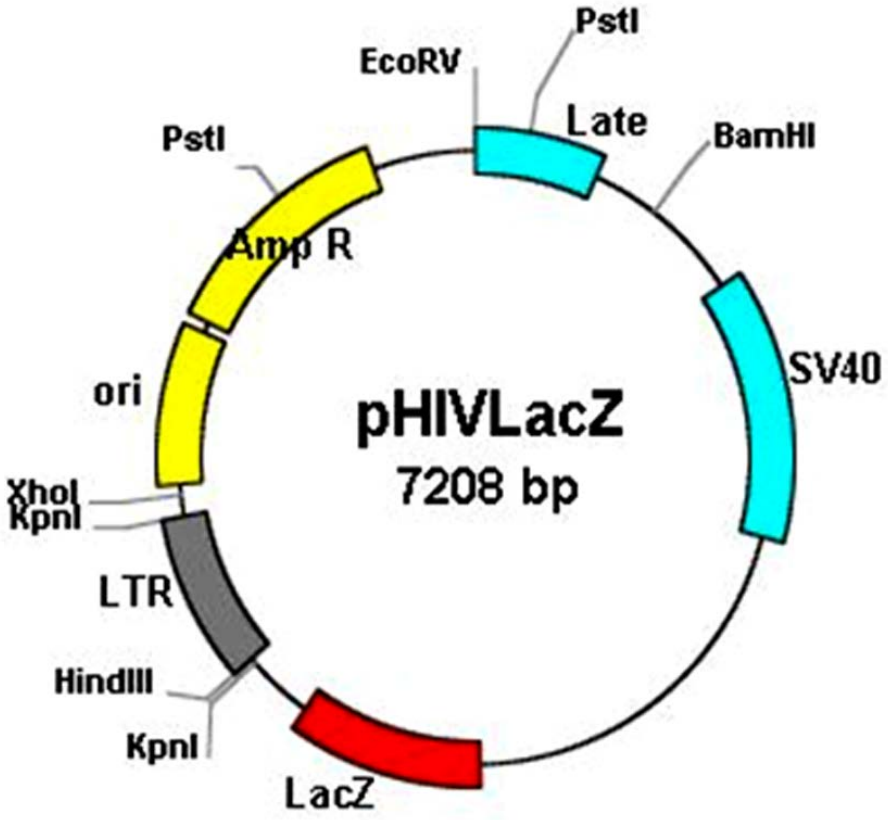

Figure 59. The approximate plasmid structure of 5KBpHIV-LacZ, five copies of the NF-κB site (5'-GGGGACTTTCC-3') were inserted into LTR sequence (Plasm 2.0.4.29, plasmid drawing software). The plasmid was extracted from bacterial cells using PureYield™ Plasmid Midiprep System from Promega.

Plasmid sequence and primers (Eurofins MWG Operon (Huntsville, AL 35805) are shown below;

Gene: HIV 3'LTR

8641 tgtagatctt agccactttt taaaagaaaa ggggggactg gaagggctaa ttcactccca
8701 acgaagacaa gatatccttg atctgtggat ctaccacaca caaggctact tccctgattg
8761 gcagaactac acaccagggc caggggtcag atatccactg acctttggat ggtgctacaa
8821 gctagtacca gttgagccag ataaggtaga agaggccaat aaaggagaga acaccagctt
8881 gttacaccct gtgagcctgc atggaatgga tgaccctgag agagaagtgt tagagtggag
8941 gtttgacagc cgcctagcat ttcatcacgt ggcccgagag ctgcatccgg agtacttcaa
9001 gaactgctga catcgagctt gctacaaggg actttccgct ggggactttc cagggaggcg
9061 tggcctgggc gggactgggg agtggcgagc cctcagatgc tgcatataag cagctgcttt
9121 ttgcctgtac tgggtctctc tggttagacc agatttgagc ctgggagctc tctggctaac
9181 tagggaaccc actgcttaag cctcaataaa gcttgccttg agtgcttca

Sequence

TGTAGATCTT AGCCACTTTT TAAAAGAAAA GGGGGGACTG GAAGGGCTAA
TTCACTCCCA ACGAAGACAA GATATCCTTG ATCTGTGGAT CTACCACACA
CAAGGCTACT TCCCTGATTG GCAGAACTAC ACACCAGGGC CAGGGGTCAG
ATATCCACTG ACCTTTGGAT GGTGCTACAA GCTAGTACCA GTTGAGCCAG
ATAAGGTAGA AGAGGCCAAT AAAGGAGAGA ACACCAGCTT GTTACACCCT
GTGAGCCTGC ATGGAATGGA TGACCCTGAG AGAGAAGTGT TAGAGTGGAG
GTTTGACAGC CGCCTAGCAT TTCATCACGT GGCCCGAGAG CTGCATCCGG
AGTACTTCAA GAACTGCTGA

Forward: tgtggatctaccacacacaaggct
Reverse: Accagagagacccagtacag

FORWARD

NNNNNNNNNNNNNNNNNNNNNNNCNNNCCNNNNNCNGGAGTCAGATATCCACT
GACCTTTGGATGGTGCTACAAGCTAGTACCAGTTGAGCCAGATAAGGTAGAAGAGG
CCAATAAAGGAGAGAACACCAGCTTGTTACACCCTGTGAGCCTGCATGGAATGGATG
ACCCTGAGAGAGAAGTGTTAGAGTGGAGGTTTGACAGCCGCCTAGCATTTCATCACG
TGGCCCGAGAGCTGCATCCGGAGTACAAGGGACTTTCCGCTGGGGACTTTCCGCTGG
GGACTTTCCGCTGGGGGACTTCCGCTGGGGGACTTTCCAGGGAGGCGTGGCCTGGGCG
GGACTGGGGAGTGGCGAGCCCTCAGATGCTGCATATAAGCAGCTGCTTTTTGCCTGT
ACTGGGTCTCTCTGGTTAGACCAGATCTGAGCCTGGGAGCTCTCTGGCTAGCTAGGG
AACCCACTGCTTAAGCCTCAATAAAGCTTGGGATCTCTATAATCTCGCGCAACCTATT
TTCCCCTCGAACACTTTTTAAGCCGTAGATAAACAGGCTGGGACACTTCACATGAGC
GAAAAATACATCGTCACCTGGGACATGTTGCAGATCCATGCACGTAAACTCGCAAGC
CGACTGATGCCTTCTGAACAATGGAAAGGCATTATTGCCGTAAGCCGTGGCGGTCTG
GTACC
GGTGGGTGAAGACCAGAAACAGCACCTCGAACTGAGCCGCGATATTGCCCAGCGTTT
CAACGCGCTGTATGGCGAGATCGATCCCGTCGTTTTACAACGTCGTGACTGGGAAAA
CCCTGGNGTTACCCAACTTAATCGCCTTGCAGCACATCCCCCTTTCGCCAGCTGGCGT
AATAGCGAAGAGGCCCGCACCGATCGCCCTTCCCAACAGTTGCGCANCCTGAATGGC
NAATGNNGCTTTGCCTGGTTNNCGGNACCAGAAGCGGTGCCGGAAANNCTGGCTGG
NNNNCGATCNTCCTGAAGCCNATACTGTCGNNCGTCCCCNTCAAACTGGCAGATGCA

CGGNTTACGATGNNNCCCANTCTACNACCAAACGTGAACCTANCCCNTTNNNGNNN
ANCCGCCCGTTTNNNNANCNGNNNNATCCNACGGNNNNNNNCNCCTCNNNTNNNNG
NTGANGNANNNGGGCNNNNNNNANGNNNNNNCNNGNANTNNNTTNNNNNGNNNNT
ANNNNNNGNGNNN

Reverse:
NNNNNNNNNNNNNNNNNNNGNNNCATCTGANGGCTCGCCACTCCCCAGTCCCGCC
CAGGCCACGCCTCCCTGGAAAGTCCCCCAGCGGAAGTCCCCCAGCGGAAAGTCCCA
GCGGAAAGTCCCCAGCGGAAAGTCCCTTGTACTCCGGATGCAGCTCTCGGGCCACGT
GATGAAATGCTAGGCGGCTGTCAAACCTCCACTCTAACACTTCTCTCTCAGGGTCATC
CATTCCATGCAGGCTCACAGGGTGTAACAAGCTGGTGTTCTCTCCTTTATTGGCCTCT
TCTACCTTATCTGGCTCAACTGGTACTAGCTTGTAGCACCATCCAAAGGTCAGTGGAT
ATCTGACTCCTGGCCCTGGTGTGTAGTTCTGCTAATCAGGGAAGTAGCCTTGTGTGTG
GTAGATCCACAGATCAAGGATATCTTGTCTTCTTTGGGAGTGAATTAGCCCTTCCAGT
CCCCCCTTTTCTTTTAAAAAGTGGCTAAGATCTACAGCTGCCTTGTAAGTCATTGGTC
TTAAAGGTACCTGAGGTGTGACTGGAAAACCCACCTCCTCCTCCTCTTGTGCTTCTAG
CCAGGCACAAGCAGCATTGGTAGCTGCTGTATTGCTACTTGTGATTGCTCCATGTTTT
TCCAGGTCTCGAGGATACTGGCTTAACTATGCGGCATCAGAGCAGATTGTACTGAGA
GTGCACCATATGCGGTGTGAAATACCGCACAGATGCGTAAGGAGAAAATACCGCAT
CAGGCGCTCTTCCGCTTCCCTCGCTCACTGACTCGCTGCGCTCGGTCGTTCGGCTGCG
GCGAGCGGTATCAGCTCACTCAAAGGCGGTAATACGGTTATCCACAGAATCAGGGG
ATAACGCAGGAAAGAACATGTGAGCAAAAGGCCAGCAAAAGGCCAGGAACCGTAA
AAAGGCCGCGTTGCTGGCGTTTTTCCATANGCTCCGCCCCCTGACGAGCATCACAAA
AATTCGANGCTCAAGTCAGAGGTGGCGAAANCCNACAGGACTNNNAANATNCNAGN
NTTTCCCCNNGAAGCTNCNNNGTGCGNTNNCNGNTCCNACCNNCNCTACNNANNCN
GTCCNCTTTCTCCTTCGGNNCGNGNNGNTTNTNNANNNNNNNACNCTGNAGNNTNN
NCAGTCGGNGNANNNN

Transfection with 5kB-LacZ plasmid

To study the effect of water soluble fullerenes on HIV LTR promoter activity and potential inhibition, cells were transfected with pHIV.5kB-LacZ using lipofectamine-2000, in 96 well plates, with each well seeded with 2.0×10^4 cells/well and 0.2 μg (0.2 μg/well) of 5kB-LacZ plasmid DNA. Cells were grown in MEM immediately after transfection for 48 hours

1. MDCK cells with 50-70% confluency were tryptinized at 37 °C and 5% CO_2 for around 25 minutes, then they were resuspended in medium (MEM+10%) and seeded onto wells as a density of 2.0 x 10^4 cells/well.
2. Cells were incubated at 37 °C and 5% CO_2 for 24 hours,
3. Transfection was done using 0.22 µg DNA and 0.5 µl lipofectamine 2000 for each well, ratio of (1:2.3), since there are 21 wells for transfection; lipofectamine (11 µl) was diluted in 110 µl OptiMEM medium and incubated for 5 minutes at RT, then 4.78 µl of 5kB-LacZ (920 µg/ml) was diluted in 110 µl OptiMEM medium.
4. The two mixtures (DNA and lipofectamine 2000) were mixed together and allowed to form for 20 minutes.
5. The plasmid DNA- Lipofectamine™ 2000 complexes 10 µl were added directly to each well of the plates containing cells and mixed gently
6. Different concentrations of fullerenes (8.6 x 10^{-6}M and 7.8 x 10^{-7}M) were added to cells after one hour of transfection.
7. PMA was added to activate the LTR, a concentration of 300 nM was added 3 hours after transfection (2 hours after the addition of fullerenes).

Measurement of NF-κB inhibition in 5KBpHIVLacZ transfected cells by β-galactosidase reporter gene activity

Enhanced β-Galactosidase Assay Kit (genlatis A10100K) uses the chromogenic substrate chlorophenol red-β-D-galactopyranoside (CPRG). The expression of β-

galactosidase is measured by its cleavage of CPRG subsequently resulting in production of chlorophenol red, which is measured by colorimetric assay using a standard 96 well plate reader. The assay was done following the manufacture instructions and absorbance was read at 575 nm with a microtiter spectrophotometer.

- After 48 hours of incubation, cells were treated according to Enhanced β-Galactosidase Assay Kit (CPRG) protocols as following:
    a. 1X Lysis buffer was added (volume; 50 µl) to each well, and the plate was incubated for 12 minutes at room temperature by swirling it slowly several times to ensure complete lysis. The cells were observed under a microscope to confirm cells lysis.
    b. A quick freeze/thaw cycle (freeze 25 minutes at -78°C and thaw at room temperature) of the plate was done to obtain a good lysis.
    c. After thawing the plate of lysed cells at room temperature, 50 µl of standard dilution buffer was added to each of the wells of a 96-well plate except the control wells, which are set aside for standard curve.
    d. The standards were prepared by making a serial dilution of β-galactosidase (*E.coli*) standards using standard dilution buffer: according to the manufacture's instruction.
        - 50 µl of each the standards was added to the control wells of the plate - the highest recommended amount of β-galactosidase is 100 milliunits (100,000~200,000 pg). Don't add lysis buffer to the standard wells, only β-galactosidase and CPRG.

e. The blank was prepared by adding 50 µl of lysis buffer to a well and 50 µl of cell lysate from non-transfected cells (mock-transfected cells) to a well to control endogenous β-galactosidase activity.

f. 100 µl of 1X CPRG substrate solution was added to each well and the plate was incubated at room temperature until the dark red color developed (from approximately 1- 3 hours depending on the cell confluency). The standards were measured immediately after loading (10 min).

g. The absorbance was read at 575 nm with a microtiter spectrophotometer.

h. Quantify β-galactosidase expression based on a linear standard curve

Reagents preparation:

- 5X lysis buffer was diluted to 1X using distilled deionized water before use. Unused 1X Lysis buffer may be stored at 4°C for future use;
- 10X CPRG stock was diluted to 1X using substrate buffer just before performing the colorimetric assay. The unused 1X CPRG was stored at -20°C for future use. It is recommend to use 1X CPRG solution only 2 times after a freeze/thaw cycle.

Protocols for gel electrophoresis and western blot

1. Cells were seeded at a density of 3 x10^5 cells/ml per well using 6 well plate
2. After 24 hours of cell incubation at 37 °C and 5% CO_2, cells were treated with 40 µl $C_{60}OH_x$
3. Cells were stimulated with 25 µl PMA after 24 hours of incubation with $C_{60}OH_x$.

4. Proteins were extracted using NF-κB extraction kit (NFKB2, Five photon biochemical, San Diego, California) following the manufacturer's instructions.
5. Sample buffer was prepared by mixing 950 µl of Laemmli Sample buffer (161-0737) with 50 µl of 2- Mercaptoethanol BME (161-0710).
6. Protein was diluted with the prepared sample buffer in 1:1 ratio and then samples were heated at 95°C for 5 min and thereafter loaded onto SDS-PAGE gels.
7. Cell lysates were fractionated using precast polyacrylamide gel, 4–20% SDS-PAGE gel (mini- Protean TGX, Bio-Rad. Cat. 456-1093), this gel is suitable to resolve p65 (molecular weight approximately 65kD). Protein samples were loaded into each well (30 µl/well). Using sample buffer (Laemmli, dilute 1:1 with sample). Precision plus protein standards, dual color, catalogue number 161-0374. 10 µl was loaded into a well
8. After loading the gel apparatus with running buffer (standard Tris-glycine running buffer, Tris/glycine/SDS, cat. # 161-0732), it was run for 15 minutes at 300 volts for approximately 15 minutes).
9. After SDS-PAGE gel is resolved, proteins were transferred to a nitrocellulose membrane (Trans-Blot® Turbo™ Mini Nitrocellulose Transfer Packs, (170-4158) using Trans-Blot Turbo kit (Bio-Rad Cat. # 170-4155) which performs semi dry blotting within 3 minutes.
10. After the disassembly of the cassette, the membrane was incubated with a freshly made blocking solution (1X PBS + 5% non-fat dry milk) at room temperature with shaking.

11. The blot was incubated with primary antibody P65 (No. p65Ab, Rab IgG, Lot 388 , Five photon Biochemicals) at a dilution of 1:400 in PBS-T solution (1X PBS + 0.05% Tween20) in a total volume 4 ml in a falcon tube 50 ml at room temperature with shaking.
12. The membrane was washed five times with PBS-T (1X PBS containing+ 0.05% Tween20) washing for 5 times, with the first wash at 15 minutes and the remaining washes each at 5 minute intervals afterwards.
13. The wash solution was discarded and the membrane was incubated with secondary antibody goat anti–rabbit IgG- HRP at a dilution 1:3000 in PBS-T (1X PBS containing+ 0.05% Tween20).
14. The membrane was washed five times with PBS-T (1X PBS containing+ 0.05% Tween20) washing for 5 times, with the first wash at 15 minutes and the remaining washes each at 5 minute intervals afterwards.
15. Membrane was washed and NF-κB proteins were detected using an enhanced chemiluminescence (ECL) reagent, ECL kit, (the detection kit was applied following the manufacture's instruction of mixing reagent A with reagent B), the mixture was applied to the membrane for 5 minutes with shaking. Bio-Rad ChemiDoc™ XRS+ System was used for the detection of chemiluminescence controlled by Image Lab™ software.